



Open access
virtual testing protocols
for enhanced
road user safety

Test protocols for virtual testing and future continuation of the OpenVT platform

WP number: 1

Deliverable: D1.2



Test protocols for virtual testing and future continuation of the OpenVT platform

Work package 1, Deliverable D1.2

Please refer to this report as follows:

Keller, A., Klug, C., Kranjec, M., Leo, C., Martinez, L., Muser, M., Schachner, M., Thomson, R., Trummler, L., Linder, A. (2022): Test protocols for virtual testing and future continuation of the OpenVT platform, Deliverable D1.2 of the H2020 project VIRTUAL.

Project details:

| | |
|----------------------------|---|
| Project start date: | 01/06/2018 |
| Duration: | 54 months |
| Project name: | Open access virtual testing protocols for enhanced road user safety – VIRTUAL |

| | |
|---------------------|---|
| Coordinator: | Astrid Linder, Prof, PhD – Research Director Traffic Safety Swedish National Road and Transport Research Institute (VTI) Regnbågsgatan 1, 417 55 Lindholmen, Göteborg, Sweden |
|---------------------|---|



This project has received funding from the European Union's Horizon 2020 research and innovation programme under grant agreement No 768960.

Deliverable details:

| | |
|-----------------------------|---|
| Version: | Final |
| Dissemination level: | PU (Public) |
| Due date: | 2022/06/20 |
| Submission date: | 2022/06/20 |
| Online location: | Webforum link: https://secure.webforum.com/atvirtual/doc/?dfRefID=2892094 |

Lead contractor for this deliverable:

Arne Keller– AGU Zürich

| | |
|--------------------------|--|
| Report Author(s): | Keller, A., Muser, M., Trummler, L. (AGU Zürich), Switzerland Klug, C., Leo, C., Schachner, M. (TU Graz), Austria Linder, A. (VTI), Sweden Thomson, R. (Chalmers University), Sweden Kranjec, M. (University of Ljubljana), Slovenia Martinez, L. (University of Madrid), Spain |
|--------------------------|--|

Legal Disclaimer

All information in this document is provided "as is" and no guarantee or warranty is given that the information is fit for any particular purpose. The user, therefore, uses the information at its sole risk and liability. For the avoidance of all doubts, the European Commission and INEA has no liability in respect of this document, which is merely representing the authors' view.

© 2018 by VIRTUAL Consortium

Revision history

| Date | Version | Reviewer | Description |
|------------|---------------------------------------|---|----------------------|
| 2022/06/01 | Preliminary draft for language review | Kelly Hess | Language review |
| 2022/06/08 | Final draft for review | QM Ingrid Skogsmo, Internal reviewer Simon Krašna | QM + internal review |
| 2022/06/20 | Final deliverable | Astrid Linder – VTI → EC | |



Table of contents

| | |
|---|-----------|
| Executive summary | 7 |
| Abbreviations and definitions | 8 |
| 1 Introduction | 9 |
| 2 Injury risk assessment manual: introduction..... | 10 |
| 2.1 Injury risk assessment in VIRTUAL | 10 |
| 2.2 Approaches to injury risk assessment | 10 |
| 2.3 Injury risk curves and protection limits | 11 |
| 2.4 Risk curves for tissue-based criteria | 11 |
| 2.5 Implementation of injury criteria: Dynasaur and VIVA+ output channels | 12 |
| 2.6 Tasks for future research | 12 |
| 3 Test protocols for virtual testing | 13 |
| 3.1 Rear impact | 13 |
| 3.1.1 Tasks for future research | 14 |
| 3.2 Vulnerable road users..... | 14 |
| 3.2.1 Tasks for future research:..... | 15 |
| 3.3 Standing passenger..... | 15 |
| 4 Concept for the future evolution of the VIRTUAL contents and the OpenVT platform | 17 |
| 4.1 Dimensions of the sustainability problem | 17 |
| 4.2 Possible solution routes | 17 |
| 4.3 OVTO: The OpenVT Organisation..... | 18 |
| 4.3.1 Purposes and objectives of OVTO..... | 18 |
| 4.3.2 Organisational structure..... | 19 |
| 4.3.3 Future funding of OVTO | 19 |
| 4.4 Outlook and tasks to address in the future | 20 |
| 5 Conclusion..... | 21 |
| References | 22 |
| 6 Appendix A – Injury criteria manual..... | 26 |
| 6.1 Non-HBM based criteria: overview ordered by body region | 26 |
| 6.1.1 Head | 26 |
| 6.1.2 Spine..... | 27 |
| 6.1.3 Thorax..... | 29 |

| | | |
|------------|--|-----------|
| 6.1.4 | Lower extremities..... | 30 |
| 6.2 | Injury criteria for children..... | 32 |
| 6.3 | Tissue-based Tissue-based injury criteria | 34 |
| 6.3.1 | General: Output definitions in VIVA+..... | 34 |
| 6.3.2 | Head | 35 |
| 6.3.3 | Spine..... | 35 |
| 6.3.4 | Thorax..... | 36 |
| 6.3.5 | Lower extremities..... | 36 |
| 6.4 | References..... | 38 |
| 7 | Appendix B: Rear impact protocol | 40 |
| 7.1 | Introduction | 40 |
| 7.1.1 | Purpose | 40 |
| 7.1.2 | Definitions | 40 |
| 7.1.3 | Overview of assessment procedure | 40 |
| 7.1.4 | General requirements | 40 |
| 7.2 | Device model to be tested | 41 |
| 7.2.1 | Calibration | 41 |
| 7.2.2 | Validation | 41 |
| 7.2.3 | Documentation of validation | 41 |
| 7.2.4 | Output definitions | 41 |
| 7.3 | Virtual occupant model (measurement device)..... | 41 |
| 7.3.1 | Prerequisites | 41 |
| 7.3.2 | Qualification procedure..... | 42 |
| 7.3.3 | Output definitions | 42 |
| 7.3.4 | Model preparation | 42 |
| 7.4 | Test preparation and pre-simulation..... | 43 |
| 7.4.1 | Test environment | 43 |
| 7.4.2 | Installation and preparation of device model and HBM | 43 |
| 7.4.3 | Installation of the HBM | 45 |
| 7.4.4 | Posture adjustment | 45 |
| 7.4.5 | Contact definitions | 45 |
| 7.4.6 | Pre-simulation..... | 45 |
| 7.4.7 | Evaluation and documentation of the pre-simulation | 46 |
| 7.4.8 | Virtual test (main simulation) | 46 |
| 7.4.9 | Crash pulse..... | 46 |
| 7.4.10 | Quality criteria | 46 |
| 7.5 | Evaluation of virtual testing results | 47 |
| 7.5.1 | Post-processing definitions..... | 47 |

| | | |
|------------|--|-----------|
| 7.5.2 | Injury assessment | 47 |
| 7.5.3 | Test report | 47 |
| 7.6 | References..... | 48 |
| 7.7 | Appendix: recommended method for positioning process | 48 |
| 7.7.1 | Preparation of positioning simulation | 48 |
| 7.7.2 | Data recording and read-out | 49 |
| 7.7.3 | Statistical model by Park et al. | 49 |
| 8 | Appendix C: Standing passenger protocol..... | 52 |
| 8.1 | Introduction | 52 |
| 8.1.1 | General Purpose..... | 52 |
| 8.1.2 | Definitions/Abbreviations used in the Report..... | 52 |
| 8.1.3 | General Requirements | 52 |
| 8.1.4 | User interfaces for in-crash simulation | 53 |
| 8.2 | Virtual Models to be tested (Device to be tested) | 53 |
| 8.2.1 | Calibration of vehicle interior model for passenger safety simulations | 53 |
| 8.2.2 | Validation | 54 |
| 8.2.3 | Documentation of validation | 54 |
| 8.3 | Virtual SP models (measurement device) | 54 |
| 8.3.1 | Prerequisites | 54 |
| 8.3.2 | Model preparation | 56 |
| 8.3.3 | Test setups..... | 57 |
| 8.3.4 | Virtual test conditions (test runs) | 64 |
| 8.3.5 | Evaluation of virtual testing results..... | 64 |
| 8.4 | References..... | 64 |
| 9 | Appendix D: Test protocol vulnerable road users (VRU)..... | 66 |
| 9.1 | Introduction | 66 |
| 9.1.1 | General Purpose..... | 66 |
| 9.1.2 | Definitions/Abbreviations used in the Report..... | 66 |
| 9.1.3 | Overview of Assessment procedure | 66 |
| 9.1.4 | General Requirements | 67 |
| 9.1.5 | Tooling and user interfaces for pre-crash simulation..... | 67 |
| 9.1.6 | User interfaces for in-crash simulation | 76 |
| 9.2 | JupyterVirtual Models to be tested..... | 76 |
| 9.2.1 | Calibration of the vehicle under test | 76 |
| 9.2.2 | Validation | 81 |
| 9.2.3 | Documentation of Validation | 83 |
| 9.3 | Virtual VRU Models (Measurement Device)..... | 85 |

| | | |
|------------|--|------------|
| 9.3.1 | Prerequisites | 85 |
| 9.3.2 | Model preparation | 88 |
| 9.3.3 | Qualification procedure..... | 94 |
| 9.4 | Test setups | 95 |
| 9.4.1 | Test environment | 95 |
| 9.4.2 | Outputs definitions of test setups | 100 |
| 9.4.3 | Simulation Time | 104 |
| 9.5 | Virtual test conditions (test runs) | 104 |
| 9.5.1 | Simulation Matrix | 104 |
| 9.5.2 | Quality Criteria | 106 |
| 9.6 | Evaluation of virtual testing results | 108 |
| 9.6.1 | Postprocessing definitions..... | 108 |
| 9.6.2 | Injury Assessments | 108 |
| 9.6.3 | Overall injury assessment | 108 |
| 9.6.4 | Cost-benefit analysis (CBA)..... | 108 |
| 9.6.5 | Documentation and Data Specification..... | 109 |
| 9.7 | References..... | 109 |
| 9.8 | Appendix | 110 |
| 9.8.1 | Bicycle model validation..... | 110 |
| 10 | Appendix E: Articles of the OpenVT Organisation | 112 |

Executive summary

This document covers the main results of VIRTUAL's work package 1: (i) the injury risk assessment manual, (ii) test protocols for virtual testing of three generic load cases and (iii) a concept for the future sustainable evolution of the VIRTUAL project results and the OpenVT platform.

The presented injury risk assessment manual provides definitions and instructions for all injury criteria currently implemented for evaluation with the VIVA+ HBMs. These comprise established criteria as well as novel tissue-based approaches. Furthermore, additional criteria are described which should be implemented in the future.

Generic test protocols for virtual testing of three load cases are presented. The protocols have been tested and implemented using the VIVA+ HBMs and serve as prototypes of virtual test protocols for application in future consumer and regulatory tests.

Finally, we propose a concept for the sustainable evolution of the VIRTUAL project results (including open source contents as well as the OpenVT platform) and identify the OpenVT Organisation (OVTO) as the main governing and coordinating body. As a non-profit organisation, OVTO will be the legal entity owning these results in the future and will oversee subsequent developments.

For each topic, a short summary is provided in the main part of the document, with more details found in the respective appendix.

Abbreviations and definitions

| Abbreviation | Description |
|--------------|--|
| 50F | Human Body Model representing the 50th percentile (average) Female |
| 50M | Human Body Model representing the 50th percentile (average) Male |
| AEB | Automatic emergency braking |
| ATD | Anthropometric test device |
| Baseline | Baseline simulations are based on the original virtual testing scenarios. Active safety systems have not been considered (w/o AEB) |
| CBA | Cost-benefit analysis |
| DoE | Design of Experiments |
| GUI | Graphical user interface |
| HBM | Human Body Model |
| IS-Scores | Injury Severity Scores |
| MaxPro | Maximum Projection |
| PMHS | Post Mortem Human Subject |
| QALY | Quality Adjusted Life Year |
| SUT | Structure Under Test |
| Viva+ SP | VIVA+ Standing Passenger model |
| VRU | Vulnerable Road User |
| VRU VISAFE | Virtual Integrated Safety Assessment of Vulnerable Road Users |
| VUT | Vehicle Under Test |

1 Introduction

This document covers several fields within VIRTUAL's work package 1, which at first seem fairly unrelated: test protocols for virtual testing, the future continuations of the OpenVT platform and the injury criteria manual. However, they are connected more closely than it seems. Bridging the gap between virtual and physical testing was the core motivation of Project VIRTUAL. In order to reach this, the key elements are (i) suitable numerical models and tools that are available open access and under open licences, (ii) detailed instructions on how to apply the open models and tools in standardised test procedures and (iii) an approach to injury risk assessment applicable to human body models and comparable between physical and virtual testing. The three topics covered in this document address exactly these key ingredients. The OpenVT platform and the OpenVT Organisation that oversees its future are the instruments that allow the VIRTUAL models and tools to be continuously available under open access conditions. The three generic test protocols for the use cases "rear impact on seated occupants" (Section 3.1), "vulnerable road users" (Section 3.2) and "standing passengers of public transport in non-collision incidents" (Section 3.3) are prototypes for the application of virtual testing in future consumer and (at a later stage) regulatory tests. Finally, VIRTUAL's injury criteria manual is a comprehensive guide to injury risk assessment with human body models, summarising the most commonly used, established injury criteria and enhancing them with tissue based approaches applicable exclusively on numerical HBMs.

In order to keep the document readable, the following chapters contain a short introduction and a summary for each of the three main topics "Injury assessment manual," "Test protocols for virtual testing" and "Concept for the future evolution of the OpenVT platform and OpenVT platform," explaining the key concepts and results. The corresponding appendices provide more detailed information, i.e. the documentation of all injury criteria, the full test protocols for the three use cases and the articles of the OpenVT organisation. The appendices, particularly the test protocols (appendices B, C and D), are also intended to serve as stand-alone documents in the future when they might be used as templates for virtual test protocols in consumer or regulatory testing. This explains why there are some redundancies and overlaps between them.

The results presented in this work reflect the status at M48 of project VIRTUAL – they are likely and even intended to evolve further in the future and beyond the end of the project. Therefore, the contents are closely linked to the OpenVT platform, where continuously updated versions can be found. Also, example load cases for each of the test protocols are available as complete source code on OpenVT. Interested users can not only download them, but can also contribute their own modifications and improvements and (under the surveillance of the OpenVT Organisation) make them available to the user community in an open source spirit. The links to the respective repositories are given in each of the chapters. Furthermore, at the end of each chapter, a paragraph "Tasks for future research" can be found, containing a list of problems which were beyond the scope of Project VIRTUAL, but should urgently be addressed in the future. These tasks are not only meant as an inspiration for future research projects, but also as an invitation to the interested reader to participate in the open source development process on the OpenVT platform, to find solutions to these problems and to help making the open contents developed within VIRTUAL even more powerful in the future.

2 Injury risk assessment manual: introduction

2.1 Injury risk assessment in VIRTUAL

Injury risk assessment is the primary purpose of the different HBMs developed within VIRTUAL. Whether they replicate vehicle occupants or other road users, such as pedestrians, all these models aim at quantifying the injury risk that these person groups face in certain hazardous traffic situations. Therefore, the injury detection framework is a core component of each of the computational models developed within VIRTUAL.

As a general approach, VIRTUAL applies a mix of established (or, more correctly, non-HBM based) injury criteria and novel tissue-based methods. The choice of criterion used in each situation depends on different factors, such as the level of detail of the HBM for a certain body part, the intended load cases and the available validation data for that particular case. An overlap of the two categories may be useful to compare the outcome in some cases – however, comparing different injury criteria is conceptually not always straightforward. Also, the application of injury criteria developed for quasi-rigid parts of dummies to a HBM somewhat contradicts the purpose of making a HBM in the first place, since the advantage of a HBM lies precisely in the fact that it offers more detailed and realistic insights into the injury mechanisms. Nevertheless, the dummy-based criteria may serve a useful purpose in relating the two domains to each other. Ultimately, it is expected that only (well-validated) tissue-based criteria will be used in HBMs.

This chapter provides a short introduction and some conceptual background of the injury to be used with the VIVA+ HBMs. The comprehensive list of criteria is provided in Appendix A. This list, sorted according to established and tissue-based criteria and according to body regions, contains all criteria which currently can be evaluated with the VIVA+ HBMs. Furthermore, it also lists criteria which are frequently used (e.g. in regulatory or consumer tests) but have not been implemented for the VIVA+ models yet. The implementation of these is an open task, which in an open source spirit we encourage the users of the VIVA+ HBMs to address in the future.

2.2 Approaches to injury risk assessment

Traditionally, safety of road vehicles is tested in physical tests using anthropomorphic test devices (ATDs). In order to estimate the injury risk in these situations, injury criteria have been developed which compare the kinematics, dynamics or (visco)elastic deformation of ATDs to values obtained in experiments with post mortem human subjects (PMHS tests). In spite of obvious shortcomings (such as the limited possibilities of ATDs to realistically replicate the behaviour of the living human body in different situations and their limited ability to cope with anthropomorphic diversity), this procedure is based on a solid foundation of research and data and is well-established in regulatory safety tests.

Unlike mechanical components, which can be precisely tested numerically with the computational methods available today, the direct numerical assessment of injury risk remains a tricky task. Essentially, two approaches can be applied for that: (1) the traditional injury criteria developed for ATDs are evaluated with the results of numerical simulations with HBMs, or (2) the deformations, strains and stresses as given by the numerical solution are analysed directly, either by comparing

them to failure criteria known from tissue-level biomechanical experiments, or by implementing a damage or failure model into the numerical model – this is known as tissue-based injury assessment.

The next step after application of the presented virtual test protocols would be deriving input to a cost-benefit analysis (CBA) with VIRTUAL's cost-benefit tool, assessing the safety benefits of the products under consideration. However, given the still somewhat experimental status of the test protocols, a readily useable input to CBA is still difficult to generate. Nevertheless, particularly in the vulnerable road user test protocol, basic guidelines how to perform this task are formulated

2.3 Injury risk curves and protection limits

In order to derive an injury risk assessment from the values of (either established or tissue-based) injury criteria, there are essentially two approaches. The first is to specify an injury risk curve, which is a function that maps the values of the criteria to a probability of a certain injury or to an expected injury severity (e.g. an AIS value). An injury risk curve can be inferred, e.g., from PMHS tests or from analysis of accident data. This approach makes the criterion an injury criterion in the proper sense, as it enables the determination of whether or not a certain injury seems likely.

In many technical applications, the purpose of the criterion is not so much to derive a probability of a certain injury, but rather to define limits up to which the loads under consideration are not harmful to the human body (where 'harmful' could mean, e.g., not causing any injuries, not causing permanent damage, not causing life-threatening injuries). In these cases, an injury risk curve is often not specified, instead a second approach, a threshold value, the protection limit, is given. Such a criterion is called protection criterion or performance criterion (Schmitt et al. 2019). In regulatory testing, this is the most common approach. However, in most cases such protection criteria are themselves based on injury risk curves.

For a criterion associated with an injury risk curve, in principle a protection limit can be derived by imposing a threshold on the injury risk.

If neither a risk curve nor a protection limit is known, a measurement parameter cannot be directly applied as an injury criterion.

In the list of injury criteria in Appendix A, we specify for each criterion whether or not an injury risk curve and/or a protection limit is known from either the scientific literature or from the application of the criterion in regulatory and consumer testing. For each body part, criteria with a risk curve are listed first, followed by the ones with a known protection limit and thereafter the ones for which neither is known.

2.4 Risk curves for tissue-based criteria

In principle, (peak) principal strains or other strain measures may be used to determine a risk of bone fracture (or soft tissue failure) instead of a simple fracture / no fracture output. For this purpose, the corresponding risk curves must be derived from e.g. biomechanical test with PMHS parts. The loading conditions of these tests can be used to reproduce the tests in a corresponding FE model. Many factors may influence the results of e.g. PMHS experiments with long bones, such as bone cross-sections, cortical bone strength, trabecular bone density, age, gender. Some of these factors may be reproduced in the FE model, while others might be unknown or not reproducible in a FE model. Thus, the resulting risk curve will always represent the injury risk vs. the factors that are not or not completely reproduced in the model. The injury risk curve may furthermore be multi-dimensional, in which case it may prove difficult to find a sufficient amount of experimental data to represent all the different parameters of the experiments.

2.5 Implementation of injury criteria: Dynasaur and VIVA+ output channels

The evaluation of injury criteria is a vital part of any HBM simulation. This task requires knowledge on the definition, interpretation and scientific background of the respective criteria, which are provided in the injury criteria manual. However, the necessary input data also has to be extracted from the model output and processed correctly. To facilitate this task, VIRTUAL recommends the Python library Dynasaur, which has been developed for this purpose by Schachner et al. (2018). Dynasaur is capable of reading LS-DYNA binary output files (binout) and contains implementations of most injury criteria recommended so far for the use with the VIVA+ HBMs. The tool is available on a pip repository and, as open source content, can also be modified and adapted further by the users. For the injury criteria implemented so far in Dynasaur, the corresponding commands and their syntax are summarised in the injury criteria manual. Furthermore, for a number of examples and validation load cases, the use of Dynasaur for the evaluation of relevant injury criteria has been demonstrated in Jupyter notebooks which can be found on the OpenVT platform. More details on the use of Dynasaur can be found on the Dynasaur repository at <https://gitlab.com/VSI-TUGraz/Dynasaur>.

Concerning the HBM, the implementation of an injury criterion essentially consists of including the necessary sensors in the HBM source code, which record the quantities needed for the calculation of the criterion during the model run. For the most relevant injury criteria, these sensors have already been implemented in the VIVA+ HBMs. The output can be read by Dynasaur using def-files (i.e., ASCII files defining output data and calculation procedures), which are supplied together with the HBMs. The def-files identify the different sensors with ID channels, through which the corresponding data can easily be found in the Dynasaur output. In the injury criteria manual, the status of this implementation is summarised for each criterion and the names of the applied ID channels are documented.

2.6 Tasks for future research

- Create Dynasaur implementations and VIVA+ output channels for not yet implemented injury criteria
- Define/find HBM based criterion that reflects forces and moments in upper neck and implement it in Dynasaur and VIVA+
- Further validate Aldman pressure criterion and implement in Dynasaur (problem: CFD solver required)

3 Test protocols for virtual testing

The virtual test protocols developed within the project are outlined in this chapter, with full text versions found in Appendices B, C and D. These protocols should guide the user to apply virtual testing methods with HBMs in a harmonised way. They must be considered as a starting point and describe the procedures applied or drafted within the VIRTUAL project. After further refinement, these protocols could serve as a baseline for the design and application of virtual test protocols for consumer information organisations or legislation.

Before establishing such a virtual test procedure in consumer information testing or similar, further discussions with different stakeholders are needed to fine-tune the procedure and check feasibility of all steps.

The procedures described focus on methods used in the VIRTUAL project. However, in the development it was considered that the procedures should be as tool- and code independent as possible. Further work would be needed to finally implement the procedures in multiple codes and to derive guidelines on the same level as for the environments used in VIRTUAL.

The VIRTUAL cost-benefit analysis (CBA) tool for vehicle safety systems was developed by Wijnen et al. (2020). The tool converts the reduction of injuries through the safety system into the reduction of QALYs. The calculated QALYs incorporate disability weights, which account for the severity and the impact on the quality of life of the injury, as well as the duration of quality of life loss.

Inserting the injury risks derived from the application of each of the test protocols into the "injury probability" sheet of the CBA tool will lead to the calculation of "benefits" in the "CBA" sheet, which can be compared to the costs of introducing a specific safety measure when a baseline is available. However, it should be kept in mind that the presented test protocols are still on a somewhat experimental level and a meaningful application for CBA might still require further refinements.

3.1 Rear impact

The topic of seated occupants subject to rear end impact loading is closely linked to that of whiplash associated disorder (WAD). WAD represents an important type of injury in road traffic that, in spite of typically not being of high severity, has a considerable socio-economic impact (e.g. Kullgren et al. (2007)). Therefore, this subject was extensively researched during the past decades (for an overview, cf. Schmitt et al. (2019)). The injury mechanisms are complex and still not fully understood. Furthermore, females have a higher risk of sustaining WAD than males (Linder et al. 2012). Simulations using HBMs with detailed models of the cervical spine appear to be a very promising approach for future research on WAD.

In safety testing, HBM simulations of the rear end impact load case open new possibilities. While physical testing using dummies is costly and limited to very few load cases and anthropometries, HBM simulations offer the possibilities to test a higher diversity of loading conditions and anthropometries. This is particularly interesting in rear-end impact, given the observed gender differences in injury risk.

To date, neither European nor American authorities require homologation tests related to whiplash injuries. However, consumer organisations have performed systematic testing of vehicle seats in low speed rear end impact situations. Many of these tests are carried out according to the EuroNCAP (2021) rear end testing protocol, which to date is considered the "state of the art" of physical testing in this scenario.

(collision speed VRU and vehicle, collision angle and collision point) that are not avoided by the active safety system are combined with occurrence probabilities from the accident data analysis which results in a matrix of collision scenarios for the in-crash simulations with related occurrence probabilities.

With the help of a Design of Experiments (DoE) method, a certain number of collision scenarios for the in-crash simulation matrix is selected. By conducting in-crash simulations with HBMs and vehicle models, injury probabilities for different body regions of the selected collision scenarios can be determined. With the help of metamodels, the injury probability for collision scenarios which are not included in the in-crash simulations should be obtained. Based on the injury probability for all remaining scenarios that cannot be avoided by the active safety system, an overall injury probability can be calculated and used for a cost-benefit analysis.

3.2.1 Tasks for future research:

- Refinement / feasibility studies of validation of the vehicle model (geometry and stiffness)
- Injury Risk assessment for upper extremities
- Injury risk curves for tibia and pelvic fractures
- Implementation in other FE codes

3.3 Standing passenger

The safety of standing passengers in public transport is a relatively undeveloped area when compared to passenger car occupants or pedestrians struck by passenger cars. There are well developed experimental and numerical assessment tools that have been developed to predict injury in automotive applications such as those described in Sections 3.1 and 3.2. This does not imply that standing passenger safety has been ignored by manufacturers or government agencies, but it does not have the same level of regulations and standards as other aspects of traffic safety.

The VIRTUAL project has used the HBM development activities in the project to address public transport safety with state-of-the-art tools that use biomechanical information to assess safety. The HBMs developed in VIRTUAL, VIVA+, can assess injury for many body regions. The objective of the standing passenger activities in VIRTUAL was to adapt the capabilities of an existing HBM to include the standing passenger situation. As this case is analogous with the pedestrian activities described in Section 3.2, the pedestrian version of the VIVA+ was the basis for the standing passenger HBM, defined as VIVA+ Standing Passenger (VIVA+ SP).

The full development of the HBM technical specifications is detailed in Deliverable 2.5 and the motivation for loading conditions used in the test protocol is provided in Deliverable 5.2. These two documents describe:

- 1) Types of loading events (e.g. braking and acceleration) that describe the external loads causing and injury event inside a public transport vehicle
- 2) The types of injuries and objects struck that produce injuries inside a public transport vehicle
- 3) The biomechanical performance requirements that describe how a standing passenger reacts to vehicle motions and possibly lead to injuries
- 4) Validation data for a test device, in this case the VIVA+ SP, to a) present the motions of a standing passenger and b) provide biomechanical information that can assess injury risk
- 5) Recommended procedures that define the criteria for a) a model describing the interior of a vehicle, b) loading conditions (vehicle motions) relevant for injury assessment, c) positioning of a HBM relative to a structure under investigation, and d) injury assessment processing

Details of the test procedure are provided in APPENDIX C (CHAPTER **Error! Reference source not found.**).

The VIRTUAL project was able to define a first protocol that describes a loading condition relevant for standing passenger safety assessment. The literature indicated that head and chest impacts to vertical structures were important sources of injury to assess. Although the floor of the vehicle was the most frequent source of injuries, it was recognised in the project that a numerical model that could accurately describe a falling human, including all protective reflexes of the upper and lower extremities, was out of scope for the project. Thus, the protocol is based on the early parts of a non-collision event, where the passenger attempts to maintain balance during sudden, but low magnitude vehicle accelerations. A set of volunteer tests were used to gather validation data that can describe the reflexive and voluntary motions of a human when their support surface (floor) is quickly moved beneath their feet. This data provided the insight and quantitative data needed to develop a standing HBM.

The VIVA+SP was validated against male and female volunteer data, so that 50th percentile male and female standing passengers can be represented. For the worst case load condition (hard braking), the model is able to represent human response up until the time of the first compensatory step that occurs around 1.25 seconds for both male and female passengers. Initial falling directions can be investigated until 1.5 seconds, after which the model is not considered valid as it cannot currently reproduce the protective motions of the upper and lower limbs.

The test protocol specifies two main impact configurations of the passenger and the interior structures. The first case is a direct head impact on the structure and the second is a direct chest impact on the structure. The literature recommends that vertical handrails should be the primary structure of interest. Head and chest injuries can currently be predicted with the Head Injury Criterion (HIC) and the rib fracture risk. The latter is based on strains predicted in the ribs and is an important feature of HBMs that cannot be reproduced in other numerical formulations, such as rigid body formulations.

The current protocol is the first of its kind for public transport safety evaluations. It should be evaluated and developed further with international working groups to ensure the protocol leads to improved vehicle designs and safety. The use of finite element HBMs allows for future studies to expand injury prediction to low severity injuries (bruising, strains, minor fractures) that lead to short- and long-term disability or impairment. The possibility to use tissue level injury criteria and the ability to simulate a standing person are unique features of the VIVA+ SP.

4 Concept for the future evolution of the VIRTUAL contents and the OpenVT platform

The OpenVT platform is both a work bench for collaborative development and a dissemination vessel that makes the VIVA+ HBMs and other VIRTUAL results available to users all around the world (for more details, see Deliverable D 1.1 (Keller and Schmitt 2019)). Therefore, from the beginning, the OpenVT platform was designed as a temporary infrastructure to be used during the active project phase of VIRTUAL. Additionally, it is an actual result of VIRTUAL, on which the VIRTUAL contents will be brought to users, who can further improve and develop the contents in an open source approach.

The future survival of the OpenVT platform beyond the end of VIRTUAL is a crucial requirement for the overall success of the VIRTUAL project; therefore, a dedicated task has been planned within VIRTUAL's work package 1. Furthermore, the survival of the OpenVT platform is required for the survival and sustainable evolution of the hosted contents. In the following, the results of this task are presented.

4.1 Dimensions of the sustainability problem

Due to the fact that the OpenVT platform (as an infrastructure that could be applied to various contents) gets its value and life from the contents (most of all, the VIVA+ HBM family), while the contents require the platform as an infrastructure, the survival of both is inherently coupled. Therefore, a useful concept for the sustainable evolution of the VIRTUAL results must simultaneously address both sides of the problem.

Additionally, three separate problem levels can be identified related to the permanent availability of the OpenVT platform and the VIRTUAL contents. The most immediate level (subsequently referred to as "**server availability level**") is the actual physical availability of the server infrastructure. This includes expenses for hardware, software and energy, as well as costs for necessary server maintenance (e.g. software upgrades).

The next level beyond these technical issues is the user support and issue tracking that will be required for the system to be of true benefit to the users. Therefore, a person with expert knowledge would need to have appropriate availability to answer possible questions and to fix possible bugs. This problem level will be referred to as "**user support level**."

Apart from that, the long-term development of the models in a true open source sense will require coordination of updates, branches and merges. Consequently, a party has to be responsible for making decisions and guiding the further evolution in an efficient manner (referred to as "**continuous project development level**"). This problem level also addresses the question of who should own the copyright of the contents on OpenVT and, therefore, has the right to take legal action in case of licence violations.

4.2 Possible solution routes

As pointed out above, any useful solution has to attack the dependency issue and three problem levels. During the work on this task, several possible solutions have been evaluated:

- **A solution amongst VIRTUAL partners:** One or several consortium members take the responsibility for the future evolution of the project results.
- **Involving external companies or organisations:** The VIRTUAL results would be handed over to an external partner, e.g. an existing non-profit organisation.
- **Handing over to follow-up projects:** If there is a continuation of VIRTUAL in a future project, OpenVT could be used there and a similar organisational structure as already in use could be applied.
- **Creating an own legal entity for OpenVT and contents:** A legal entity would be the owner of OpenVT and (possibly) the copyrights of the contents. This could be a not-for-profit organisation as well as a company.

While the solution “handing over to follow-up projects” probably would solve most problems on all levels in the most straightforward way, it depends on the future availability of external project funding, which was not foreseeable during the duration of VIRTUAL. “Involving external companies or organisations” comes with the risk of giving up control of the VIRTUAL results and possibly losing the open source character. “A solution amongst VIRTUAL partners” comes with the advantage that the original developers of the VIRTUAL contents can still be involved, however, the organisational structures, e.g. of public research institutions, may not be ideal for handling intellectual property with short decision routes. The disadvantage of “creating an own legal entity” is that it must be designed wisely in order to protect it from possible “hostile take-overs” which could potentially corrupt the open character of the VIRTUAL contents in the future – while this approach probably allows most flexibility and short-handed decision routes for future challenges.

After evaluation of the different proposed solution routes, it was determined that the advantages of the “solution amongst VIRTUAL partners” and the “legal entity” approach could be combined by founding a non-profit organisation with a small number of natural persons as members, mainly the original developers of the VIRTUAL contents (employed by VIRTUAL partners). This legal entity can be the owner of the OpenVT platform and of the copyrights of OpenVT contents. If the membership requirements are rather restrictive, the risk of “hostile take-over” is minimised. With the lead of WP 1 being at the Switzerland-based AGU Zurich, it was decided to found an association according to Swiss civil code as a legal entity to represent the OpenVT platform and its contents in the future: OVTO, the OpenVT organisation.

4.3 OVTO: The OpenVT Organisation.

The OpenVT organisation was founded on October 25, 2021, as an association according to art. 60ff of the Swiss civil code and is based in Zürich, Switzerland. Such an association becomes a legal entity as soon as the written articles of the association ‘indicate the objects of the association, its resources and its organisation’. Furthermore, the association has been registered in the commercial register of the state of Zürich. The articles of the association can be found in Appendix E.

4.3.1 Purposes and objectives of OVTO

The purposes of OVTO are mainly to own and maintain the OpenVT platform, to oversee the future evolution of the VIVA+ HBM family and other tools and models resulting from VIRTUAL, to provide user support and, as legal entity, to own the copyright of these open contents. As copyright owner, OVTO can make decisions about future changes in the licence policy of any of these open source contents and would be the legal entity that could possibly take legal action in case of licence violations.

When the articles of OVTO were written, these purposes were condensed into the “objectives of the association”, where a somewhat more general formulation was chosen to widen the future field of action to support biomechanical research in general:

- *Run and own The OpenVT platform and the associated domain openvt.eu.*
- *Provide OpenVT as an open platform for virtual testing (VT) in road safety and injury biomechanics in general.*
- *Own the copyrights of open source projects related to VT and biomechanics.*
- *Host open source projects related to VT and biomechanics on The OpenVT platform, maintain them and ensure the sustainable evolution in the future, provide user support.*
- *Promote and support research related to virtual testing and computer modelling in biomechanics and traffic safety.*

All three problem levels and the dependency issue are covered by the objectives. These objectives can only be changed with the consent of all OVTO members in the future.

4.3.2 Organisational structure

Authorities of OVTO are the General Meeting of members (GM), the Committee and the Auditor. Furthermore, there can be a Subcommittee for each of the open source projects hosted on the OpenVT platform.

The GM is the highest authority of OVTO. It elects the Committee and oversees its actions, decides on open source projects hosted on the OpenVT platform and approves or rejects membership applications. The GM convenes for an annual regular assembly and, at the request of the Committee, for extraordinary assemblies. At the assemblies, all members have equal voting rights.

The Committee is responsible for the daily business of OVTO. It consists of the President, the Vice President, the Secretary and the Treasurer. During the founder’s meeting on October 25, 2021 (which at the same time was the first GM assembly), the GM elected the following Committee: Arne Keller (President), Mats Svensson (Vice President), Corina Klug (Secretary), Markus Muser (Treasurer).

As Auditor, the GM can decide to hire a person external of the association.

Subcommittees represent the developers of the open source projects within OVTO. Their members (natural persons) are appointed by the Committee on nomination of the group of active developers. The subcommittees report to the GM; however, the GM only has an indirect influence on their activities in the sense that the GM can decide to end hosting the corresponding open source project (which also terminates the Subcommittee). This structure has been implemented in order to grant the project developers a high degree of freedom of self-administration and to facilitate providing adequate user support.

Only natural persons can become members of OVTO. Currently, there are 15 members. The articles limit the relative number of members affiliated with the same organisation or company. The GM has decided on strict membership criteria, only allowing proven experts in the scientific field and/or active contributors to OpenVT as members. Furthermore, by decision of the GM, the total number of members is limited to 25. Currently, there is no membership fee, but each member must report their contribution to the contents of OpenVT annually. This rather strict membership policy has been implemented to keep OVTO independent, fast and operative in the future and to prevent “hostile takeovers,” where the decisions of the associations could be majorly influenced by one single company or institution.

4.3.3 Future funding of OVTO

OVTO’s daily business will cause expenses on all three problem levels. To cover these, it is planned to explore several routes of funding:

- **Sponsoring and donations:** companies as well as interested individuals are invited to either donate to OVTO or to become sponsors (i.e., agreeing to pay an annual sponsoring fee). According to the amount donated or sponsored, adequate visibility, e.g. on the OVTO website, will be granted. Sponsors, furthermore, may participate in the GM assembly in an advisory role.
- **Conference and workshop fees:** if the user workshops for the VIVA+ models and the OpenVT platform turn into regular events, the participants could be asked for a participation fee.
- **Fees for user support:** in keeping with the open source character, the actual contents on the OpenVT platform are available free of charge. However, it is possible to charge future users of the VIRTUAL models for support services. The registration of OVTO in the commercial register is the first step to being able to offer these fee-based services.
- **In-kind project or institutional funding:** the VIVA+ models and other OpenVT content are mainly used by active researchers at public or private research institutions (which might even be members of OVTO in the future). If as part of their work they develop the VIVA+ models further and these developments are re-submitted to the OpenVT platform, the future evolution of the OVTO-owned models indirectly benefits from their research funding. Similarly, some research institutions or companies might allow their employees to devote a part of their work time to the development of the VIVA+ models. This is how most major open source projects are developed.

4.4 Outlook and tasks to address in the future

Currently, the transition process from VIRTUAL to OVTO is under way. This includes handing over the OpenVT platform as well as the copyrights of as many OpenVT contents as possible. Furthermore, a website on the domain ovto.org will be active presently.

As next steps, OVTO will be promoted at several events and conferences in order to acquire sponsors and donations. Nevertheless, providing consistent funding for an adequate budget for the planned activities remains a challenge in the future.

Other open issues include organising user support and exploiting the “indirect project or institutional funding” route further. These issues will be addressed during and after the transition period from VIRTUAL to OVTO.

5 Conclusion

In this document, three main results of VIRTUAL's work package 1 are presented. These include the injury assessment framework and test protocols for virtual testing of three generic load cases. Furthermore, the OpenVT organisation OVTO is described, which will serve to ensure the sustainable evolution of the OpenVT platform and of other VIRTUAL project results.

The core part of the injury assessment framework is a complete injury criteria manual for the VIVA+ HBMs, specifying the criteria that can already be evaluated with the HBMs and giving instructions on how to evaluate them. The list includes established injury criteria, which were developed for use with ATDs or corresponding simulation models, as well as novel tissue-based criteria. The latter allow extensive application of finite element modelling and are expected to provide more detailed injury risk assessments in the future. Further research is, however, required to establish a solid data basis for risk curves and protection thresholds. With this combination of novel and established injury criteria, the manual lays the foundation for the injury assessment procedures described in the test protocols. Furthermore, the manual also contains criteria which are established today (i.e., described in the literature and/or commonly used in physical tests for regulatory or consumer testing), but are currently not implemented for the use with the VIVA+ HBMs – a task which should be addressed by future research.

The three presented test protocols for virtual testing cover the load cases "seated vehicle occupants in rear impact", "standing passengers in busses and trams" and "vulnerable road users." Each test protocol provides a generic example outlining how to apply VIVA+ models to test products such as vehicle seats, vehicle interior or vehicle fronts to assess their protection potential. These test protocols are intended as prototypes of virtual test protocols and are not immediately applicable in consumer or regulatory testing. Within this project, corresponding virtual tests have been carried out successfully, hence, more complete future test protocols may be designed using the protocols presented here as guidelines. This represents an important step towards virtual testing in consumer and regulatory tests of vehicle components.

Finally, we address the question of how the VIRTUAL project results will be kept available, maintained and evolving in the future. This was analysed on different levels, ranging from the availability of resources for the OpenVT platform to the scientific expertise for future improvements of the VIVA+ HBM family. The OpenVT platform and the open source contents developed in VIRTUAL are dependent on one another, so their survival is a coupled problem. After evaluation of different solution routes, it was decided to found the OpenVT organisation (OVTO) as an association according to Swiss law to govern and maintain the project. To date, OVTO has 15 members (scientific experts and developers active on OpenVT). As a legal entity, OVTO will own and manage the OpenVT platform in the future and will oversee the development of the open source contents developed within project VIRTUAL.

Together, these project results provide a solid basis for the future evolution and exploitation of the VIVA+ HBM family and other VIRTUAL results and, furthermore, will allow these open source contents to further evolve into useful tools to help ensure the safety of all road users.

References

- Barrow, A., Edwards, A., Smith, L., Khatry, R., Kalaiyarasan, A., and Hynd, D. *Effectiveness estimates for proposed amendments to the EU's General and Pedestrian Safety Regulations*. Wokingham, Berkshire, United Kingdom: TRL, 2018.
- Bartsch H.-J., Sachs M. *Taschenbuch mathematischer Formeln für Ingenieure und Naturwissenschaftler*. München: Hanser, 2014.
- Bose, Dipan, Kavi S. Bhalla, Costin D. Untaroiu, B. Johan Ivarsson, Jeff R. Crandall, and Shepard Hurwitz. «Injury tolerance and moment response of the knee joint to combined valgus bending and shear loading.» *Journal of biomechanical engineering* (American Society of Mechanical Engineers Digital Collection) 130 (2008).
- Boström, O., Y. Håland, L. Lövsund, and M. Y. Svenssom. «Neck injury criterion (NIC) and its relevance to various possible neck injury mechanisms.» *Eds. Yoganandan, N; Pintar, FA: Frontiers in Whiplash Trauma. IOS Press, The Netherlands*, 2000.
- Boström, Ola, et al. «A new neck injury criterion candidate-based on injury findings in the cervical spinal ganglia after experimental neck extension trauma.» *Proceedings of The 1996 International Ircobi Conference On The Biomechanics Of Impact, September 11-13, Dublin, Ireland*. 1996. 123-136.
- Cho, Jin-Rae, Seung-Bum Park, Sung-Hyun Ryu, Sung-Ho Kim, and Shi-Bok Lee. «Landing impact analysis of sports shoes using 3-D coupled foot-shoe finite element model.» *Journal of mechanical science and technology* (Springer) 23 (2009): 2583–2591.
- Duvenaud, David. «The Kernel cookbook: Advice on covariance functions.» URL <https://www.cs.toronto.edu/~duvenaud/cookbook>, 2014.
- Edwards, Mervyn, Alix Edwards, Josh Appleby, and Dean Beaumont. «Banging heads onboard buses: assessment scheme to improve injury mitigation for bus passengers.» *Traffic injury prevention* (Taylor & Francis) 20 (2019): S71–S77.
- Eichberger, Arno, Mario Darok, Hermann Steffan, Peter E. Leinzinger, Ola Boström, and Mats Y. Svensson. «Pressure measurements in the spinal canal of post-mortem human subjects during rear-end impact and correlation of results to the neck injury criterion.» *Accident Analysis & Prevention* (Elsevier) 32 (2000): 251–260.
- Eriksson, Linda, and Anders Kullgren. «Influence of seat geometry and seating posture on NICmax long-term AIS 1 neck injury predictability.» *Traffic injury prevention* (Taylor & Francis) 7 (2006): 61-69.
- EuroNCAP. «Pedestrian Human Model Certification. TB 024.» <https://cdn.euroncap.com/media/56949/tb-024-pedestrian-human-model-certification-v20.pdf>, 2019a.
- EuroNCAP. «Pedestrian testing protocol.» <https://cdn.euroncap.com/media/41769/euro-ncap-pedestrian-testing-protocol-v85.201811091256001913.pdf>, 2019b.
- EuroNCAP. «The Dynamic Assessment of Car Seats for Neck Injury: Protection Testing Protocol Version 4.1.1.» 2021.
- Gabler, Lee F., Jeff R. Crandall, and Matthew B. Panzer. «Development of a second-order system for rapid estimation of maximum brain strain.» *Annals of biomedical engineering* (Springer) 47 (2019): 1971-1981.
- Gruber, Michael, et al. «The effect of P-AEB system parameters on the effectiveness for real world pedestrian accidents.» *Proceedings of the 26th ESV Conference Proceedings*. 2019.
- Hainisch, T. *Erstellung von FE Fahrradmodellen zum Abbilden unterschiedlicher Rahmen-Geometrien und -Größen für Crashesimulationen*. Bachelorarbeit, Graz: TU Graz, Institut für Fahrzeugsicherheit., 2015.

- Hertz, Ellen. «A note on the head injury criterion (HIC) as a predictor of the risk of skull fracture.» *Proceedings: Association for the Advancement of automotive medicine annual conference*. 1993. 303-312.
- John, J ., et al. «Validated seated OS-HBM models published on the OpenVT platform and described in scientific papers.» *Deliverable D2.2 of the H2020 project VIRTUAL*. 2021.
- Joseph, V. Roshan, Evren Gul, and Shan Ba. «Designing computer experiments with multiple types of factors: The MaxPro approach.» *Journal of Quality Technology* (Taylor & Francis) 52 (2020): 343–354.
- Keller, A., and K. U. Schmitt. «The OpenVT platform: A collaboration and dissemination platform for open access virtual testing.» *Deliverable D1.1 of the H2020 project VIRTUAL*. 2019.
- Kleinberger, Michael, Emily Sun, Rolf Eppinger, Shashi Kuppa, and Roger Saul. «Development of improved injury criteria for the assessment of advanced automotive restraint systems.» *NHTSA Docket 4405* (1998).
- Klug, C., P Luttenberger, M Schachner, J Micorek, R Greimel, and W Sinz. «Postprocessing of Human Body Model Results – Introduction of the Open Source Tool DYNASAUR.» *7th International Symposium: Human Modeling and Simulation in Automo*. 2018.
- Kroell, Charles K., Dennis C. Schneider, and Alan M. Nahum. «Impact tolerance and response of the human thorax II.» *SAE Transactions* (JSTOR), 1974: 3724-3762.
- Kullgren, Anders. «Dose-response models and EDR data for assessment of injury risk and effectiveness of safety systems.» *IRCOBI Conference, Bern, Switzerland*. 2008. 3-14.
- Kullgren, Anders, Linda Eriksson, Ola Boström, and Maria Krafft. «Validation of neck injury criteria using reconstructed real-life rear-end crashes with recorded crash pulses.» *Proc. 18th ESV Conf*. 2003. 1-13.
- Kullgren, Anders, Maria Krafft, Anders Lie, and Claes Tingvall. «The effect of whiplash protection systems in real-life crashes and their correlation to consumer crash test programmes.» *Proc. 20th ESV Conf.(07-0468), Lyon (France)*. 2007. 1–7.
- Larsson, Karl-Johan, Amanda Blennow, Johan Iraeus, Bengt Pipkorn, and Nils Lubbe. «Rib cortical bone fracture risk as a function of age and rib strain: updated injury prediction using finite element human body models.» *Frontiers in bioengineering and biotechnology* (Frontiers) 9 (2021): 412.
- Linder, Astrid, et al. «Test specifications for VT of erect passengers on public transport.» *Milestone Report M5.3 of the H2020 project VIRTUAL*. Gothenburg, Sweden, 2020.
- Linder, Astrid, Stefan Olsén, Jenny Eriksson, Mats Y. Svensson, and Anna Carlsson. «Influence of gender, height, weight, age, seated position and collision site related to neck pain symptoms in rear end impacts.» *Proceedings: IRCOBI Conference*. 2012. 12–14.
- McLundie, W. M. «Investigation of Two-Wheeled Road Traffic Accidents using Explicit FE Techniques.» (Cranfield University) 2007.
- Nahum, Allan., Charles W. Gadd, Dennis C. Schneider, and Charles K. Kroell. «The biomechanical basis for chest impact protection: I. Force-deflection characteristics of the thorax.» *Journal of Trauma and Acute Care Surgery* (LWW) 11 (1971): 874-882.
- Nusia, Jiota, Jia Cheng Xu, Reimert Sjöblom, Johan Knälmann, Astrid Linder, and Svein Kleiven. «Injury risk functions for the four primary knee ligaments.» *Under Review (Journal of the Mechanical Behavior of Biomedical Material)*, 2022.
- Örtengren, Tore, H.-A. Hansson, Per Lövsund, Mats Y. Svensson, A. Suneson, and Annette Säljö. «Membrane leakage in spinal ganglion nerve cells induced by experimental whiplash extension motion: a study in pigs.» *Journal of neurotrauma* 13 (1996): 171–180.
- Panjabi, M. M., J. L. Wang, and N. Delson. «Neck injury criterion based on intervertebral motions and its evaluation using an instrumented neck dummy.» *Proceedings of the International Research Council on the Biomechanics of Injury conference*. 1999. 179-190.
- Park, Jangwoon, Sheila M. Ebert, Matthew P. Reed, and Jason J. Hallman. «Statistical models for predicting automobile driving postures for men and women including effects of age.» *Human factors* (SAGE Publications Sage CA: Los Angeles, CA) 58 (2016): 261–278.

- Pedregosa, Fabian, et al. «Scikit-learn: Machine learning in Python.» *the Journal of machine Learning research* (JMLR. org) 12 (2011): 2825–2830.
- Prasad, Priya, and Roger P. Daniel. «A biomechanical analysis of head, neck, and torso injuries to child surrogates due to sudden torso acceleration.» *SAE transactions* (JSTOR), 1984: 784-799.
- Sahoo, D., C. Deck, and R. Willinger. «Brain injury tolerance limit based on computation of axonal strain.» *Journal of Accident Analysis & Prevention*, 2016: Vol 92, 53-70.
- Schachner, M, J Micorek, P Luttenberger, and R Greimel. *Dynasaur*. 2018. <https://gitlab.com/VSI-TUGraz/Dynasaur>.
- Schachner, Martin, Wolfgang Sinz, Robert Thomson, and Corina Klug. «Development and evaluation of potential accident scenarios involving pedestrians and AEB-equipped vehicles to demonstrate the efficiency of an enhanced open-source simulation framework.» *Accident Analysis & Prevention* (Elsevier) 148 (2020): 105831.
- Schmitt, K.-U., Markus H. Muser, and P. Niederer. «A new neck injury criterion candidate for rear-end collisions taking into account shear forces and bending moments.» Tech. rep., SAE Technical Paper, 2001.
- Schmitt, Kai-Uwe, Markus H. Muser, Felix H. Walz, and Peter F. Niederer. «N km--a proposal for a neck protection criterion for low-speed rear-end impacts.» *Traffic injury prevention* (Taylor & Francis) 3 (2002): 117-126.
- Schmitt, Kai-Uwe, Peter F. Niederer, Duane S. Cronin, Barclay Morrison III, Markus H. Muser, and Felix Walz. *Trauma biomechanics: an introduction to injury biomechanics*. Springer, 2019.
- Schubert, Alexander, Nico Erlinger, Christoph Leo, Johan Iraeus, Jobin John, and Corina Klug. «Development of a 50th Percentile Female Femur Model.» *International Research Council on the Biomechanics of Injury 2021*. 2021. 308–332.
- Silvano, Ary P., and Maria Ohlin. «Non-collision incidents on buses due to acceleration and braking manoeuvres leading to falling events among standing passengers.» *Journal of Transport & Health* (Elsevier) 14 (2019): 100560.
- Snedeker, Jess G., Markus H. Muser, and Felix H. Walz. «Assessment of pelvis and upper leg injury risk in car-pedestrian collisions: comparison of accident statistics, impactor tests and a human body finite element model.» Tech. rep., SAE Technical Paper, 2003.
- Thomson, Robert, and Matej Kranjec. «Test case simulations for erect passengers on public transport to be used for validation including instructions/documentation.» *Milestone M 5.4 of the H2020 project VIRTUAL*. 2021.
- Thomson, Robert, Matej Kranjec and Luis Martinez. «Validated erect transit passenger model on OpenVT platform and documented in scientific publications.» *Deliverable D2.5. of the H2020 project VIRTUAL*. 2021.
- TRL, CEESAR, ACEA. «General Safety Regulation: accident analysis assesses effectiveness of proposed safety measures.» <https://www.acea.auto/publication/general-safety-regulation-accident-analysis-assesses-effectiveness-of-proposed-safety-measures/>, 2018.
- Viano, David C., and Ian V. Lau. «Thoracic impact: a viscous tolerance criterion.» Tech. rep., SAE Technical Paper, 1985.
- Wijnen, W., Elvik, R., Bützer, D. «Preliminary cost-benefit calculation tool for vehicle safety systems.» *Milestone 6.3 of the H2020 project VIRTUAL*. 2020.
- Williams, Christopher K. I., and Carl Edward Rasmussen. *Gaussian processes for machine learning*. Bd. 2. MIT press Cambridge, MA, 2006.
- Wu, Ge, et al. «ISB recommendation on definitions of joint coordinate system of various joints for the reporting of human joint motion—part I: ankle, hip, and spine.» *Journal of biomechanics* (Elsevier) 35 (2002): 543–548.
- Wu, Ge, et al. «ISB recommendation on definitions of joint coordinate systems of various joints for the reporting of human joint motion—Part II: shoulder, elbow, wrist and hand.» *Journal of biomechanics* (Elsevier) 38 (2005): 981–992.
- Wu, Ge, and Peter R. Cavanagh. «ISB recommendations in the reporting for standardization of kinematic data.» *J. Biomech* 28 (1995): 1257–1261.

Xu, J-C., et al. «Description of safe operation envelope for erect passengers on public transport.»
Deliverable D 5.2 of the H2020 project VIRTUAL. 2022.

Yamada, Hiroshi. *Strength of biological materials*. Baltimore - Md: Williams and Wilkins, 1970.

Yao, Hua-Dong, Mats Y. Svensson, and Håkan Nilsson. «Transient pressure changes in the vertebral canal during whiplash motion--A hydrodynamic modeling approach.» *Journal of biomechanics* (Elsevier) 49 (2016): 416-422.

6 Appendix A – Injury criteria manual

6.1 Non-HBM based criteria: overview ordered by body region

6.1.1 Head

Head injury criterion (HIC)

- **Input quantities:** Acceleration time history of the centre of gravity of the head. A node must be defined in the model to represent the CoG.
- **Definition:**

$$HIC = \max \left[\frac{1}{t_2 - t_1} \int_{t_1}^{t_2} a(t) dt \right]^{2.5} (t_2 - t_1),$$

where $a(t)$ is the resulting CoG acceleration as a function of the time and t_1, t_2 are any arbitrary points in time during the acceleration pulse. For HIC36, $t_2 - t_1$ must be ≤ 36 ms, likewise for HIC15 a limit of 15 ms applies.

- **Application in regulatory tests:** FMVSS 208, UN R94/R95 (as Head Protection Criterion HPC)
- **Implementation:** Dynasaur commands HIC15, HIC36

- | |
|---|
| <ul style="list-style-type: none">• HIC15(a_res, t)• HIC36(a_res, t) |
|---|

- **ID channel in VIVA+ model:** Head_COG, id: [8390000]
- **Injury risk curve:** According to Mertz (1993), the probability of a skull fracture relates to the natural logarithm of HIC with a cumulative normal distribution with mean 6.96352 and standard deviation 0.84664 (values valid for a 50-percentile male).
- **Protection limit(s):** Different values depending on test procedure and load case, ranging from 700 to 2500
- **Load case:** Frontal impact, pedestrian head impactor tests, helmet tests etc.
- **Literature, validation data:** very well-documented in the biomechanics literature, cf. Schmitt et al (2019).
- **Comment:** widely used in many test procedures. Based on rigid-body dynamics, i.e. application in HBMs is limited. Possible for VIVA+ (rigid head)

DAMAGE criterion

- **Input quantities:** Rotational time history of the centre of gravity of the head. A node must be defined in the model to represent the CoG with outputs in a local coordinate system.
- **Definition:** See Gabler et al. (2019)
- **Application in regulatory test:** n/a
- **Implementation in Dynasaur:** Dynasaur command DAMAGE

- | |
|---|
| <ul style="list-style-type: none">• DAMAGE_MPS• DAMAGE_AIS1• DAMAGE_AIS2• DAMAGE_AIS4+ |
|---|

- **ID channel in VIVA+ model:** Head-CoG-Seatbelt-Accelerometer, id: [1090000]
- **Injury risk curve:** According to Gabler et al. (2019)
- **Protection limit(s):**n/a
- **Applied filtering:** n/a
- **Literature, validation data:** Gabler, Crandall & Panzer (2019)
- **Comment:** not widely used. Based on rigid-body dynamics, i.e. application in HBMs is limited. Possible for VIVA+ (rigid head).

6.1.2 Spine

Neck Injury Criterion NIC

- **Input quantities:** anterior-posterior (x) components of the acceleration and velocity of head COG relative to the T1 vertebra.
- **Definition:**

$$NIC = l \cdot a_{rel}(t) + v_{rel}^2(t),$$

where a_{rel} is the relative x acceleration, v_{rel} is the the relative x velocity and l is a length parameter set at 0.2 m. Thus, the dimension of NIC is $\frac{m^2}{s^2}$.

- **Application in regulatory tests:** n/a., but used in consumer tests
- **Implementation:** Dynasaur command NIC:

- NIC_curve(a_T1, a_head, time)
- NIC_risk(a_T1, a_head, time)
- NIC_max(a_T1, a_head, time)

- **ID channel in VIVA+ model:** Node T1_center, id: [8382015],
- **Injury risk curve:** Kullgren et al. (2003), Eriksson and Kullgren (2006), Kullgren (2008), Ono et al. (2009)
- **Protection limit:** suggested: for the average male 15 m²/s²
- **Load case:** low speed rear/frontal impact
- **Literature, validation data:** Boström et al. (1996), Boström et al. (2000)
- **Comment:** In ATDs, the accelerations and velocities are measured by accelerometers; the x component thus corresponds to the anterior-posterior axis of the head and T1 accelerometer with a_{rel} representing the difference of the two x acceleration components. This may cause problems when the head rotates strongly before it touches the head restraint, or if head / T1 are not aligned or if the frankfort plane is not parallel to the x-y-plane at the beginning. In HBMs, it is suggested to measure the head and T1 accelerations in a global coordinate system, project the results into a local T1 coordinate system (the x axis of which is oriented in anterior-posterior direction) and to consider a_{rel} as the difference of the x components of the two accelerations (same for the velocities). The evaluation of NIC in a sleeping position, for example, is still objectionable.

Neck Injury Criterion Nij

- **Input quantities:** Axial force, sagittal bending moment
- **Definition:**

$$N_{ij} = \frac{F_z}{F_{int}} + \frac{M_y}{M_{int}},$$

where F_z and M_y represent the axial force and sagittal bending moment, respectively, and the denominator values are the respective critical intercept values. The latter are defined for various dummy types, sizes and for extension/flexion. These values need to be adapted for use in HBMs.

- **Application in regulatory tests:** FMVSS 208
- **Implementation:** Dynasaur function nij:

- nij(force_x, force_z, moment_y, distance_occipital_condyle, nij_fzc_te, nij_fzc_co, nij_myc_fl, nij_myc_ex)

- **ID channel in VIVA+ model:** Not yet implemented
- **Injury risk curve:** Kleinberger et al. (1998)
- **Protection limit:** 1.0 (FMVSS), 0.2 (0.16) for AIS 1 injuries of long (short) duration. These values, however, depend on the critical intercepts.
- **Load case:** frontal impact
- **Literature, validation data:** Prasad & Daniel (1984), Kleinberger et al. (1998).
- **Comment:** criterion based on the assumption that all forces and moments pass through / act on the occipital condyles. In HBMs, this is not the case. New evaluation methods (e.g. cross-sectional analysis) must be found to apply this criterion to HBMs.

Neck Protection Criterion Nkm

- **Input quantities:** Shear force, flexion/extension bending moment, both measured at the upper neck load cell.
- **Definition:**

$$N_{km}(t) = \frac{F_x(t)}{F_{int}} + \frac{M_y(t)}{M_{int}},$$

where F_x and M_y are the shear force and axial bending moment, respectively, and the denominator values are the respective critical intercept values.

- **Application in regulatory tests:** none, but used in several consumer tests
- **Injury risk curve:** Kullgren et al. (2003), Kullgren (2008)
- **Protection limit:** 1.0 (depends on critical intercepts)
- **Implementation:** see Nij
- **ID channel in VIVA+ model:** Not yet implemented
- **Load case:** low speed rear/frontal impact
- **Literature, validation data:** Schmitt et al. (2001), Schmitt et al. (2002).
- **Comment:** criterion based on the assumption that all forces and moments pass through / act on the occipital condyles. In HBMs, this is not the case. New evaluation methods (e.g. cross-sectional analysis) must be found to apply this criterion to HBMs.

Inter-Vertebral Neck Injury Criterion IV-NIC / IV-NIC(R) / IV-NIC_{rot}

- **Input quantities:** Intervertebral motion of intervertebral joint i .
- **Definition:**

$$IV - NIC_i = \frac{\theta_{trauma,i}}{\theta_{physio,i}},$$

where $\theta_{trauma,i}$ and $\theta_{physio,i}$ are the angular range of motion causing injury and the physiological motion range, respectively.

- **Application in regulatory tests:** n.a.
- **Implementation:** Dynasaur function IV-NIC:

- IV_NIC(r_displacement, limit, flexion_tension="")

- **ID channel in VIVA+ model:** can be applied to all nodes on vertebrae, see landmark table.
- **Injury risk curve:** n/a.
- **Protection limit:** n/a.
- **Load case:** low speed rear impact
- **Literature, validation data:** Panjabi et al. (1999)
- **Comment:** Rarely used since these parameters are difficult to measure / not validated in an ATD. Other authors have employed a similar principle to analyse shear / compression motion. For clarity, the IV-NIC based on rotation is called IV-NIC(R). Used mainly in PMTO tests, but applicable for HBMs as long as vertebrae are not deformed or rigid bodies.

Upper neck loads

- **Input quantities:** Forces and moments measured at the upper neck load cell.
- **Definition:** Direct interpretation of forces and moments in place of calculated criteria such as Nkm or Nij
- **Application in regulatory tests:** n/a
- **Implementation:** No Dynasaur implementation needed
- **ID channel in VIVA+ model:** Not yet implemented
- **Injury risk curve:** n/a
- **Protection limit:** depends on load case and parameter
- **Load case:** rear/frontal impact
- **Literature, validation data:** Various.
- **Comment:** criterion based on the assumption that all forces and moments pass through / act on the occipital condyles. In HBMs, this is not the case. New evaluation methods (e.g. cross-sectional analysis) must be found to apply this criterion to HBMs. Use for comparison with strain-based criteria.

6.1.3 Thorax

Viscous Criterion VC

- **Input quantities:** chest deflection rate, compression
- **Definition:**

$$VC(t) = \frac{d}{dt} D(t) * \frac{D(t)}{b},$$

with D and d analogous to the compression criterion (see below).

- **Application in regulatory tests:** UN R94, UN R95, SAE J1727
- **Implementation:** Dynasaur function VC:

- VC(Scaling_factor, deformation_constant, y, time)

- **ID channel in VIVA+ model:** not implemented
- **Injury risk curve/protection limit:** cf Viano and Lau (1985) / 1.0
- **Load case:** frontal impact, side impact
- **Literature, validation data:** Viano and Lau (1985)
- **Comment:** depends on the viscous properties of the thorax / thorax model. Difficult to transfer between ATD and HBM.

Compression Criterion C

- **Input quantities:** Chest deflection, thorax thickness
- **Definition:**

$$C = \frac{D}{b},$$

where D is the chest deflection and b the initial thorax depth

- **Application in regulatory tests:**

- **Implementation:** Not implemented.
- **Injury risk curve/protection limit:**

$$AIS = -3.78 + 19.56 C$$
- **Load case:** frontal impact
- **Literature, validation data:** Nahum et al. (1971), Kroell et al. (1974)
- **Comment:** outdated for HBMs

Chest deflection

- **Definition:** Maximum chest deflection
- **Application in regulatory tests:** FMVSS 208
- **Implementation:** cf. VC criterion
- **Load case:** frontal impact
- **Literature, validation data:** various.
- **Comment:** outdated for HBMs. Use tissue-based criteria instead.

Peak spinal acceleration

- **Input data:** cfc1000 filtered T12 resultant acceleration as function of time
- **Definition:** 3ms peak spinal resultant acceleration at T12.
- **Application in regulatory tests:** FMVSS 208
- **Implementation:** Dynasaur function A3MS:

- | |
|--|
| <ul style="list-style-type: none"> • A3ms(a_res, t) |
|--|

- **ID channel in VIVA+ model:** T12_center, id: [8382125]
- **Injury risk curve/protection limit:** n/a
- **Load case:** frontal impact
- **Literature, validation data:** n/a
- **Comment:** outdated for HBMs.

Rib Deflection Criterion RDC

- **Definition:** Rib deflection in mm as measured in side impact dummy EUROSID
- **Application in regulatory tests:** UN R95
- **Injury risk curve/protection limit:** RDC < 42mm
- **Implementation:** No Dynasaur implementation needed
- **ID channel in VIVA+ model:** not implemented
- **Load case:** side impact
- **Literature, validation data:** n/a
- **Comment:** depends heavily on the spring-damper assembly of the EuroSID. Probably not useful for HBMs.

Thoracic Compression Criterion ThCC

- **Definition:** Absolute value of the compression of the thorax in mm
- **Application in regulatory tests:** UN R94
- **Implementation:** No Dynasaur implementation needed
- **ID channel in VIVA+ model:** not yet implemented
- **Injury risk curve/protection limit:** ThCC < 50 mm
- **Load case:** frontal impact
- **Literature, validation data:** n/a
- **Comment:** simple criterion, questionable for HBMs

6.1.4 Lower extremities

Tibia Index TI

- **Input quantities:** Bending moment and axial force in tibia
- **Definition:**

$$TI = \frac{M}{M_{crit}} + \frac{F}{F_{crit}},$$

where M, F are the bending moment and the axial force, respectively. The denominator values are the corresponding critical intercept values, $M_{crit} = 225$ Nm and $F_{crit} = 35.9$ kN (values for the 50th percentile male according to Yamada (1970)).

- **Application in regulatory tests:** UN R94
- **Implementation:** Dynasaur function tibia-index:

- `tibia_index(Mx, My, Fz, critical_bending_moment, critical_compression_force)`

- **ID channel in VIVA+ model:** not implemented
- **Injury risk curve/protection limit:** $TI < 1.3$ at the top and bottom of each tibia, with a maximum compression force of 8 kN.
- **Load case:** frontal impact
- **Literature, validation data:** Yamada (1970)
- **Comment:** needs intersect values for different sizes of HBMs. Criterion based on the assumption that all forces and moments pass through / act on a cross-section in the centre of the tibia. In HBMs, this is not the case. New evaluation methods (e.g. cross-sectional analysis) must be found to apply this criterion to HBMs. Use for comparison with strain-based criteria.

Femur Force Criterion FFC

- **Definition:** compression force transmitted axially on each femur of a dummy as a function of time
- **Application in regulatory tests:** UN R94
- **Injury risk curve/protection limit:** $FFC < 9.07$ kN @ $t = 0$, FFC not exceeding 7.58 kN for more than 10 ms.
- **Load case:** frontal impact
- **Literature, validation data:** n/a
- **Implementation:** No Dynasaur implementation needed
- **ID channel in VIVA+ model:** not implemented
- **Comment:** Criterion based on the assumption that all forces pass through a cross-section in the centre of the femur. In HBMs, this is not the case. New evaluation methods (e.g. cross-sectional analysis) must be found to apply this criterion to HBMs. Use for comparison with strain-based criteria.

Femur bending moment

Tibia Compression Force Criterion TCFC

- **Definition:** Compression force transmitted axially through the tibiae of test dummy
- **Application in regulatory tests:** UN R94
- **Injury risk curve/protection limit:** $TCFC < 8$ kN
- **Load case:** frontal impact
- **Literature, validation data:** n/a
- **Implementation:** Not yet implemented
- **ID channel in VIVA+ model:** Not implemented
- **Comment:** Criterion based on the assumption that all forces pass through a cross-section in the centre of the tibia. In HBMs, this is not the case. New evaluation methods (e.g. cross-sectional analysis) must be found to apply this criterion to HBMs. Use for comparison with strain-based criteria.

Maximum tibia displacement

- **Definition:** Maximum displacement of the tibia with respect to the femur as measured in dummy filtered with CFC 180
- **Application in regulatory tests:** UN R94
- **Injury risk curve/protection limit:** displacement < 15mm as protection criterion for the knee ligaments.
- **Implementation:** Not yet implemented
- **ID channel in VIVA+ model:** Not yet implemented
- **Load case:** frontal impact
- **Literature, validation data:** n/a
- **Comment:** actual displacement depends on the mechanical properties of the (ATD) knee. May be used in HBMs, but different values / protection limits will apply.

Pubic Symphysis Peak Force PSPF

- **Definition:** Maximum force measured by a load cell at the pubic symphysis of the pelvis, filtered at channel frequency class 600 Hz
- **Application in regulatory tests:** UN R95
- **Implementation:** Not yet implemented
- **ID channel in VIVA+ model:** Not yet implemented
- **Injury risk curve/protection limit:** PSPF < 6 kN as protection criterion for pelvis
- **Load case:** side impact
- **Literature, validation data:** n/a
- **Comment:** Criterion based on the assumption that a given fraction of all forces pass through a cross-section in the pubic symphysis. In HBMs, this is not the case. New evaluation methods (e.g. cross-sectional analysis) must be found to apply this criterion to HBMs. Use for comparison with strain-based criteria.

6.2 Injury criteria for children

In general, injury risk assessment for children is complicated by the lack of validation data. The existing (protection) criteria are either based on accident reconstruction or on scaled versions of protection criteria for adults. To date, no VIVA+ child HBM is available. The remarks below therefore refer to other HBMs where child versions are available, such as PIPER or Thums. Consequently, the point "ID channels in VIVA+" is not applicable for these criteria.

Head excursion

- **Definition:** geometrical constraint, cf. UN R44
- **Input quantities:** Kinematics of CoG of head of child dummy
- **Application in regulatory tests:** UN R44
- **Implementation:** Not yet implemented
- **Injury risk curve:** n/a
- **Protection limit:**
- **Load case:** frontal/rear impact (child protection criterion)
- **Literature, validation data:**
- **Comment:** purely geometrical constraint. May be used with HBMs, but outdated by UN R129

3ms head acceleration:

- **Definition:** Maximum Value of the resultant head COG acceleration (CFC 1000 filtered) exceeded for 3 ms cumulatively.
- **Application in regulatory tests:** UN R129

- **Implementation:** Dynasaur command A3MS (see 3ms chest acceleration in 6.1.3)
- **Injury risk curve:** subject to ongoing research
- **protection limit:** 75-80 g
- **Load case:** frontal impact
- **Literature, validation data:** n/a
- **Comment:** similar to adult ATD criterion.

Head protection criterion HPC15:

- **Definition:** See HIC15
- **Application in regulatory tests:** UN R129
- **Implementation:** see HIC
- **Injury risk curve:** n/a
- **protection limit:** 600-800
- **Load case:** frontal impact
- **Literature, validation data:** n/a
- **Comment:** requirements similar to adult HIC. widely used in many test procedures. Based on rigid-body dynamics, i.e. application in HBMs is limited. Possible, with limitations, for PIPER. Restrictions similar to adult HIC.

Upper neck tension force

- **Definition:** Upper neck tension force as measured by dummy, CFC 600 filtered.
- **Application in regulatory tests:** UN R129
- **Implementation:** in preparation
- **Injury risk curve:** n/a
- **protection limit:** For monitoring purpose only
- **Load case:** frontal impact
- **Literature, validation data:** n/a
- **Comment:** criterion based on the assumption that all forces and moments pass through / act on the occipital condyles. In HBMs, this is not the case. New evaluation methods (e.g. cross-sectional analysis) must be found to apply this criterion to HBMs. Use for comparison with strain-based criteria.

Upper neck moment

- **Definition:** Upper neck moment as measured by dummy, CFC 600 filtered.
- **Application in regulatory tests:** UN R129
- **Injury risk curve:** n/a
- **protection limit:** For monitoring purpose only
- **Load case:** frontal impact
- **Implementation:** in preparation
- **Literature, validation data:** n/a
- **Comment:** criterion based on the assumption that all forces and moments pass through / act on the occipital condyles. In HBMs, this is not the case. New evaluation methods (e.g. cross-sectional analysis) must be found to apply this criterion to HBMs. Use for comparison with strain-based criteria.

3ms chest acceleration:

- **Definition:** Maximum Value of the resultant chest acceleration (CFC 600 filtered) exceeded for 3 ms cumulatively
- **Application in regulatory tests:** UN R129
- **Implementation:** see 3ms chest acceleration (6.1.3)
- **Injury risk curve:** n/a
- **protection limit:** 55 g
- **Load case:** frontal impact

- **Literature, validation data:** n/a
- **Comment:** cf. adult chest acceleration criterion. The same limitations for HBMs apply. The relevance of this criterion is heavily debated.

6.3 Tissue-based Tissue-based injury criteria

6.3.1 General: Output definitions in VIVA+

Table 6-1 List of Landmarks according to Wu and Cavanagh, 1995; Wu et al., 2002; Wu et al., 2005 and IDs for VIVA+ models

| # | Id | Name | # | Id | Name | # | Id | Name | # | Id | Name | |
|---------|------------------------------------|------|---------|-----------------------|------|---------|-------------------|------|---------|-----------------------|---------|-------------------------|
| 109000 | HE-Head-CoG-Seatbelt-Accelerometer | | 3091200 | UX-Scapula-PC-AA-MP-L | | 4091033 | TX-T3_top | | 4091106 | TX-T9_T10_MP_y_off | 6091030 | PE-Acetabulum-ACL-L |
| 2091010 | NE-C1_COG | | 3091201 | UX-Scapula-AI-L | | 4091034 | TX-T3_center | | 4091110 | TX-T11_COG | 6091052 | PE-Coccyx-inferior |
| 2091011 | NE-C1_post_sup | | 3091202 | UX-Scapula-TS-L | | 4091036 | TX-T2_T3_MP_y_off | | 4091112 | TX-T11_bottom | 6091053 | PE-Sacrum-anterior |
| 2091012 | NE-C1_bottom | | 3091203 | UX-Scapula-AA-L | | 4091040 | TX-T4_COG | | 4091113 | TX-T11_top | 6091054 | PE-Sacrum-posterior |
| 2091020 | NE-C2_COG | | 3091310 | UX-GH-Humerus-L | | 4091042 | TX-T4_bottom | | 4091114 | TX-T11_center | 6591001 | PE-ASIS-R |
| 2091022 | NE-C2_bottom | | 3091204 | UX-Scapula-PC-L | | 4091043 | TX-T4_top | | 4091116 | TX-T10_T11_MP_y_off | 6591002 | PE-PSIS-R |
| 2091023 | NE-C2_top | | 3091330 | UX-Humerus-EL-EM-MP-L | | 4091044 | TX-T4_center | | 4091120 | TX-T12_COG | 6591021 | PE-Ischium-inferior-R |
| 2091024 | NE-C2_center | | 3091331 | UX-Humerus-EM-L | | 4091046 | TX-T3_T4_MP_y_off | | 4091122 | TX-T12_bottom | 6591030 | PE-Acetabulum-ACL-R |
| 2091026 | NE-C1-C2_MP_y_off | | 3091332 | UX-Humerus-EL-L | | 4091050 | TX-T5_COG | | 4091123 | TX-T12_top | 7091110 | LX-Femur-head-O-L |
| 2091030 | NE-C3_COG | | 3091430 | UX-Ulna-US-L | | 4091052 | TX-T5_bottom | | 4091124 | TX-T12_center | 7091190 | LX-Femur-FEL-FEM-MP-F-L |
| 2091032 | NE-C3_bottom | | 3091530 | UX-Radius-RS-L | | 4091053 | TX-T5_top | | 4091126 | TX-T11_T12_MP_y_off | 7091191 | LX-Femur-FEM-L |
| 2091033 | NE-C3_top | | 3091600 | UX-Carpal-RS-US-MP-L | | 4091054 | TX-T5_center | | 4093501 | TX-Sternum_IJ | 7091192 | LX-Femur-FEL-L |
| 2091034 | NE-C3_center | | 3591121 | UX-Clavicle-med-R | | 4091056 | TX-T4_T5_MP_y_off | | 4093502 | TX-Sternum_PX | 7091300 | LX-Patella-CoG-L |
| 2091036 | NE-C2_C3_MP_y_off | | 3591122 | UX-Clavicle-lat-R | | 4091060 | TX-T6_COG | | 5091012 | AB-L1_bottom | 7091410 | LX-Tibia-IC-L |
| 2091040 | NE-C4_COG | | 3591200 | UX-Scapula-PC-AA-MP-R | | 4091062 | TX-T6_bottom | | 5091013 | AB-L1_top | 7091411 | LX-Tibia-MC-L |
| 2091042 | NE-C4_bottom | | 3591201 | UX-Scapula-AI-R | | 4091063 | TX-T6_top | | 5091014 | AB-L1_center | 7091412 | LX-Tibia-LC-L |
| 2091043 | NE-C4_top | | 3591202 | UX-Scapula-TS-R | | 4091064 | TX-T6_center | | 5091016 | AB-T12_L1_MP_y_off | 7091431 | LX-MM-Tibia-Fibula-L |
| 2091044 | NE-C4_center | | 3591203 | UX-Scapula-AA-R | | 4091066 | TX-T5_T6_MP_y_off | | 5091022 | AB-L2_bottom | 7091432 | LX-LM-Tibia-Fibula-L |
| 2091046 | NE-C3_C4_MP_y_off | | 3591204 | UX-Scapula-PC-R | | 4091070 | TX-T7_COG | | 5091023 | AB-L2_top | 7091700 | LX-Calcanus-CoG-L |
| 2091050 | NE-C5_COG | | 3591310 | UX-GH-Humerus-R | | 4091072 | TX-T7_bottom | | 5091024 | AB-L2_center | 7091703 | LX-Calcanus-post-L |
| 2091052 | NE-C5_bottom | | 3591330 | UX-Humerus-EL-EM-MP-R | | 4091073 | TX-T7_top | | 5091026 | AB-L1_L2_MP_y_off | 7094110 | LX-IM-Talus-L |
| 2091053 | NE-C5_top | | 3591331 | UX-Humerus-EM-R | | 4091074 | TX-T7_center | | 5091032 | AB-L3_bottom | 7091110 | LX-Femur-head-O-R |
| 2091054 | NE-C5_center | | 3591430 | UX-Ulna-US-R | | 4091076 | TX-T6_T7_MP_y_off | | 5091033 | AB-L3_top | 7591190 | LX-Femur-FEL-FEM-MP-F-R |
| 2091056 | NE-C4_C5_MP_y_off | | 3591530 | UX-Radius-RS-R | | 4091080 | TX-T8_COG | | 5091034 | AB-L3_center | 7591191 | LX-Femur-FEM-R |
| 2091060 | NE-C6_COG | | 3591600 | UX-Carpal-RS-US-MP-R | | 4091082 | TX-T8_bottom | | 5091036 | AB-L2_L3_MP_y_off | 7591192 | LX-Femur-FEL-R |
| 2091062 | NE-C6_bottom | | 4091010 | TX-T1_COG | | 4091083 | TX-T8_top | | 5091042 | AB-L4_bottom | 7591300 | LX-Patella-CoG-R |
| 2091063 | NE-C6_top | | 4091012 | TX-T1_bottom | | 4091084 | TX-T8_center | | 5091043 | AB-L4_top | 7591410 | LX-Tibia-IC-R |
| 2091064 | NE-C6_center | | 4091013 | TX-T1_top | | 4091086 | TX-T7_T8_MP_y_off | | 5091044 | AB-L4_center | 7591411 | LX-Tibia-MC-R |
| 2091066 | NE-C5_C6_MP_y_off | | 4091014 | TX-T1_center | | 4091090 | TX-T9_COG | | 5091046 | AB-L3_L4_MP_y_off | 7591412 | LX-Tibia-LC-R |
| 2091070 | NE-C7_COG | | 4091016 | NE-C7_T1_MP_y_off | | 4091092 | TX-T9_bottom | | 5091052 | AB-L5_bottom | 7591431 | LX-MM-Tibia-Fibula-R |
| 2091071 | NE-C7_post_sup | | 4091020 | TX-T2_COG | | 4091093 | TX-T9_top | | 5091053 | AB-L5_top | 7591432 | LX-LM-Tibia-Fibula-R |
| 2091072 | NE-C7_bottom | | 4091022 | TX-T2_bottom | | 4091094 | TX-T9_center | | 5091054 | AB-L5_center | 7591700 | LX-Calcanus-CoG-R |
| 2091073 | NE-C7_top | | 4091023 | TX-T2_top | | 4091096 | TX-T8_T9_MP_y_off | | 5091056 | AB-L4_L5_MP_y_off | 7591703 | LX-Calcanus-post-R |
| 2091074 | NE-C7_center | | 4091024 | TX-T2_center | | 4091100 | TX-T10_COG | | 6091000 | PE-Acetabulum-MP-AC | 7594110 | LX-IM-Talus-R |
| 2091076 | NE-C6_C7_MP_y_off | | 4091026 | TX-T1_T2_MP_y_off | | 4091102 | TX-T10_bottom | | 6091001 | PE-ASIS-L | | |
| 3091121 | UX-Clavicle-med-L | | 4091030 | TX-T3_COG | | 4091103 | TX-T10_top | | 6091002 | PE-PSIS-L | | |
| 3091122 | UX-Clavicle-lat-L | | 4091032 | TX-T3_bottom | | 4091104 | TX-T10_center | | 6091021 | PE-Ischium-inferior-L | | |

Table 6-2 Body Parts of the VIVA+ models for strain-based tissue assessment

| Type | Name | Type | Name |
|---------------|-----------------------------------|---------------|-------------------------|
| Cortical Bone | LX-Bone-Femur-Cortical-Proximal-L | Knee Ligament | LX-Knee-Ligament-MCL-L |
| Cortical Bone | LX-Bone-Femur-Cortical-Proximal-R | Knee Ligament | LX-Knee-Ligament-MCL-R |
| Cortical Bone | LX-Bone-Femur-Cortical-Shaft-L | Knee Ligament | LX-Knee-Ligament-LCL-L |
| Cortical Bone | LX-Bone-Femur-Cortical-Shaft-R | Knee Ligament | LX-Knee-Ligament-LCL-R |
| Cortical Bone | LX-Bone-Femur-Cortical-Distal-L | Knee Ligament | LX-Knee-Ligament-aACL-L |
| Cortical Bone | LX-Bone-Femur-Cortical-Distal-R | Knee Ligament | LX-Knee-Ligament-aACL-R |
| Cortical Bone | PE-Bone-Pelvis-Cortical | Knee Ligament | LX-Knee-Ligament-pACL-L |
| Cortical Bone | LX-Bone-Tibia-Cortical-L | Knee Ligament | LX-Knee-Ligament-pACL-R |
| Cortical Bone | LX-Bone-Tibia-Cortical-R | Knee Ligament | LX-Knee-Ligament-aPCL-L |
| Cortical Bone | TX-Ribcage-R12-Cortical-L | Knee Ligament | LX-Knee-Ligament-aPCL-R |
| Cortical Bone | TX-Ribcage-R12-Cortical-R | Knee Ligament | LX-Knee-Ligament-pPCL-L |
| Cortical Bone | TX-Ribcage-R11-Cortical-L | Knee Ligament | LX-Knee-Ligament-pPCL-R |

| | |
|---------------|---------------------------|
| Cortical Bone | TX-Ribcage-R11-Cortical-R |
| Cortical Bone | TX-Ribcage-R10-Cortical-L |
| Cortical Bone | TX-Ribcage-R10-Cortical-R |
| Cortical Bone | TX-Ribcage-R9-Cortical-L |
| Cortical Bone | TX-Ribcage-R9-Cortical-R |
| Cortical Bone | TX-Ribcage-R8-Cortical-L |
| Cortical Bone | TX-Ribcage-R8-Cortical-R |
| Cortical Bone | TX-Ribcage-R7-Cortical-L |
| Cortical Bone | TX-Ribcage-R7-Cortical-R |
| Cortical Bone | TX-Ribcage-R6-Cortical-L |
| Cortical Bone | TX-Ribcage-R6-Cortical-R |
| Cortical Bone | TX-Ribcage-R5-Cortical-L |
| Cortical Bone | TX-Ribcage-R5-Cortical-R |
| Cortical Bone | TX-Ribcage-R4-Cortical-L |
| Cortical Bone | TX-Ribcage-R4-Cortical-R |
| Cortical Bone | TX-Ribcage-R3-Cortical-L |
| Cortical Bone | TX-Ribcage-R3-Cortical-R |
| Cortical Bone | TX-Ribcage-R2-Cortical-L |
| Cortical Bone | TX-Ribcage-R2-Cortical-R |
| Cortical Bone | TX-Ribcage-R1-Cortical-L |
| Cortical Bone | TX-Ribcage-R1-Cortical-R |

6.3.2 Head

SUFEHM (Strasbourg University Finite Element Head Model)

Since the head (i.e. the skull) is implemented as a rigid body in VIVA+, only kinematic injury criteria can be used. In principle, the nodal point history i.e. the kinematic data of the head CoG might be input into evaluation tools such as the SUFEHM, which, in turn, implements tissue-based criteria in an isolated brain / skull environment.

- **Literature, validation data:** Sahoo et al. (2016).

6.3.3 Spine

Aldman pressure

This criterion is kinematics based and addresses a mechanism thought to cause nerve tissue injury. This mechanism was described in more detail by Yao et al. (2018) and the nerve tissue damage has been hypothesised to be the origin of whiplash injury symptoms by Örtengren (1996), Eichberger et al. (2000).

- **Input quantities:** Kinematics of vertebrae in cervical spine. Angular displacement in each cervical vertebral joint.
- **Definition:** Pressure time history is calculated in software of Yao et al. (2016). The hands-on use of the software is described in the VIRTUAL Milestone M3.5 (pages 17-21).

- **Implementation:** MATLAB code on OpenVT platform. No Dynasaur implementation, as a CFD solver is required.
- **Load case:** rear impact.
- **Injury risk curve/protection limit:** Needs to be determined for female and male
- **Literature, validation data:** Yao et al. (2016)

6.3.4 Thorax

Rib fracture

Fractures of single or multiple ribs can be assessed by observing the rib strain in an HBM.

- **Input quantities:** Maximum principle strain of each rib
- **Definition:** From Larsson et al. (2021)

$$Fracture\ risk(strain, AGE) = \frac{1}{2} + \frac{1}{2} \left[\frac{LN(strain) - (\beta_0 + \beta_1 * AGE)}{\sqrt{2} * \alpha} \right]$$

Table 6-3 Injury risk curve for rib fractures from Larsson et al. (2021)

| Injury risk function | Distribution | α | β_0 | β_1 |
|----------------------|--------------|----------|-----------|-----------|
| Rib Fractures | Log-Normal | 0.3026 | -2.9866 | -0.0130 |

- **Application in regulatory test:** n/a
- **Implementation:** Dynasaur user function erf_rib_risk_age
- **Injury risk curve:** According to Larsson et al. (2021)
- **Protection limit(s):** n/a
- **Used ID channel in VIVA+ model:** Cortical Rib bones (ids see Table 6-2)
- **Applied filtering:** n/a
- **Literature, validation data:** Larsson et al. (2021)

Pelvic Fractures

The pelvic bone will be further refined outside of VIRTUAL. A preliminary injury criterion is used in VIRTUAL (Snedeker et al., 2003), which should be used for qualitative evaluations only.

6.3.5 Lower extremities

Femur Fractures

Fractures of proximal femur and femur shaft can be assessed by observing the cortical bone strain in an HBM.

- **Input quantities:** 99th percentile principle strain of cortical femur bone (mean of IP)
- **Definition:** From Schubert et al. (2021)

$$Fracture\ risk(PS99\ strain) = 1 - e^{-\left(\frac{strain}{k}\right)^\lambda}$$

Table 6-4 Injury risk curves for femur fractures (95 % confidence intervals are presented within brackets) from Schubert et al. (2021)

| Injury risk function | Distribution | Shape factor (k) | Scale parameter (λ) |
|----------------------|--------------|-----------------------------|-------------------------------|
| Proximal femur | Weibull | 2.2244 (1.4187 - 3.4877) | 0.0149 (0.0114 - 0.0195) |
| Femur shaft | Weibull | 2.7426 | 0.0342 |

(1.7878 - 4.2072)

(0.0279 - 0.0418)

- **Application in regulatory test:** n/a
- **Implementation:** Dynasaur 99th percentile strain and Jupyter notebook (post_processing_single.ipynb)
- **Injury risk curve:** According to Schubert et al. (2021)
- **Protection limit(s):** n/a
- **Used ID channel in VIVA+ model:** Cortical femur bone (ids see Table 6-2)
- **Applied filtering:** n/a
- **Literature, validation data:** Schubert et al. (2021)

Tibia Fractures

Injury risk curves for tibia fractures are currently under development. They will be added in the next version of the test protocol.

Knee Injuries

Ligament injuries are assessed based on measured total elongation of the knee ligaments/initial length.

- **Input quantities:** Elongation (strain) of Knee Ligaments
- **Definition:** From Nusia et al. (2021)

$$\text{Weibull Fracture risk}(\text{strain}) = 1 - e^{-\left(\frac{\text{strain}}{k}\right)^\lambda}$$

$$\text{Log - Logistic Fracture risk}(\text{strain}) = \frac{\text{strain}^\lambda}{\text{strain}^\lambda + k^\lambda}$$

Table 6-5 Injury risk curves for knee ligaments (95 % confidence intervals are presented within brackets) from Nusia et al. (2021)

| Injury risk function | | Distribution | Scale parameter (λ) | Shape parameter (k) |
|----------------------|--------------|--------------|-------------------------------|-------------------------|
| ACL DYNAMIC BLB | Log-Logistic | | 26.23 (22.98 - 29.94) | 3.88 (3.05 - 4.94) |
| PCL DYNAMIC BLB | Log-Logistic | | 18.62 (16.88 - 20.54) | 6.39 (4.76 - 8.59) |
| MCL STATIC LIG | Weibull | | 26.10 (24.91 - 27.34) | 7.19 (5.60 - 7.78) |
| LCL DYNAMIC BLB | Log-Logistic | | 13.90 (12.40 - 15.59) | 5.65 (4.11 - 7.78) |

- **Application in regulatory test:** n/a
- **Implementation:** Dynasaur ligament elongation and Jupyter notebook (post_processing_single.ipynb)
- **Injury risk curve:** According to Nusia et al. (2021)
- **Protection limit(s):** n/a
- **Used ID channel in VIVA+ model:** Knee Ligaments (ids see Table 6-2)
- **Applied filtering:** n/a
- **Literature, validation data:** Nusia et al. (2021)

6.4 References

- Boström, O., Y. Håland, L. Lövsund, and M. Y. Svenssom. «Neck injury criterion (NIC) and its relevance to various possible neck injury mechanisms.» *Eds. Yoganandan, N; Pintar, FA: Frontiers in Whiplash Trauma. IOS Press, The Netherlands, 2000.*
- Boström, Ola, et al. «A new neck injury criterion candidate-based on injury findings in the cervical spinal ganglia after experimental neck extension trauma.» *Proceedings of The 1996 International Ircobi Conference On The Biomechanics Of Impact, September 11-13, Dublin, Ireland.* 1996. 123-136.
- Eichberger, Arno, Mario Darok, Hermann Steffan, Peter E. Leinzinger, Ola Boström, and Mats Y. Svensson. «Pressure measurements in the spinal canal of post-mortem human subjects during rear-end impact and correlation of results to the neck injury criterion.» *Accident Analysis & Prevention* (Elsevier) 32 (2000): 251–260.
- Eriksson, Linda, and Anders Kullgren. «Influence of seat geometry and seating posture on NICmax long-term AIS 1 neck injury predictability.» *Traffic injury prevention* (Taylor & Francis) 7 (2006): 61-69.
- Gabler, Lee F., Jeff R. Crandall, and Matthew B. Panzer. «Development of a second-order system for rapid estimation of maximum brain strain.» *Annals of biomedical engineering* (Springer) 47 (2019): 1971-1981.
- Hertz, Ellen. «A note on the head injury criterion (HIC) as a predictor of the risk of skull fracture.» *Proceedings: Association for the Advancement of automotive medicine annual conference.* 1993. 303-312.
- Kleinberger, Michael, Emily Sun, Rolf Eppinger, Shashi Kuppa, and Roger Saul. «Development of improved injury criteria for the assessment of advanced automotive restraint systems.» *NHTSA Docket 4405* (1998).
- Kroell, Charles K., Dennis C. Schneider, and Alan M. Nahum. «Impact tolerance and response of the human thorax II.» *SAE Transactions* (JSTOR), 1974: 3724-3762.
- Kullgren, Anders. «Dose-response models and EDR data for assessment of injury risk and effectiveness of safety systems.» *IRCOBI Conference, Bern, Switzerland.* 2008. 3-14.
- Kullgren, Anders, Linda Eriksson, Ola Boström, and Maria Krafft. «Validation of neck injury criteria using reconstructed real-life rear-end crashes with recorded crash pulses.» *Proc. 18th ESV Conf.* 2003. 1-13.
- Kullgren, Anders, Maria Krafft, Anders Lie, and Claes Tingvall. «The effect of whiplash protection systems in real-life crashes and their correlation to consumer crash test programmes.» *Proc. 20th ESV Conf.(07-0468), Lyon (France).* 2007. 1–7.
- Larsson, Karl-Johan, Amanda Blennow, Johan Iraeus, Bengt Pipkorn, and Nils Lubbe. «Rib cortical bone fracture risk as a function of age and rib strain: updated injury prediction using finite element human body models.» *Frontiers in bioengineering and biotechnology* (Frontiers) 9 (2021): 412.
- Linder, Astrid, Stefan Olsén, Jenny Eriksson, Mats Y. Svensson, and Anna Carlsson. «Influence of gender, height, weight, age, seated position and collision site related to neck pain symptoms in rear end impacts.» *Proceedings: IRCOBI Conference.* 2012. 12–14.
- Nahum, Allan., Charles W. Gadd, Dennis C. Schneider, and Charles K. Kroell. «The biomechanical basis for chest impact protection: I. Force-deflection characteristics of the thorax.» *Journal of Trauma and Acute Care Surgery* (LWW) 11 (1971): 874-882.
- Nusia, Jiota, Jia Cheng Xu, Reimert Sjöblom, Johan Knälmann, Astrid Linder, and Svein Kleiven. «Injury risk functions for the four primary knee ligaments.» *Under review* (Journal of the Mechanical Behavior of Biomedical Materials), 2022.
- Örtengren, Tore, H.-A. Hansson, Per Lövsund, Mats Y. Svensson, A. Suneson, and Annette Säljö. «Membrane leakage in spinal ganglion nerve cells induced by experimental whiplash extension motion: a study in pigs.» *Journal of neurotrauma* 13 (1996): 171–180.

- Panjabi, M. M., J. L. Wang, and N. Delson. «Neck injury criterion based on intervertebral motions and its evaluation using an instrumented neck dummy.» *Proceedings of the International Research Council on the Biomechanics of Injury conference*. 1999. 179-190.
- Park, Jangwoon, Sheila M. Ebert, Matthew P. Reed, and Jason J. Hallman. «Statistical models for predicting automobile driving postures for men and women including effects of age.» *Human factors* (SAGE Publications Sage CA: Los Angeles, CA) 58 (2016): 261–278.
- Prasad, Priya, and Roger P. Daniel. «A biomechanical analysis of head, neck, and torso injuries to child surrogates due to sudden torso acceleration.» *SAE transactions* (JSTOR), 1984: 784-799.
- Sahoo, D., C. Deck, and R. Willinger. «Brain injury tolerance limit based on computation of axonal strain.» *Journal of Accident Analysis & Prevention*, 2016: Vol 92, 53-70.
- Schmitt, K.-U., Markus H. Muser, and P. Niederer. «A new neck injury criterion candidate for rear-end collisions taking into account shear forces and bending moments.» Tech. rep., SAE Technical Paper, 2001.
- Schmitt, Kai-Uwe, Markus H. Muser, Felix H. Walz, and Peter F. Niederer. «N km--a proposal for a neck protection criterion for low-speed rear-end impacts.» *Traffic injury prevention* (Taylor & Francis) 3 (2002): 117-126.
- Schmitt, Kai-Uwe, Peter F. Niederer, Duane S. Cronin, Barclay Morrison III, Markus H. Muser, and Felix Walz. *Trauma biomechanics: an introduction to injury biomechanics*. Springer, 2019.
- Schubert, Alexander, Nico Erlinger, Christoph Leo, Johan Iraeus, Jobin John, and Corina Klug. «Development of a 50th Percentile Female Femur Model.» *International Research Council on the Biomechanics of Injury 2021*. 2021. 308–332.
- Snedeker, Jess G., Markus H. Muser, and Felix H. Walz. «Assessment of pelvis and upper leg injury risk in car-pedestrian collisions: comparison of accident statistics, impactor tests and a human body finite element model.» Tech. rep., SAE Technical Paper, 2003.
- Viano, David C., and Ian V. Lau. «Thoracic impact: a viscous tolerance criterion.» Tech. rep., SAE Technical Paper, 1985.
- Yamada, Hiroshi. *Strength of biological materials*. Baltimore - Md: Williams and Wilkins, 1970.
- Yao, Hua-Dong, Mats Y. Svensson, and Håkan Nilsson. «Transient pressure changes in the vertebral canal during whiplash motion--A hydrodynamic modeling approach.» *Journal of biomechanics* (Elsevier) 49 (2016): 416-422.

7 Appendix B: Rear impact protocol

7.1 Introduction

7.1.1 Purpose

This protocol provides specifications for a virtual test to evaluate the performance of vehicle seat models and/or models of the vehicle interior in protection of adult seated occupants in rear end impact loading conditions. In principle, the virtual test does not evaluate the performance of the respective physical item, but the performance of the virtual models thereof. If a physical counterpart of the device model exists, it depends on the quality of the virtual models how well they correspond to the physical version. This should be evaluated in specific validation tests (see the respective subchapter). As an experimental prototype, this protocol is not tailored and tested for any specific application, but can be adapted to consumer or product development tests, for example.

7.1.2 Definitions

7.1.2.1 Human Body Model (HBM):

A finite element model of the human body.

7.1.2.2 50M/ 50F:

HBM representing the 50th percentile (average) male/female.

7.1.2.3 Virtual occupant model

HBM positioned, morphed and validated in a way to replicate the behaviour of a (seated) vehicle occupant. In virtual rear impact tests, the occupant model serves as the measurement device (analogous to a dummy in a physical test).

7.1.2.4 Device model:

Finite element model representing a device such as a seat or other parts of vehicle interior. The device model can either consist of linked rigid bodies or deformable materials. The model shall be validated and the validation documented. In this protocol, the device model under test is primarily a seat model; hence, "seat model" and "device model" are used interchangeably. However, other parts of the vehicle interior could also be included in the test, for which the general requirements for device models hold as far as applicable.

7.1.2.5 Solver

A software approximating the solution of an initial and boundary value problem with a time dependent finite element method. Usually, explicit methods are used for the time scales relevant in safety testing. However, this is not a strict requirement (see subchapter "general requirements").

7.1.3 Overview of assessment procedure

The assessment procedure consists of 4 parts: (i) preparation of the HBM and device model, (ii) pre-simulation (positioning), (iii) main simulation, (iv) postprocessing. Even though the preparation of the models includes the validation and its documentation, this task is not part of the actual test procedure and does not have to be repeated for new test runs with the same model. However, validation and proper documentation thereof must be performed before the test procedure can be applied.

7.1.4 General requirements

Simulations need to be performed with a freely or commercially available state-of-the-art simulation software that can also be used by third parties. Reference simulations / verifications of the code shall be performed when changing to other code versions to make sure that results are still valid. For all steps described in this document, the same simulation framework shall be used (one pre-crash and

one in-crash environment). Solver versions or decomposition for the FE solver must not be changed throughout the whole procedure.

An HBM validated for rear end impact with the 50F and 50M anthropometry as specified in the documentation of the VIVA+ model (see <https://vivaplus.readthedocs.io>) shall be used. It is recommended to use the VIVA+ 50F and 50M HBMs, which are free and open source and come in a seated version with documented validation.

7.2 Device model to be tested

The device model to be tested using this test protocol is a model of a driver or passenger seat. The protocol could in principle be extended to test other parts of the vehicle interior in the future; however, this might require additional validation of the HBM and modifications in the assessment procedure.

If the goal of the test is not to test the performance of a particular seat or seat model, a generic seat model can be used. As a validated seat model, the VIRTUAL open source driver's seat model is freely available on the OpenVT platform.

7.2.1 Calibration

The goal of the calibration is that the general properties of the device model (such as geometry, mass and material properties) agree with the physical device. While the validation is to be documented in a dedicated report, there are no formal standards for calibration. However, the following guidelines may be helpful:

- The geometry should be measured with 3D scans of the physical seat.
- For the steel parts, a generic material model for steel is applicable in most cases.
- For the calibration of the foam properties, ideally a test according to the ISO standards for foam testing (ISO3386, cyclic compression tests of foam samples) should be done.

At the end of the calibration procedure, the model developers should be confident that the device model reasonably replicates the physical properties of the device to be tested.

7.2.2 Validation

The device model shall be validated with dynamic laboratory tests and simulations replicating the tests. These tests can include impactor tests as well as sled experiments. The validation shall at least include an impactor test for the seat cushion, the seat back and the head restraint with an impactor instrumented with an accelerometer.

7.2.3 Documentation of validation

The documentation shall include all relevant information for a third party to reproduce the experimental and virtual tests. Templates described in IMVITER deliverables can be used as reference. Curve ratings/scores comparing measured and simulated acceleration time series according to ISO/TS 18571:2022 shall be provided. For a successful validation, the scores shall be greater than 0.58 (i.e., at least "fair agreement" according to ISO/TS 18571:2022).

The validation of the VIRTUAL open-source driver seat model is documented on the OpenVT platform.

7.2.4 Output definitions

N/A for seat model.

7.3 Virtual occupant model (measurement device)

7.3.1 Prerequisites

See subchapter "General requirements." In principle, any finite element HBM can be used as long as it is positioned accordingly and validated for use as an occupant model in rear impact. The applicability

of the HBM as an occupant model in rear end impact shall be demonstrated with the qualification procedure described below. This qualification procedure is still somewhat experimental; more details have to be specified in the future. It is recommended to use the VIVA+ HBM, for which the qualification procedure has already been evaluated.

7.3.2 Qualification procedure

7.3.2.1 Anthropometry requirements

The anthropometry of the HBM shall correspond to the 50F/50M parameters as specified in the VIVA+ model documentation at <https://vivaplus.readthedocs.io/en/latest/model/anthro/>.

7.3.2.2 Validation of the models

The standard for the validation of the HBM is set by the validation of the VIVA+ model as documented in Deliverable D 2.2 (John et al. 2021).

7.3.2.3 Certification load case

For a certification load case, a generic rear impact test with VIRTUAL's open access vehicle seat model is used. The implementation of the load case can be found on the OpenVT platform at https://openvt.eu/load_cases/generic_rear_impact. The guidelines for the evaluation of the certification load case still have to be set by future research.

7.3.3 Output definitions

- 7.3.3.1 For each of the anatomical landmarks used to control the positioning procedure (see Chapter 7.3.4.3), the position and velocity shall be recorded. If the HBM does not come with pre-defined reference points for these landmarks, they shall be defined by the user according to the definitions used by Park et al. (2016).
- 7.3.3.2 All output data mentioned in 7.3.3.3 shall be output with a minimum sampling frequency of 10 kHz / a sampling interval no longer than 0.0001 sec.
- 7.3.3.3 The following parameters shall be recorded as a function of time:
 - The position and velocity of the anatomical landmarks
 - The kinematics of the centre of mass of the head. Head accelerations shall be recorded in a local coordinate system oriented along the Frankfort plane.
 - The kinematics of the centre of mass of the T1 vertebra. Accelerations shall be recorded in a local coordinate system oriented parallel to the head local coordinate system at the beginning of the main simulation.

7.3.4 Model preparation

7.3.4.1 Posture: target positions

- 7.3.4.2 The seated posture of the HBM at the beginning of the test (main simulation) is defined by the position of a set of anatomical landmarks (target positions). The target positions shall be computed as a function of the geometry of the HBM and the vehicle interior using the regressions specified below. The target positions shall be specified in the test report. The target positions are used later to evaluate the success of the pre-simulation.
- 7.3.4.3 The regression models for the target positions have been inferred by Park et al. (2016) according to seated postures measured on volunteer participants. The posture prediction models for females and males are provided in 7.7.3.

7.4 Test preparation and pre-simulation

7.4.1 Test environment

7.4.1.1 Units

7.4.1.2 The units used in the simulation shall be specified in the test report. It is recommended to use SI units. Throughout this protocol, the units kg, mm and ms will be used. Additionally, kN and GPa, derived from the aforementioned units, will be used.

7.4.1.3 Coordinate System

7.4.1.4 The global and local coordinate systems used shall be Cartesian coordinate systems.

7.4.1.5 While the positive x-direction of the global coordinate system shall be oriented in the direction of travel of the seat, the positive z-direction shall be oriented upward (Coordinate system according to e.g. SAE J211).

7.4.2 Installation and preparation of device model and HBM

7.4.2.1 Device model installation

7.4.2.2 A vehicle floor shall be included in the model. This may be a detailed model of a real vehicle floor pan, or a rigid plate with sufficient dimensions to provide support for e.g. the feet of the model during the entire simulation.

7.4.2.3 If no structure resembling a footrest is present, a toe board shall be modelled to keep the feet of the HBM in place. A rigid plate with sufficient dimensions to provide support for e.g. the feet of the model during the entire simulation may be used. The toe board shall be inclined 45° degrees with respect to the horizontal plane.

7.4.2.4 Both structures in 7.4.2.2 and 7.4.2.3 shall be rigidly connected. The fore/aft position should be adjustable. These structures may be implemented as rigid bodies or plates of steel¹.

7.4.2.5 The device model shall be rigidly attached to the vehicle floor. If there is a physical counterpart of the seat available, the inclination with respect to horizontal should be the same as specified by the manufacturer. The inclination shall be reported. The same procedure applies for the height of the seat above the vehicle floor. If the model is supplied with adjustable seat slides, the vehicle-side part shall be rigidly attached to the floor, and the (longitudinal) position shall be recorded.

7.4.2.6 The position of the H-point of the device model relative to the coordinate system of the seat shall be specified in the test report. The H-point can either be measured with an H-point machine on the physical counterpart of the seat model or directly on the device model using a virtual model of an H-point machine. In either case, the measurement shall be carried out according to the H-point procedure specified by Euro NCAP (2021).

7.4.2.7 Device model adjustments

7.4.2.8 For the determination of the head restraint height two scenarios are possible. If a physical counterpart of the seat model is available, find the geometric midpoint as described in 7.4.2.10 and use the same height in the virtual seat model.

7.4.2.9 If no physical counterpart is available, identify the highest point that lies in the centreline of the head restraint cushion. Adjust the head restraint height such that this point corresponds to the vertex of the head of the occupant model.

7.4.2.10 The geometric midpoint can either be defined for seats with a non-locking or a locking adjustable head restraint.

- Non-locking adjustable: Set the headrest to the lowest and highest vertical position at the horizontal centre line and mark both. The geometric midpoint marks the half-distance between the lowest and highest positions. This is only applicable if the sliding motion of

¹ Mass Density: 7.89E-6kg/mm³, E-Module: 210 GPa, Poisson-Ratio: 0.3

the adjustment mechanism is modelled realistically. Otherwise, adjust the head restraint to the lowest position.

- Locking adjustable: Set the headrest to the lowest and highest vertical locking position. The half-distance between the two locking positions marks the geometric midpoint. If there is no locking position at the geometric midpoint raise the headrest by up to 10mm. If a locking position exists in this range, this will be the test position. In case no position exists, lower the head restraint to the next lower locking position.

7.4.2.11 In case of a validation test, the settings used in the physical tests shall be replicated on the device model. If no physical counterpart is available or no validation test is performed, adjust the device model with the following modifications (According to EuroNCAP (2021)):

- Seat track (slide) should be in its most rearward locking position.
- Seat height should be set to its lowest position.
- Seat tilt should be adjusted in order to achieve a cushion angle of zero (± 1 degree). The measurement of the cushion angle is described in 7.4.2.12.
- Set the seat back angle to the position specified by the manufacturer (± 1 degree). If no position is provided, a seat back angle of 23° ($\pm 1^\circ$) shall be used. The measurement of the seat back angle is described in 7.4.2.13.
- Cushion height should be set to its lowest level.
- Lumbar support should be set to its most rearward or least prominent position.
- If adjustable relative to the lower portion, the upper seat back should be rotated fully rearward.
- Cushion extension should be set to its most rearward or least extended position.
- Side bolsters should be set to the widest position
- Arm rests should be set in the stowed position.

All adjustments shall be documented in the test report. Adjustments not implemented in the model shall be documented as well.

- 7.4.2.12 The cushion angle should be measured using two distinct nodes on the cushion. The first node is located in the middle of the forward edge. Locate a second node that is 400mm rearward along the global x-direction. Determine the angle between a line connecting these two nodes and the horizontal axis.
- 7.4.2.13 The seat back angle should be measured using two distinct nodes on the seat back. The first node is located on the middle upper edge of the seat back. Locate a second node in the middle of the lower seat back. Determine the angle between a line connecting these two nodes and the vertical axis.

7.4.3 Installation of the HBM

- 7.4.3.1 The HBM shall be positioned in the device model using translations and/or rotations. Its mid-sagittal plane shall align with the longitudinal centreline of the device model. The centreline should go through the origin of the global y-axis ($y = 0$).
- 7.4.3.2 It shall be ensured that no initial penetrations between the surfaces of the HBM and the device model occur.
- 7.4.3.3 Adjust the fore/aft position of the toe board according to the position of the feet of the HBM. They should slightly hover above the toe board. Initial penetrations between the feet and the toe board must be avoided.

7.4.4 Posture adjustment

- 7.4.4.1 An HBM suitable as occupant model should already be pre-positioned in a seated posture close to the final posture after pre-simulation (see 7.4.6). The initial posture might be changed using validated positioning tools to alter joint angles or to rotate the HBM, for example. All modifications to the HBM shall be documented.

7.4.5 Contact definitions

- 7.4.5.1 Contact formulations shall be established between the HBM and the model device. The HBM shall be defined as the slave surface, and the device model shall be defined as the master surface. A symmetric behaviour in terms of a surface-to-surface contact is recommended.
- 7.4.5.2 A friction coefficient is normally required in the contact definition. The coefficient should be chosen according to the surface properties of the utilised HBM and model device.
- 7.4.5.3 The contact force between the slave and master surface(s) in 7.4.5.1 shall be recorded as a function of time. The sampling frequency shall not be lower than 1 kHz.

7.4.6 Pre-simulation

- 7.4.6.1 The goal of the pre-simulation is to place the HBM on the seat in a position where (i) all landmarks lie within the required tolerances of the defined positions, (ii) the velocity of all landmarks at the end of the pre-simulation is less than the required tolerance and (iii) the seat and seat cushion are deformed such that the HBM is supported in equilibrium.
- 7.4.6.2 The method for the pre-simulation may be chosen freely. A recommended method using gravity settling and constant-force beam elements is given in Section 7.7.
- 7.4.6.3 A global damping coefficient of 0.05 to 0.1 may be applied in order to remove unphysical oscillations.
- 7.4.6.4 Gravitational force should be enabled for the whole pre-simulation.
- 7.4.6.5 During the pre-simulation, the positions and velocities of the landmarks on the HBM shall be recorded as defined in 7.3.3.
- 7.4.6.6 The duration of the pre-simulation can be chosen according to the needs of the positioning method (typically, 200 - 300 ms are needed). Relevant for the positioning targets is the state at the end of the pre-simulation (i.e. at the beginning of the main simulation).

7.4.7 Evaluation and documentation of the pre-simulation

- 7.4.7.1 Report the positions and velocities of the landmarks for which positioning targets exist.
- 7.4.7.2 Report the residual distance of each landmark, i.e. the distance between the target position according to the regressions by Park et al. (2016) and the position at the end of the pre-simulation.
- 7.4.7.3 Report the residual speed of each landmark, i.e. the absolute value of the velocity at the end of the pre-simulation.
- 7.4.7.4 Positional requirements are fulfilled if for each landmark the residual distance of each landmark is less than 10 mm and the residual speed is less than 0.1 m/s.
- 7.4.7.5 Report the total contact forces between the HBM and the device model, i.e. the vector sum of all contact forces between the HBM and the device model. The resulting contact forces shall lie within $\pm 5\%$ of the weight of the HBM.
- 7.4.7.6 Report the head-to-head restraint distance at the end of the pre-simulation, i.e. the horizontal distance from the most occipital point of the head to the surface of the head restraint.
- 7.4.7.7 The positioning of the HBM shall be modified until all requirements mentioned above are met. A recommended positioning method is specified in the appendix of this protocol (Section 7.7).

7.4.8 Virtual test (main simulation)

- 7.4.8.1 The main simulation is carried out immediately after the pre-simulation. This may be done either by simply continuing the pre-simulation while applying the acceleration pulse of the main simulation, or by using a restart mechanism using stored pre-simulation data. In the latter case, it shall be ascertained that all stresses, strains, deformations, and nodal initial conditions are carried over from the pre-simulation.
- 7.4.8.2 No global damping shall be used during the main simulation.
- 7.4.8.3 The gravitational force shall stay enabled for the entire main simulation.

7.4.9 Crash pulse

- 7.4.9.1 The test pulse can be applied either as a prescribed motion of the vehicle floor or as a gravity-type load. The latter is preferred. In case a gravity load is used, the acceleration originating from the crash pulse shall be deducted from the measured kinematics.
- 7.4.9.2 The crash pulse can be chosen according to the purpose of the test. Crash pulses according to the corridors specified in the EuroNCAP rear impact protocol (EuroNCAP 2021) are preferred.

7.4.10 Quality criteria

- 7.4.10.1 Both the pre- and main-simulation must terminate normally. Any simulation run that results in an error termination is not valid as a test result.
- 7.4.10.2 Table 7-1 shows a list of requirements regarding the numerical stability of the main-simulation. In order to achieve a valid simulation, all requirements must be fulfilled.

Table 7-1: Numerical stability requirements for the pre- and main-simulation

| Requirement |
|--|
| Conservation of total energy |
| Hourglass energy < 5% of initial total energy and < 10% of final internal energy |
| Added mass < 5% of initial total mass |

Parts with maximum added mass have been added < 10% of their initial mass

Mobile parts of the model have been added < 5% of their initial mass

No shooting nodes

No solid elements with negative volume

7.5 Evaluation of virtual testing results

7.5.1 Post-processing definitions

- 7.5.1.1 This section defines the quantities to be extracted from the model results. Both the raw quantities and the injury criteria shall be reported/plotted in a test report.
- 7.5.1.2 Head restraint contact time: The head-to-head restraint contact time is defined as the time between the start of the crash pulse and the occupant model touching the head restraint. Contact duration has to exceed 40 ms in order to represent a valid result. It is recommended to use the contact forces between the head and the head restraint as a measure for the head restraint contact time.
- 7.5.1.3 T1 acceleration: Data acquired from the T1 sensor shall be filtered to channel frequency class (cfc) 180. It shall be reported if the resulting acceleration or the acceleration along the x-axis was used.
- 7.5.1.4 Head acceleration: For the evaluation of NIC, data acquired from the head sensor should be filtered to channel frequency class (cfc) 180. It shall be reported if the resultant acceleration or x-acceleration was used.

7.5.2 Injury assessment

- 7.5.2.1 NIC: The NIC value is calculated using the relative horizontal acceleration and velocity of the head and T1 vertebra. Hence, the acceleration and velocity in the x-direction shall be used. Data acquired from both sensors should be filtered to channel frequency class (cfc) 180 (cf. injury assessment manual). The accelerations of head and T1 shall be evaluated in a coordinate system connected to T1 and initially parallel to the Frankfort plane, i.e. parallel to the head coordinate system. If rotations of more than 5 - 10° of the head relative to the torso appear before the maximum NIC value is reached, the computation of NIC might not be reliable any more, as the definition assumes that head and T1 do not rotate with respect to each other to larger amounts. This shall be reported in the test report.
- 7.5.2.2 More injury criteria should be evaluated in the future (e.g., Aldman pressure). This is an open issue for future research.

7.5.3 Test report

- 7.5.3.1 The test shall be documented using a pdf report. In addition to that, Jupyter notebooks may be used. The test report shall contain the values or time series of the assessment quantities described above as well as a documentation of the results of the positioning procedure.
- 7.5.3.2 In future applications of this test protocol, more detailed standards for the test report (including instructions for a cost-benefit analysis and the evaluation of an overall score) may be specified.

7.6 References

Euro NCAP: «The Dynamic Assessment of Car Seats for Neck Injury Protection Testing Protocol.» *Version 4.1.1.* 2021.

Park, Jangwoon, Sheila M. Ebert, Matthew P. Reed, and Jason J. Hallman. «Statistical models for predicting automobile driving postures for men and women including effects of age.» *Human factors* (SAGE Publications Sage CA: Los Angeles, CA) 58 (2016): 261–278.

7.7 Appendix: recommended method for positioning process

There are no specific requirements on how to reach the seated position postulated in this protocol. However, in order to present a working method to reach the required position precision, the following step-by-step manual describes how to position the VIVA+ HBM on VIRTUAL’s open access driver’s seat model using a marionette method and gravity settling. LS-Dyna input files for the presented simulations are available on the OpenVT platform.

7.7.1 Preparation of positioning simulation

1. The simulation uses the following units: kg –mm – ms (kN, GPa).
2. Rotate and/or translate the HBM to reach a position as close as possible to the seat. Make sure that there is no initial penetration between the HBM and the seat model.
3. Determine the distance vector from the centre of the left and right acetabulum of the HBM to the H-point of the seat.
4. Search for nodes on the HBM where a beam element can be connected. Preferably these nodes should lie on rigid parts or on parts that are relatively stiff (e.g. bones). Make sure that the nodes are distributed uniformly over the body of the HBM (Table 7-2).

Table 7-2: Amount of beams used on each body part

| Body part | Left side [Amount] | Right side [Amount] | Centre [Amount] |
|-----------|--------------------|---------------------|-----------------|
| Head | 1 | 1 | 1 |
| Shoulder | 1 | 1 | 0 |
| Ribs | 4 | 4 | 0 |
| Hip | 3 | 3 | 0 |
| Knee | 1 | 1 | 0 |
| Ankle | 0 | 0 | 0 |

5. Define the target nodes. The vector between the nodes on the HBM and the target nodes should be the same vector as measured in step 3.
6. Constrain the target nodes in space with a boundary condition (e.g. *BOUNDARY_SPC_SET).
7. Assign a mass of about 0.001 kg per target node.
8. Define a beam element between each node of the HBM and target node. Set the material to *MAT_CABLE_DISCRETE_BEAM and the section of the beam to ELFORM 6.
9. Use a ramp up time (about 10 ms) for the force of the beam. Additionally, different forces should be used for different body parts (e.g. less force for the beams on the head than on the hip). See Table 7-3.

Table 7-3: Force for each of the beams per body part

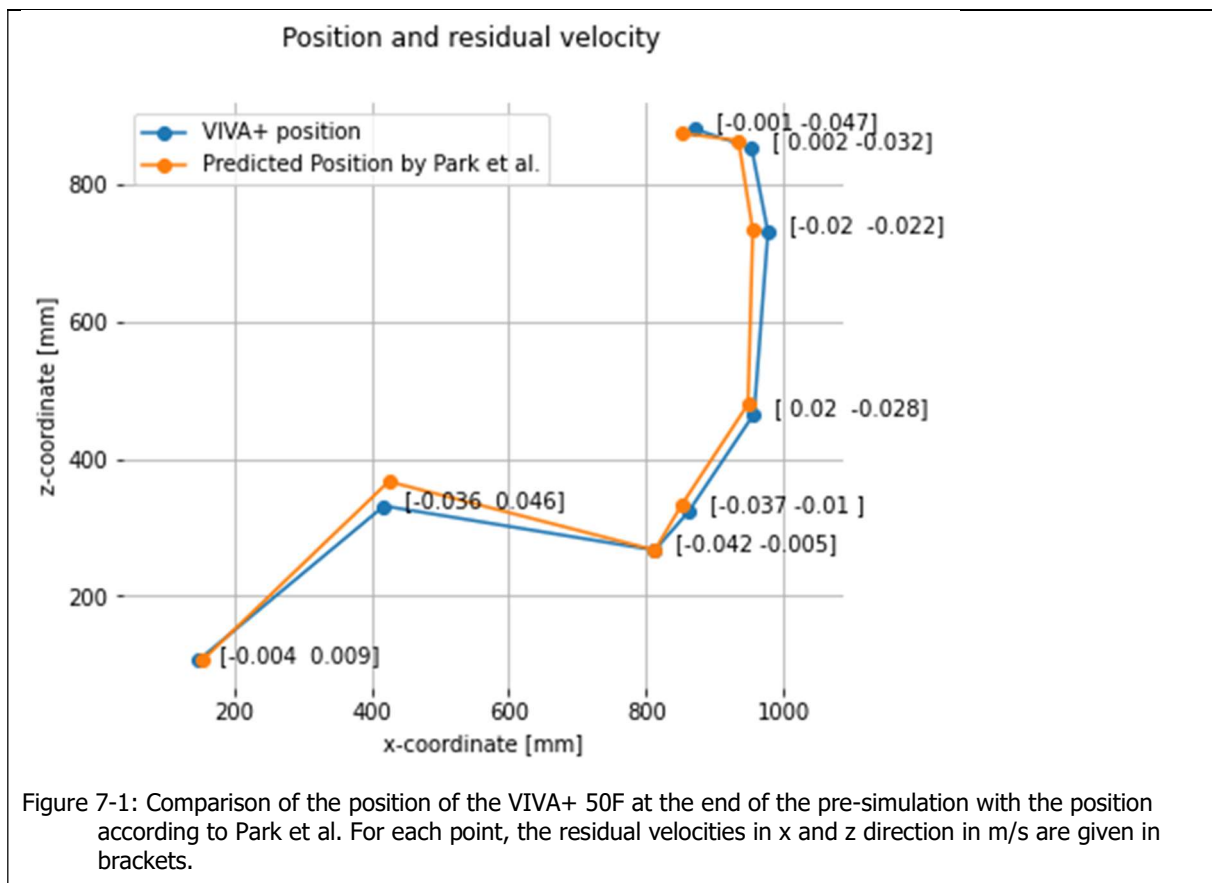
| Body part | Force [kN] |
|-----------|------------|
| Head | 0.07 |
| Shoulder | 0.15 |

| | |
|-------|------|
| Ribs | 0.15 |
| Hip | 0.15 |
| Knee | 0.1 |
| Ankle | 0 |

10. At some point in the simulation, the distance between the nodes of the HBM and the target nodes reaches or is close to zero. This is the time when the force of the beams should be terminated. This is done with the option "Tmaxf0" on the material card.
11. Let the HBM settle with only gravity acting on the model for around 50 - 100 ms.
12. A global damping coefficient of 0.07 and gravity was used during the whole seating process.

7.7.2 Data recording and read-out

Record the nodal kinematics with a *DATABASE_HISTORY_NODE_LOCAL command and store the results in a binout file. The final position before a crash pulse is applied shall be compared to the predicted position by Park et al. (2016). A Jupyter notebook script for the postprocessing analysis can be found on the OpenVT platform at <https://openvt.eu/fem/hbm-positioning>.



7.7.3 Statistical model by Park et al.

Table 7-4 and Table 7-5 provide the parameters of the posture prediction models by Park et al. (2016) for females and males, respectively.

Table 7-4: **Input values and parameters of the regression models for F50.** BMI = body mass index (kg/m²). H30 = seat height (mm). L6re = relative steering wheel center with respect to the middle location at each seat height (mm). S = stature (mm). SHS = sitting height/stature.

| Dependent variable | Regression Model |
|--------------------|---|
| Center eye x | $340.0 + (0.355 \times S) + (2.820 \times \text{BMI}) - (0.413 \times \text{H30}) + (0.550 \times \text{L6re})$ |
| Center eye z | $-432.0 + (0.347 \times S) + (942.0 \times \text{SHS}) + (0.923 \times \text{H30})$ |
| Tragion x | $426.0 + (0.348 \times S) + (3.130 \times \text{BMI}) - (0.420 \times \text{H30}) + (0.550 \times \text{L6re})$ |
| Tragion z | $-538.0 + (0.369 \times S) + (1054 \times \text{SHS}) + (0.927 \times \text{H30})$ |
| C7/T1 x | $430.0 + (0.356 \times S) + (2.990 \times \text{BMI}) - (0.394 \times \text{H30}) + (0.535 \times \text{L6re})$ |
| C7T1 z | $-399.0 + (0.299 \times S) + (699.0 \times \text{SHS}) + (1.070 \times \text{BMI}) + (0.930 \times \text{H30})$ |
| T12/L1 x | $8674 - (4.710 \times S) - (15609 \times \text{SHS}) + (3.090 \times \text{BMI}) - (0.370 \times \text{H30}) + (0.491 \times \text{L6re}) + (9.570 \times S \times \text{SHS})$ |
| T12/L1 z | $81.30 + (8.930 \times 10^{-2} \times S) + (0.939 \times \text{H30})$ |
| L5/S1 x | $9853 - (5.360 \times S) - (17602 \times \text{SHS}) - (5.400 \times \text{BMI}) - (2.840 \times \text{Age}) - (0.388 \times \text{H30}) + (0.467 \times \text{L6re}) + (10.80 \times S \times \text{SHS}) + (0.112 \times \text{BMI} \times \text{Age})$ |
| L5/S1 z | $407.0 - (673.0 \times \text{SHS}) + (1.290 \times \text{BMI}) - (7.410 \times \text{Age}) + (0.939 \times \text{H30}) + (13.80 \times \text{SHS} \times \text{Age})$ |
| Mid-hip x | $9446 - (5.190 \times S) - (5.060 \times \text{BMI}) - (16970 \times \text{SHS}) - (2.750 \times \text{Age}) - (0.365 \times \text{H30}) + (0.465 \times \text{L6re}) + (10.50 \times S \times \text{SHS}) + (0.109 \times \text{BMI} \times \text{Age})$ |
| Mid-hip z | $276.0 - (680.0 \times \text{SHS}) + (4.540 \times \text{BMI}) - (5.550 \times \text{Age}) + (0.906 \times \text{H30}) - (5.760 \times 10^{-2} \times \text{BMI} \times \text{Age}) + (12.90 \times \text{SHS} \times \text{Age})$ |
| Right knee x | $5036 - (2.730 \times S) - (8853 \times \text{SHS}) - (0.429 \times \text{H30}) + (0.346 \times \text{L6re}) + (5.400 \times S \times \text{SHS})$ |
| Right knee z | $600.0 + (7.890 \times 10^{-2} \times S) - (1049 \times \text{SHS}) - (0.405 \times \text{Age}) + (0.748 \times \text{H30}) - (0.233 \times \text{L6re})$ |
| Right ankle x | $409.0 - (0.137 \times S) - (1.230 \times \text{BMI}) - (0.382 \times \text{Age}) + (0.115 \times \text{H30}) + (0.142 \times \text{L6re})$ |
| Right ankle z | $63.40 + (0.479 \times \text{BMI}) + (0.115 \times \text{H30})$ |

Table 7-5: **Input values and parameters of the regression models for M50.** BMI = body mass index (kg/m²). H30 = seat height (mm). L6re = relative steering wheel center with respect to the middle location at each seat height (mm). S = stature (mm). SHS = sitting height/stature.

| Dependent variable | Regression model |
|--------------------|--|
| Center eye x | $291.0 + (0.436 \times S) - (0.482 \times H30) + (0.591 \times L6re)$ |
| Center eye z | $-413.0 + (0.313 \times S) + (878.0 \times SHS) + (2.240 \times BMI) + (0.968 \times H30)$ |
| Tragion x | $357.0 + (0.447 \times S) - (0.482 \times H30) + (0.597 \times L6re)$ |
| Tragion z | $-365.0 + (0.305 \times S) + (830.0 \times SHS) + (1.990 \times BMI) - (0.198 \times Age) + (0.974 \times H30)$ |
| C7/T1 x | $367.0 + (0.452 \times S) - (0.454 \times H30) + (0.552 \times L6re)$ |
| C7T1 z | $-290.0 + (0.209 \times S) + (659.0 \times SHS) + (3.180 \times BMI) + (0.972 \times H30)$ |
| T12/L1 x | $-420.0 + (0.862 \times S) + (11.50 \times Age) - (0.414 \times H30) + (0.541 \times L6re) - (6.110 \times 10^{-3} \times S \times Age)$ |
| T12/L1 z | $62.50 + (8.400 \times 10^{-2} \times S) + (0.806 \times BMI) + (0.965 \times H30) + (3.210 \times 10^{-2} \times L6re)$ |
| L5/S1 x | $1619 + (0.380 \times S) - (2286 \times SHS) - (2.340 \times BMI) - (15.50 \times Age) - (0.410 \times H30) + (0.524 \times L6re) + (30.50 \times SHS \times Age)$ |
| L5/S1 z | $11.20 + (2.140 \times BMI) + (0.960 \times H30)$ |
| Mid-hip x | $214.0 + (0.616 \times S) - (680.0 \times SHS) + (7.210 \times Age) - (0.392 \times H30) + (0.546 \times L6re) - (3.860 \times 10^{-3} \times S \times Age)$ |
| Mid-hip z | $533.0 - (1051 \times SHS) - (25.10 \times BMI) - (0.182 \times Age) + (0.935 \times H30) + (50.80 \times SHS \times BMI)$ |
| Right knee x | $4082 - (1.850 \times S) - (6958 \times SHS) + (0.838 \times BMI) - (0.474 \times H30) + (0.391 \times L6re) + (3.680 \times S \times SHS)$ |
| Right knee z | $-68.90 + (0.256 \times S) - (361.0 \times SHS) + (0.731 \times H30) - (0.272 \times L6re)$ |
| Right ankle x | $131.0 + (0.725 \times BMI) + (7.530 \times 10^{-2} \times H30) + (0.141 \times L6re)$ |
| Right ankle z | $-34.50 + (6.900 \times 10^{-2} \times S) + (0.107 \times Age) + (9.740 \times 10^{-2} \times H30)$ |

8 Appendix C: Standing passenger protocol

8.1 Introduction

8.1.1 General Purpose

The general purpose of this document is to outline the process, an assessment protocol, for the evaluation of protection provided by interior structures of public transport vehicles. Of particular interest is the case when a standing passenger loses their balance and stumbles, falls, or strikes vertical structures in the vehicle.

The load cases of interest for this model are based on a review of literature ((Silvano and Ohlin 2019), (Edwards et al. 2019)) that describes scenarios and types of interior contacts relevant for study. Deliverable 5.2 (Xu et al. 2022) outlines the development process of this test protocol and justifies recommended placements of the model inside the vehicle and the recommended pulses relevant for study. Detailed descriptions of the specific features for the VIVA+ Standing Passenger are described in Deliverable 2.5 (Thomson and Kranjec 2021).

8.1.2 Definitions/Abbreviations used in the Report

| Abbreviation | Description |
|--------------|--|
| 50F | Human Body Model representing the 50th percentile (average) Female |
| 50M | Human Body Model representing the 50th percentile (average) Male |
| AEB | Automatic emergency braking |
| HBM | Human Body Model |
| Viva+ SP | VIVA+ Standing Passenger model |
| IS-Scores | Injury Severity Scores |
| SUT | Structure Under Test |

8.1.3 General Requirements

Simulations need to be performed with a freely or commercially available state-of the art simulation software that can also be used by third parties. Reference simulations / Verifications of the code should be performed when changing to other code versions to make sure that results are still valid. All steps described in this document should be used. Solver versions or decomposition for the FE solver shall not be changed throughout the procedure.

8.1.4 User interfaces for in-crash simulation

The following Jupyter notebooks on the OpenVT platform² can be used for evaluating simulations. The notebooks are based on VIVA+ but can be updated to match other HBM models validated for use in this test protocol. Model output definitions used in the Jupyter notebooks are described on the OpenVT platform and also described in 6.3.1. As these notebooks are under constant further development, please follow the instructions and README files in the repository.

- **post_processing.ipynb:** This Jupyter notebook can be used to automatically assess your simulation results using Dynasaur (Klug et al. (2018), Schachner et al. (2018)). For more information on Dynasaur, please visit <https://gitlab.com/VSI-TUGraz/Dynasaur>.
- **post_processing_single.ipynb:** This Jupyter notebook can be used to analyse the results created with Dynasaur for a specific in-crash simulation collision scenario. Output is a pdf report which includes all the necessary information such as injury criteria of different body regions and energies.

8.2 Virtual Models to be tested (Device to be tested)

8.2.1 Calibration of vehicle interior model for passenger safety simulations

The model of interior structures (or SUT) that are subject to a virtual testing assessment must reflect the geometry and material properties of the physical objects in response to an impact by a human. The structural behaviour should be based on component tests and must be well documented. Strain-rate dependency and the deformation behaviour in the range of anticipated impact severity must be considered. The model and its calibration are the responsibility of the manufacturer or supplier. An example interior model is provided in Figure 8-1. Typical obstacles relevant for assessment are vertical and horizontal grab rails, seats, vertical partitions, etc.

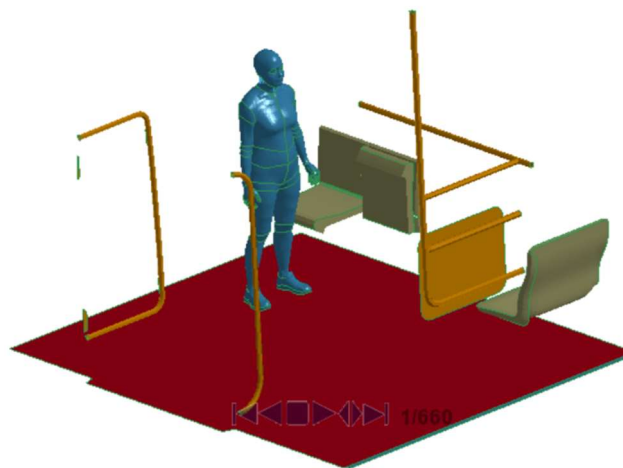


Figure 8-1: Typical interior model of a public transport vehicle

² <https://openvt.eu/wp-4/VISAFE-VRU>

8.2.2 Validation

The standing passenger virtual testing protocol in VIRTUAL is a proposed methodology without any physical implementations at this time. Thus, physical test experience must be extrapolated based on similar testing such as the free motion head form impactor for interior passenger car testing (FMVSS 201³) or the Euro NCAP pedestrian testing protocol (Euro NCAP 2019b). Validation of the vehicle interior has to be performed before the incorporation of the VIVA+ models.

It is recommended that the SUT manufacturer should validate their interior structures using similar dynamic test data to support the simulation of model performance. Impact velocities for free motion head form impacts can be expected to be between 1 and 5 m/s. Simulation results should not deviate more than 10% from the measured test values.

Impactors used for validation tests should be as simple as possible. Validated head form simulation models should be used to ensure the validity of the interior. Validation reports of the impactors should also be available for external analysis.

ISO scores of the acceleration or force vs. time signals should be calculated using the method described in ISO/TS 18571:2022. ISO scores must be higher than 0.58 to fulfil the validation process. Tests used for validation must not be used for the calibration of the interior models. On request of the test institution, tests at other locations might be performed where the manufacturer would have to predict the responses beforehand.

8.2.3 Documentation of validation

All SUT validation steps need to be properly documented. Templates described in IMVITER deliverables can be used as reference.

To ensure that the SUT model remains consistent, it is recommended to apply a procedure to ensure consistency of the files, where checksums are calculated of all included files. This checksum shall be included in the result files to enable a clear link between the output files and the simulation input files.

Test data used for validations must be stored according to ISO-TS 13499. The corresponding simulation outputs must be available in the same format. The calculated IS-Scores related to the files need to be available in table format for all calculated channels.

8.3 Virtual SP models (measurement device)

8.3.1 Prerequisites

Shoes

Shoes must be fitted on the HBM in order to conduct standing passenger simulations. Shoes developed outside the VIRTUAL project must follow the specifications given in Euro NCAP Technical Bulletin TB024 (Euro NCAP 2019a). The shoes provided for the VIVA+ SP model are available on the OpenVT platform⁴. The material properties of the VIVA+ shoes are based on Cho et al. (2009). The

³ Federal Motor Vehicle Safety Standard 201: Occupant Protection in Interior Impact

⁴ <https://openvt.eu/fem/shoes>

baseline shoe geometry is based on freely available geometry data⁵. Each shoe consists of the following parts: Fabric outer, Fabric inner, Sole inner, Sole mid and Sole outer. This can also be seen in Figure 8-2 and Figure 8-3.

To fit the shoes on the VIVA+ model, the geometry of the VIVA+ foot (50F and 50M) was used to generate the inner fabric. All other parts are then adjusted on this geometry. The specifications for the 50M and 50F shoes are given in Table 8.1. The VIVA+ Standing Passenger models are provided on the OpenVT platform⁶ with the shoes already included.

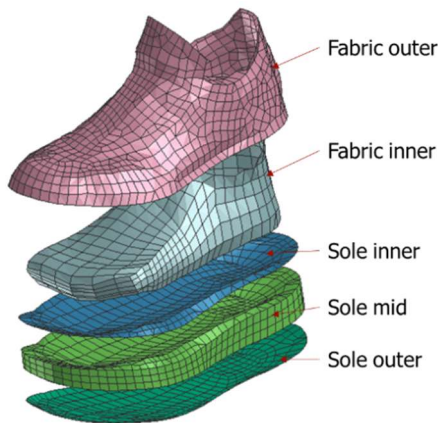


Figure 8-2: Structure of the VIVA+ Shoe Model

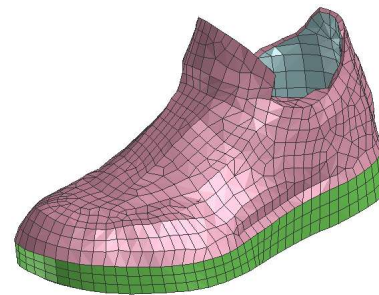


Figure 8-3 VIVA+ Shoe Model

Table 8-1 Specification of VIVA+ shoes – example shown for LS-Dyna

| | 50M | 50F |
|--------------------------------------|--|---------|
| Sole thickness (at the heels) | 26.5 mm | 26.5 mm |
| Weight of one shoe | 694 g | 532 g |
| Fabric outer | Section: Shell 1mm; Material: *MAT_ELASTIC (LS-Dyna) | |
| Fabric inner | Section: Shell 1mm; Material: *MAT_ELASTIC (LS-Dyna) | |
| Sole inner | Section: Shell 1mm; Material: *MAT_ELASTIC (LS-Dyna) | |
| Sole mid | Section: Solid; Material: *MAT_ELASTIC (LS-Dyna) | |
| Sole outer | Section: Shell 1mm; Material: *MAT_ELASTIC (LS-Dyna) | |
| Contact Fabric outer to Fabric inner | *CONTACT_AUTOMATIC_SINGLE_SURFACE (LS-Dyna) | |
| Contact right shoe to left shoe | *CONTACT_AUTOMATIC_SINGLE_SURFACE (LS-Dyna) | |
| Contact Foot to Shoe | *CONTACT_AUTOMATIC_SURFACE_TO_SURFACE (LS-Dyna) | |

⁵ <https://free3d.com>

⁶ [Robert Thomson / WP2-Task5 · GitLab \(openvt.eu\)](#)

8.3.2 Model preparation

8.3.2.1 Posture & Geometry

The standing passenger models have been pre-positioned to represent the volunteer posture used to validate the models. Alteration of the joint angles will affect the model's response resulting from the pre-programmed muscle activities in the lower limbs. Both a 50M and a 50F model are available. Figure 8-4 shows the original posture of the model and reference volunteer at the start of simulation. Positioning of the VIVA+ SP Model⁷ to recreate the position of limbs and stance width was accomplished with tools developed in the PIPER project⁸. Other HBM positioning tools may be applied.

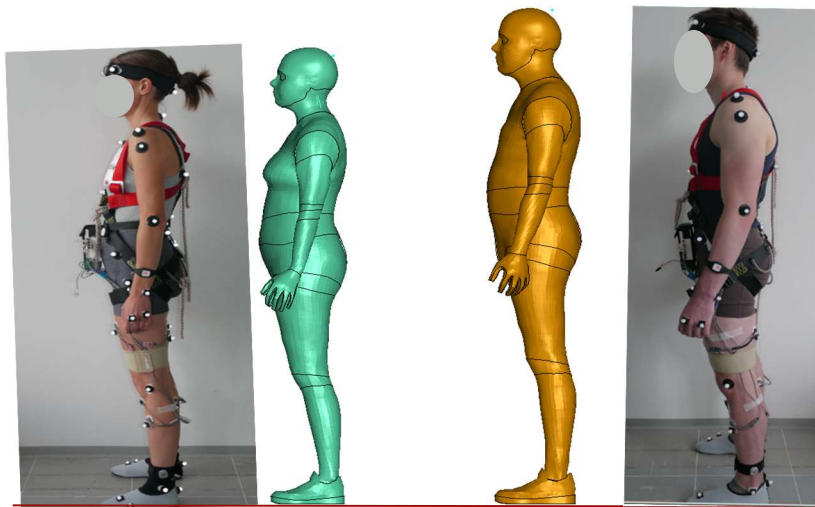


Figure 8-4: Posture of female volunteer (left), VIVA+ SP Models (Center), and male volunteer (Right)

8.3.2.2 Output definitions

The kinematic assessments of the HBM simulations can utilise predefined landmarks. A list of all landmarks can be found in Table 6-1. The landmarks are defined according to the ISB recommendations (Wu and Cavanagh, 1995; Wu et al., 2002; Wu et al., 2005). The recommended output interval for node histories is 0.1ms. In the head centre of gravity, a seatbelt-accelerometer (LS-Dyna) provides kinematic outputs in a local frame of reference relative to the xy plane parallel to the Frankfort plane. Please also see ANNEX B: HUMAN BODY MODEL OUTPUT of the Euro NCAP Technical Bulletin TB024 (Euro NCAP 2019b) for more information of how the landmarks should be connected to the HBM. All required landmarks are included in the VIVA+ models by default.

8.3.2.3 Tissue-based assessment in in-crash simulation

Strain based tissue assessments of specific cortical bones can be analysed. A list of cortical bones and ligaments suitable for analysis is given in Table 6-2. For these body parts, injury risk curves are available for the strain-based assessment. The output interval for strain values should be 1.0 ms. For LS-Dyna the strain flag (STRFLG) in *DATABASE_EXTENT_BINARY has to be set to 1 to have the strain output also for shell elements in the binary files. Note that the VIVA+ Standing Passenger cannot provide the same output as the VIVA+ Pedestrian model due to the introduction of simplified revolute joints and rigid bodies in the lower extremities.

⁷ [model · main · FE_models / VIVA / vivaplus · GitLab \(openvt.eu\)](#)

⁸ [framework \[piper-project.org\]](#)

8.3.2.4 Qualification procedure

Anthropometry requirements

Human Body Models have to be used in two different anthropometries. One should reflect the average female (50F) and the other one the average male (50M) anthropometry. The dimensions should be based on the statistical models available on humanshape.org for the settings described in Table 8-2. All landmarks should be met with a tolerance of 10 mm.

Table 8-2: Target anthropometries for 50F and 50M models

| | 50F | 50M |
|------------------------|---------|---------|
| Population | US | US |
| Gender | Female | Male |
| Stature | 1620 cm | 1750 cm |
| Weight | 62.3 kg | 77.3 kg |
| Sitting height/stature | 0.52 | 0.52 |
| Age | 50yrs | 50yrs |

Validation of the VRU in-crash Models

The VIVA+ SP is derived from a validated version of the standing occupant model used for pedestrian and cyclist impacts. Any HBM models used for the assessment of injury have to be validated according to the current state of scientific knowledge. Validation setups shared for the VIVA+ models should be used as reference. The overall stiffness should be evaluated with hub impacts (Viano et al., 1989). The full body kinematics should be evaluated using PMHS tests where vehicle models to perform the validations are openly available. Detailed descriptions of the validation procedures and all related models are available within the VIVA+ validation catalogue on <https://vivaplus.readthedocs.io>.

Validation of the muscle activity during the perturbation response is described in Deliverable 2.5 (Thomson et al., 2021). Applications of HBMs developed outside of VIRTUAL should use this or other similar test data.

8.3.3 Test setups

8.3.3.1 Test environment

For conducting the simulations of the VRU in the test environment, one must use the same models, control setting and solver as for the validation and qualification procedures.

Positioning for in-crash simulation

Figure 8-5 depicts the trajectory of three regions of the body if the HBM were to move unrestricted in an example bus interior. This figure must be generated by the user to prior to conducting a simulation as it is needed to position the HBM relative to the obstacle of interest. Different times are noted on the curves so the position of each body can be identified at the time of contact of another body part. This is also needed to define the time to switch the rigid elements in the upper torso to deformable and ensure proper injury severity prediction.

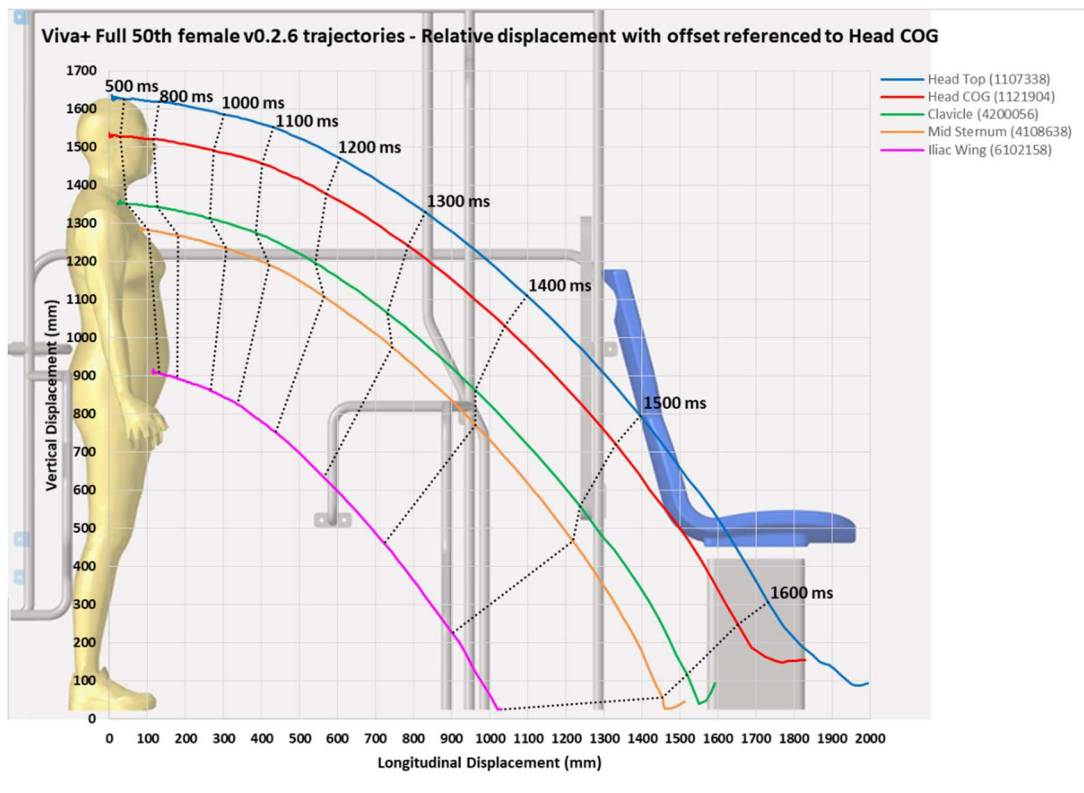


Figure 8-5 Trajectory of key body regions of 50% Female

The protocol recommends two impact conditions: 1) direct contact with the head and 2) an offset of 100 mm laterally to create an impact with the chest or clavicle. These two positions are presented in Figure 8-6. The trajectory paths in Figure 8-5 are needed to identify the maximum impact speed for the segment of interest, head or chest.

The geometric location of the reference obstacles in the horizontal plane (x,y) must be known in the coordinate system of the interior model. The interior model should be positioned relative to the sagittal plane of the VIVA+ SP. The longitudinal reference position for the VIVA+ SP is the forward edge of the Anterior Sacrum (node 8340031 in VIVA+SP) shown in Figure 8-8.

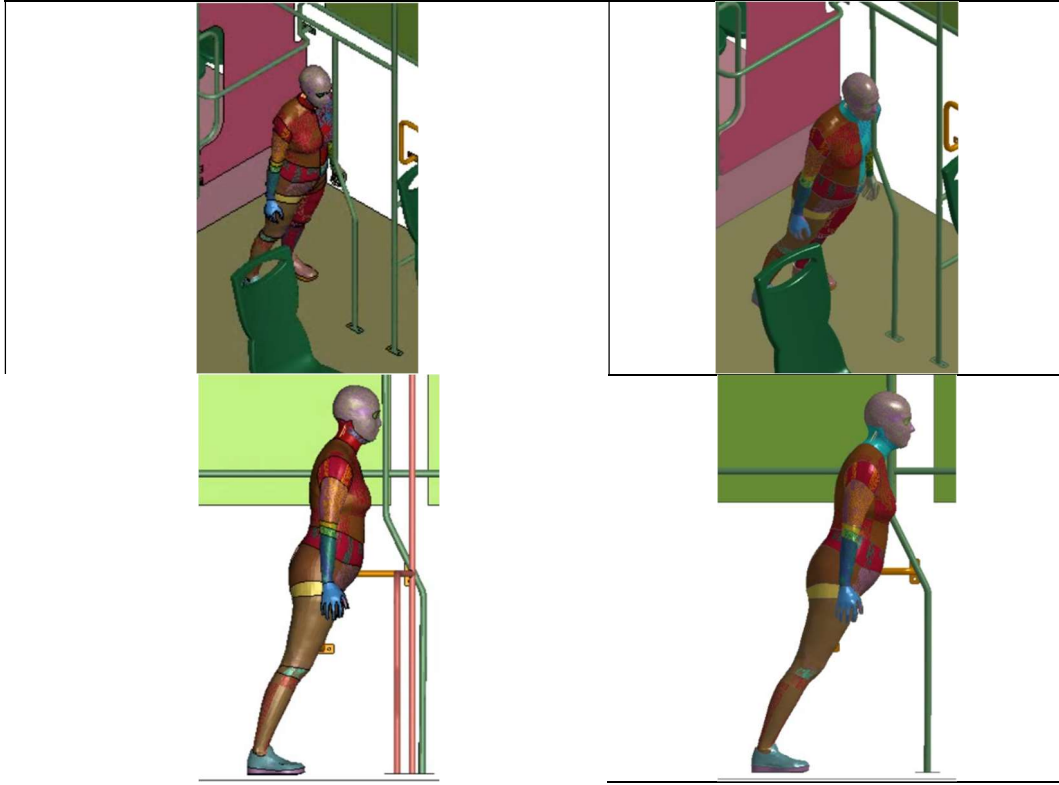


Figure 8-6: Impact Configuration-Left: Centred on head, Right: Offset 100 mm laterally

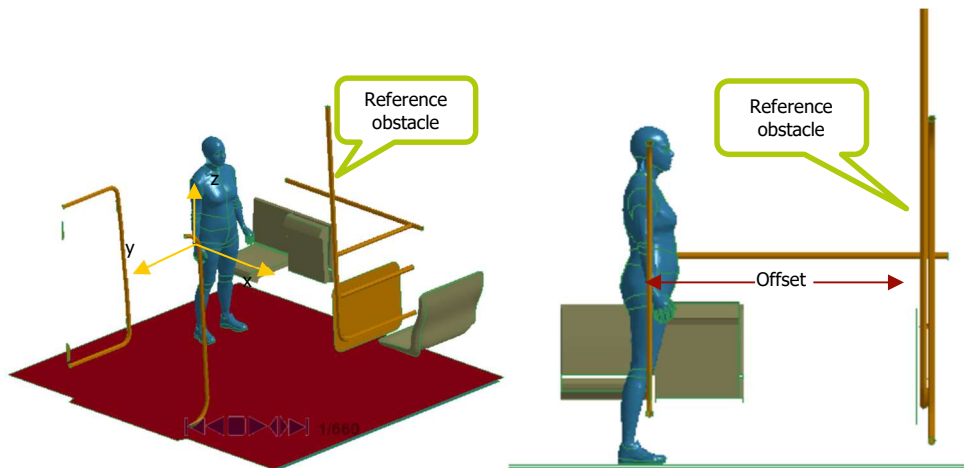


Figure 8-7: Occupant position relative to the interior reference obstacle

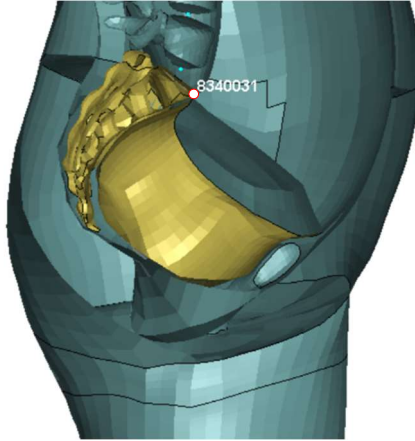


Figure 8-8: Reference position on VIVA+ SP for Positioning

In the load case shown in Figure 8-7, the passenger is aligned with the upright hand support. In the case of hard braking, the passenger would fall forward and strike the post.

The simulation input files should use the VIVA+SP as the reference coordinate system. The additional model elements (SUT) shall be included using the `*INCLUDE_TRANSFORM LS-DYNA` keyword with the translation and rotation information specified in `*DEFINE_TRANSFORMATION`:

```
*DEFINE_TRANSFORMATION
$# traid
  1
$# option   a1      a2      a3      a4      a5      a6      a7
TRANSL     x       y       z       0.0    0.0    0.0    0.0
ROTATE     a       b       c       d       e       f       g
```

Here, a1, a2, and a3 are the x, y, z translations required to position the object of interest relative to the HBM. The rotation elements define the rotation in degrees (g) about the direction cosines (a,b,c) about the x,y,z coordinates (d,e,f).

The vertical position of the passenger should include a 4 mm offset from the top floor surface to the shell elements on the soles of the shoes to account for the contact offset defined in the shell elements of the soles.

It should be noted that the motion of the passenger may not be parallel to the applied acceleration vector. The original posture of the VIVA+ SP was modified to account for the volunteer postures and this process also introduces slight asymmetries. The slight asymmetries in the model can cause lateral motions of the models due to the active muscle moments being applied through revolute joints. This will be identified in a pre-run of the passenger model described earlier to observe any lateral motions to the point of intended impact. The passenger can then be re-positioned laterally to account for the known motion. This situation is illustrated in the example simulation described in Section 3.4 in Milestone 5.4 (Thompson and Kranjec (2021)).

Pre-simulation

A gravity settling phase is required to allow the VIVA+SP to load the shoes and floor. A gravity settling period of 100 ms is recommended. Global damping is applied and removed with a Sigmoid function in the VIVA+ SP files.

Contact definitions in in-crash simulation

The simulation should be checked to ensure there are no initial penetrations of contact surfaces. For the contact between HBM and interior structures the sets shown in Table 8-3 and Table 8-4 should be created. With these sets, the following contacts should be implemented:

- **Skin Head to whole interior**
- **Skin Torso incl. Hip and Neck to whole interior**
- **Skin left Arm to whole interior**
- **Skin right Arm to whole interior**
- **Skin left Leg to whole interior**
- **Skin right Leg to whole interior**
- **Shoes to whole interior**

In LS-Dyna, the bold given contacts should be modelled as:`*CONTACT_AUTOMATIC_SURFACE_TO_SURFACE` and the other contacts. Similar contacts can be used if all quality criteria are fulfilled.

Instead of the entire interior, specific obstacles can be prioritised depending on the impact of interest. Typical interior obstacles of interest are shown in Table 8-4.

Table 8-3 Contact Sets for HBM

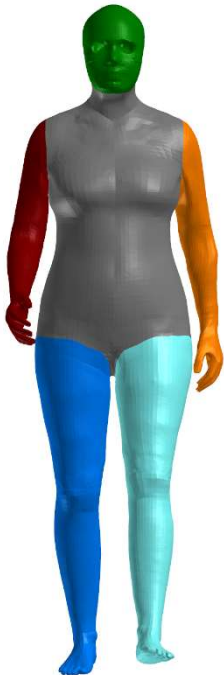
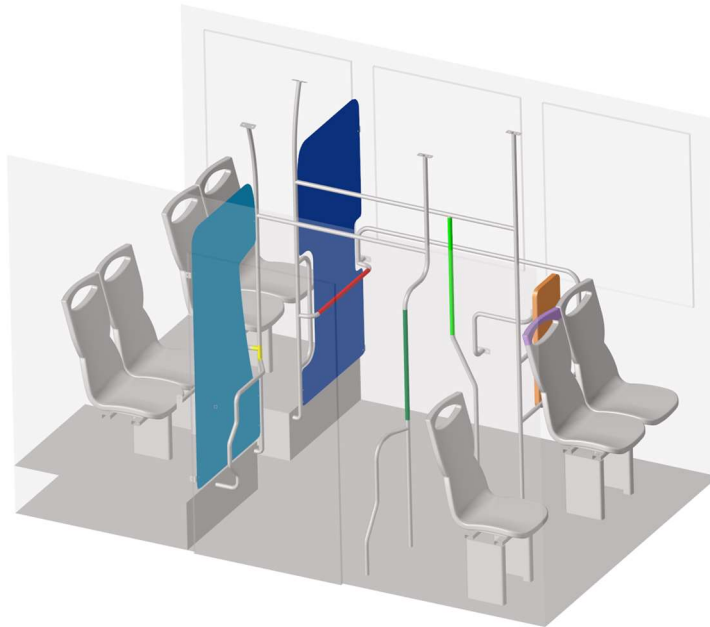
| | Contact Set |
|---|-------------------------------|
|  | Skin Head |
| | Skin Torso incl. Hip and Neck |
| | Skin left Arm |
| | Skin right Arm |
| | Skin left Leg |
| | Skin right Leg |

Table 8-4 Contact Sets for interior

Obstacles

| |
|----------------|
| Vertical bar1 |
| Vertical bar2 |
| Horizontal bar |
| Bar joint |
| PRM restrain |
| Partition |
| Seat |



8.3.3.2 Loading direction and severity

The models include one validated loading direction parallel to the sagittal plane of the HBM. The revolute joints and prescribed joint moments are only valid for longitudinal loading. A prescribed motion shall be placed on the interior structures to represent the braking motion the passenger is reacting to and that presents a risk for striking an interior structure. The motion time history is shown in Figure 8-9.

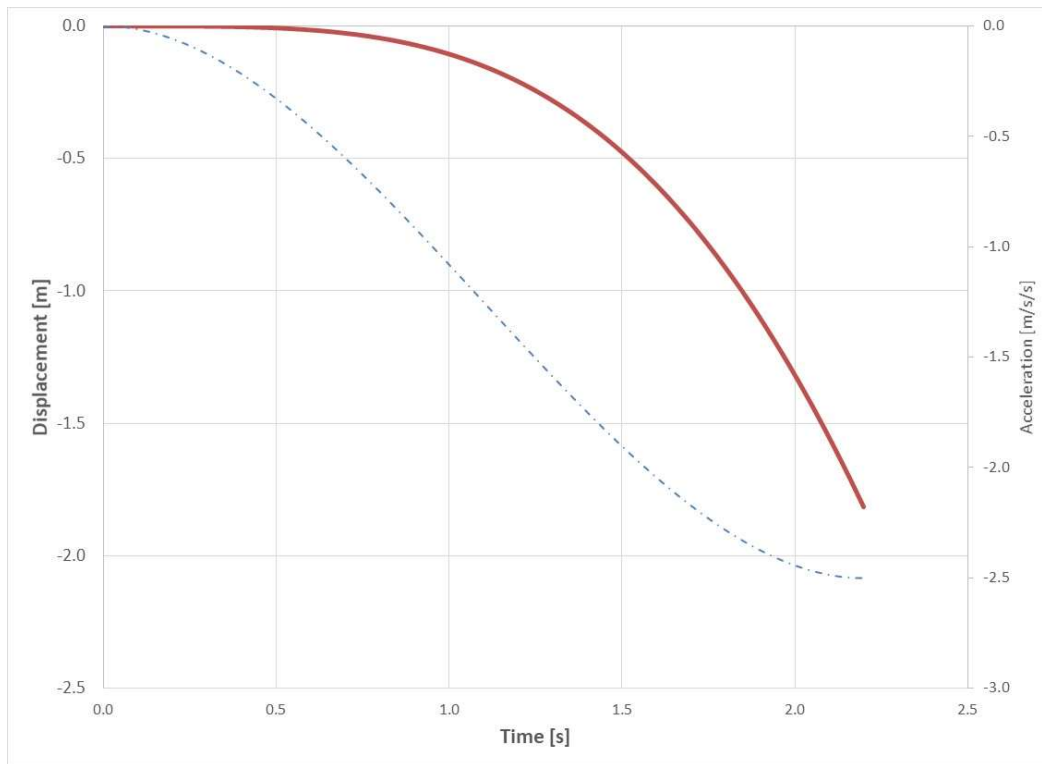


Figure 8-9: Perturbation Time History - Red Curve: Displacement (left axis), Dashed Curve: Acceleration (right axis).

The loading profile is derived from measured vehicle data and is described in Linder et al. (2020) The load curve specification for the braking motion is provided in the "simulation_control.k" input file in the OpenVT repository.

The use of any other pulses will require a new definition of the joint moment time histories. The calibration and validation of the HBM response is described by Thomson and Kranjec (2021).

8.3.3.3 Outputs definitions of test setups

Necessary outputs are activated by default in the models provided. In case other outputs are needed, please follow LS-Dyna keywords recommendations to define them.

The Dynasaur data processing routines provided on the OpenVT platform can be used as a model for user defined processing of model outputs in other post processing environments.

8.3.3.4 Simulation time

The in-crash simulations should at least last 100 ms longer than the time of head or body impact on the structure. The muscle activity is modelled and calibrated to represent the first second (1000 ms) of the balance perturbation. Volunteer variations in stepping times can even lead to simulation times of 1500 ms. Due to the limited functionality of muscles and the lack of sophisticated stepping simulations, the maximum recommended simulation time for the VIVA+ SP is 2000 ms and represents a worst case fall of an unaware standing passenger.

8.3.4 Virtual test conditions (test runs)

8.3.4.1 Simulation matrix

The position of the VIVA+ models from one of the obstacles of interest has not been standardised by international working groups. The longitudinal and lateral position of the HBM shall be determined from Figure 8-5 to recreate the head and chest impact conditions of interest outlined by 2 load cases identified in Table 8-5. The manufacturer may investigate other positions of interest.

The loading profile described in Section 8.3.3.2 is the only loading environment recommended for the VIVA+ SP without a new calibrated joint control definition.

Table 8-5: Test Matrix for Standing Passenger

| Vertical Bar | Minimum Distance [mm] | Maximum Distance [mm] |
|----------------|-----------------------|-----------------------|
| Horizontal Bar | 500 | 900 |
| PRM restraint | 500 | 900 |
| Partition | 500 | 1000 |
| Seat | 500 | 900 |

8.3.5 Evaluation of virtual testing results

8.3.5.1 Postprocessing definitions

Calculation procedures for in-crash simulation

This section describes the available injury risk assessment criteria applicable for the VIVA+ SP. Only criteria compatible with the model functionality are recommended.

8.3.5.2 Injury Assessments

The following injury criteria should be evaluated (definitions see chapter Injury Manual):

- HIC 15
- DAMAGE
- Rib fracture

8.3.5.3 CBA

The VIRTUAL cost-benefit calculation tool for vehicle safety systems was developed by Wijnen et al. (2020). This tool does not have a module for standing passenger injuries.

8.3.5.4 Documentation and Data Specification

The simulation output files (animations and time histories) must be stored with any tables generated with the Jupyter notebooks.

The results of the assessment of the in-crash simulations will be stored as PDF reports. The guidelines for the documentation of the test are currently a work in progress and will be further described in the next version of the protocol.

8.4 References

Cho, Jin-Rae, Seung-Bum Park, Sung-Hyun Ryu, Sung-Ho Kim, and Shi-Bok Lee. «Landing impact analysis of sports shoes using 3-D coupled foot-shoe finite element model.» *Journal of mechanical science and technology* (Springer) 23 (2009): 2583–2591.

- Edwards, Mervyn, Alix Edwards, Josh Appleby, and Dean Beaumont. «Banging heads onboard buses: assessment scheme to improve injury mitigation for bus passengers.» *Traffic injury prevention* (Taylor & Francis) 20 (2019): S71–S77.
- Euro NCAP. «Pedestrian Human Model Certification. TB 024.» <https://cdn.euroncap.com/media/56949/tb-024-pedestrian-human-model-certification-v20.pdf>, 2019a.
- Euro NCAP. «Pedestrian testing protocol.» <https://cdn.euroncap.com/media/41769/euro-ncap-pedestrian-testing-protocol-v85.201811091256001913.pdf>, 2019b.
- John, J ., et al. «Validated seated OS-HBM models published on the OpenVT platform and described in scientific papers.» *Deliverable D2.2 of the H2020 project VIRTUAL*. 2021.
- Linder, Astrid, et al. «Test specifications for VT of erect passengers on public transport.» *Milestone Report M5.3 of the H2020 project VIRTUAL*. Gothenburg, Sweden, 2020.
- Silvano, Ary P., and Maria Ohlin. «Non-collision incidents on buses due to acceleration and braking manoeuvres leading to falling events among standing passengers.» *Journal of Transport & Health* (Elsevier) 14 (2019): 100560.
- Thomson, Robert, and Matej Kranjec. «Test case simulations for erect passengers on public transport to be used for validation including instructions/documentation.» *Milestone M 5.4 of the H2020 project VIRTUAL*. 2021.
- Thomson, Robert, Matej Kranjec and Luis Martinez. «Validated erect transit passenger model on OpenVT platform and documented in scientific publications.» *Deliverable D2.5. of the H2020 project VIRTUAL*. 2022.
- Viano, David C., and Ian V. Lau. «Thoracic impact: a viscous tolerance criterion.» Tech. rep., SAE Technical Paper, 1985.
- Wu, Ge, et al. «ISB recommendation on definitions of joint coordinate system of various joints for the reporting of human joint motion—part I: ankle, hip, and spine.» *Journal of biomechanics* (Elsevier) 35 (2002): 543–548.
- Wu, Ge, et al. «ISB recommendation on definitions of joint coordinate systems of various joints for the reporting of human joint motion—Part II: shoulder, elbow, wrist and hand.» *Journal of biomechanics* (Elsevier) 38 (2005): 981–992.
- Wu, Ge, and Peter R. Cavanagh. «ISB recommendations in the reporting for standardization of kinematic data.» *J. Biomech* 28 (1995): 1257–1261.
- Xu, J-C., et al. «Description of safe operation envelope for erect passengers on public transport.» *Deliverable D 5.2 of the H2020 project VIRTUAL*. 2022.

9 Appendix D: Test protocol vulnerable road users (VRU)

9.1 Introduction

9.1.1 General Purpose

The general purpose of this document is to outline a holistic assessment procedure for the evaluation of VRU protection. Before establishing such a procedure further discussions with different parties are needed to fine-tune the procedure and check feasibility of all steps. The document, which describes the procedures applied or drafted within the VIRTUAL project, should be considered as a starting point.

The aim was to model a scenario-based VRU assessment taking active and passive safety measures into account. It thereby considers cyclists and pedestrians as well as female and male road users equally to assess the active and passive protection systems of the vehicle under test (VUT).

9.1.2 Definitions/Abbreviations used in the Report

| Abbreviation | Description |
|--------------|--|
| 50F | Human Body Model representing the 50th percentile (average) Female |
| 50M | Human Body Model representing the 50th percentile (average) Male |
| AEB | Automatic emergency braking |
| Baseline | Baseline simulations are based on the original virtual testing scenarios. Active safety systems have not been considered (w/o AEB) |
| DoE | Design of Experiments |
| GUI | Graphical user interface |
| HBM | Human Body Model |
| MaxPro | Maximum Projection |
| QALY | Quality Adjusted Life Year |
| VRU | Vulnerable Road User |
| VRU VISAFE | Virtual integrated safety assessment of vulnerable road users |
| VUT | Vehicle Under Test |

9.1.3 Overview of Assessment procedure

An overview of the virtual integrated safety assessment of vulnerable road users (VRU VISAFE) is given in Figure 9-1. Based on accident data a catalogue of virtual testing scenarios was created and used for the agent based pre-crash simulations. This agent based pre-crash simulations are conducted without (baseline) and with a generic autonomous emergency braking system (AEB). The accident

parameters (collision speed VRU and Vehicle, collision angle and collision point) of the accidents that are not avoided by an AEB system - are combined with occurrence probabilities from the accident data analyse which results in the collision scenarios for the in-crash simulations.

With the help of a DoE method, a certain number of collision scenarios for in-crash simulations is selected such that a good space filling is obtained. By conducting in-crash simulations with HBMs and vehicle models, injury probabilities for different body regions of the selected collision scenarios can be determined. Using a meta model, the injury probability for collision scenarios which are not included in the in-crash simulations can be obtained. Based on the injury probability for all non-avoided cases through the AEB system an overall injury probability can be calculated which can be used for a cost-benefit analysis.

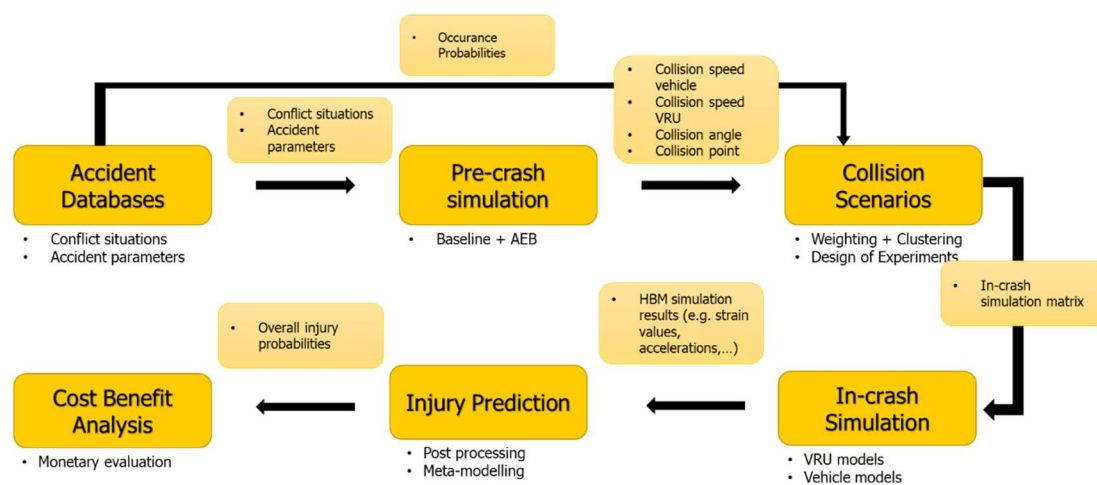


Figure 9-1 Overview of virtual integrated safety assessment of vulnerable road users VISAFAE-VRU

9.1.4 General Requirements

Simulations need to be performed with a freely or commercially available, state-of-the-art simulation software that can also be used by third parties. Reference simulations / Verifications of the code should be performed when changing to other code versions to make sure that results are still valid. For all steps described in this document the same simulation framework should be used (one pre-crash and one in-crash environment). Solver versions or decomposition for the FE solver must not be changed throughout the whole procedure.

9.1.5 Tooling and user interfaces for pre-crash simulation

Within this chapter the pre-crash tool of VISAFAE-VRU and its user interface developed within VIRTUAL are described. Detailed instructions in a manual-style are provided for the pre-crash tool.

The procedures described for the pre-crash simulation could also be applied with other type of pre-crash tools. If users wish to use a different tool, they would have to benchmark it against the described open-source tool, document the deviations and find ways to set up the scenarios and perform the analysis comparable to those described in this document.

9.1.5.1 Basic components

The virtual-pre-crash tool consists of four main components, which form a toolchain as shown in Figure 9-2. The output of one component is used as input for the subsequent one, which was described in (Schachner et al., 2020).

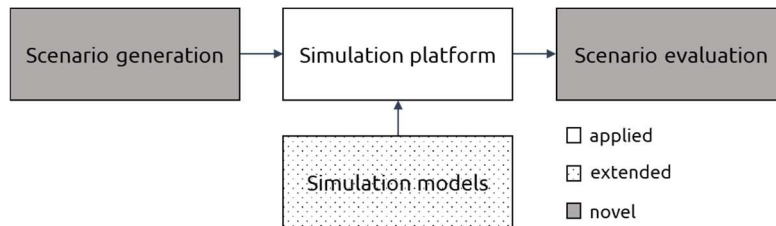


Figure 9-2: The main components of the virtual-pre-crash-tool to generate, simulate and evaluate scenario catalogue derived from potential vehicle to VRU conflict situations (Schachner et al., 2020).

9.1.5.2 Graphical User Interface

In order to evaluate future collision scenarios in a user-friendly way, a graphical user interface (GUI) has been implemented as a Dash application, which is shown in Figure 9.3. Dash is an interactive, open-source plotting library that provides online graphing, analytic and statistic tools for different programming languages, i.e. Python.

Prerequisites

The source code is part of the git repository of the vru-precrash-tool, and can either be downloaded or cloned from the OpenVT platform. In order to run the application, additional packages are required, which can be installed using the command:

```
>>> pip install -r <path/to/requirements.txt>.
```

To launch the application, the `dash_app/index.py` script has to be executed, which opens a local webserver on port `127.0.0.1:8050`

Usage

In order to run `dash_app/index.py` it is necessary to pass `--dest` `<path/to/generated/scenario/directory>` command line argument

```
>>> python dash_app/index.py --dest <path/to/generated/scenario/directory>
```

Specified `--dest` directory is created if it does not exist. Existing simulations (previously performed) are listed in the sidebar of the GUI. Simulations conducted in the session are saved in the `--dest` directory. Further information on the output directory structure can be obtained from Section 9.3.2.2.

Dash application

The dash application's welcome screen's main part represents a sidebar consisting of a dropdown, in which certain conflict types (car_ped, car_cyclist, tram_ped) can be selected, and a + button. According to the chosen Conf Type dropdown option, the simulated scenario catalogues available in the --dest directory are outlined below.

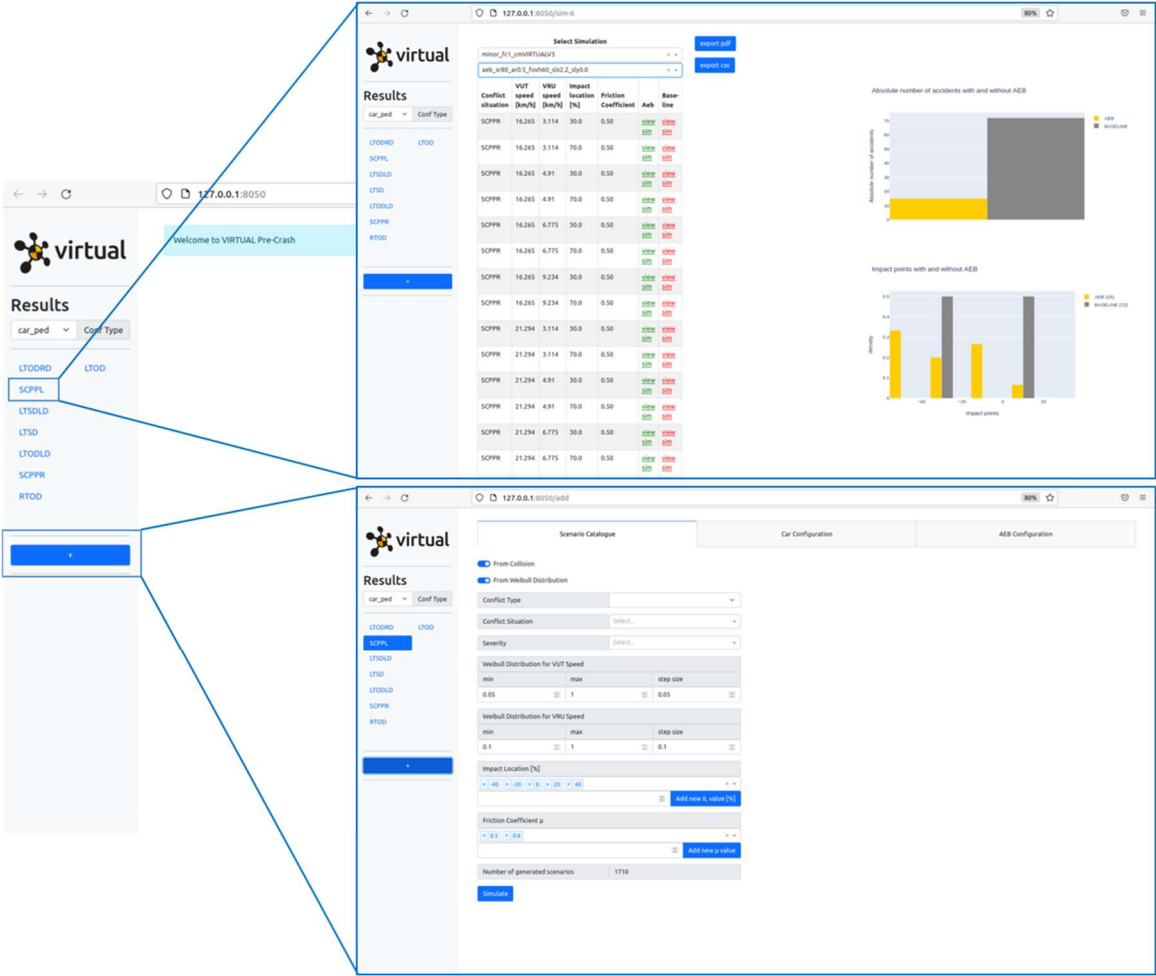


Figure 9-3: Illustration of Graphical User Interface (GUI): In the initial layout of the dash application, the user can choose further to generate new scenarios or evaluate existing ones.

How to generate a new scenario catalogue

By pushing/pressing the + button in the left of the dash application, the canvas in the right is updated to generate a scenario catalogue. To create a scenario catalogue, the user must select a conflict type, situation and severity. The accident statistics from Deliverable D4.1 are loaded by default for each configuration. Next, the user must select the required parameters for the scenario catalogue generation process, which are further discussed in the following sections (split up in scenario generation parameters, vehicle configuration parameters, and AEB parameters as seen in Figure 9-4.

How to show an evaluation of one of the already generated conflict scenarios

By clicking on one of the listed scenario catalogues in the sidebar, the canvas in the right is updated with two dropdown menus from which a specific scenario can be selected and evaluated. Further descriptions can be found in Scenario Evaluation and Postprocessing definitions for pre-crash simulation (9.6.1.1)

Simulation Models

Further explanations can be found in Virtual Models to be tested (9.2.1).

Scenario Generation

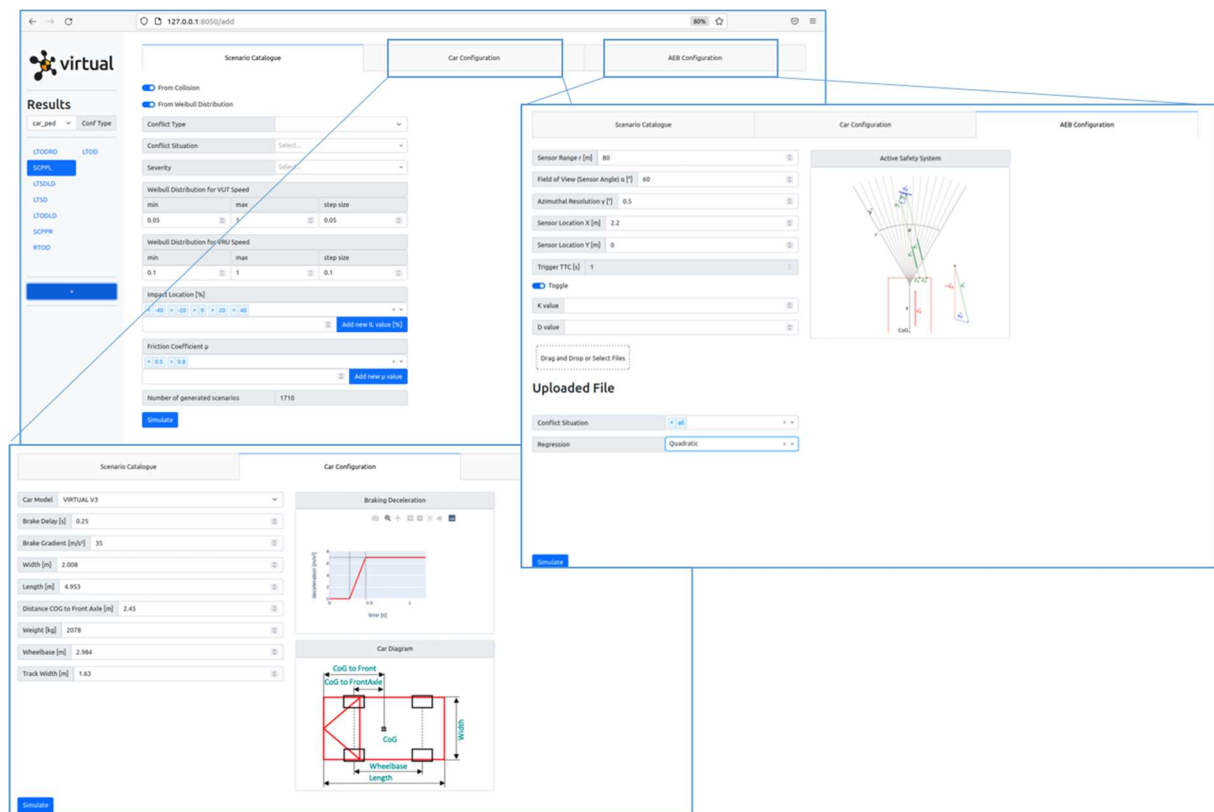


Figure 9-4: Graphical User interface (GUI) for the Scenario Generation process. The GUI is split into three parts: the scenario catalogue, the car configuration and the AEB configuration.

Parameters that can be configured to generate a particular scenario can be divided into three groups:

- Scenario Catalogue
- Car Configuration
- AEB Configuration

Once all the desired parameters are selected, the user can generate the scenario by pressing the **Simulate** button at the bottom.

Scenario Catalogue

In this section, `Conflict Type`, `Conflict Situation` and `Severity` are mandatory fields. Depending on the selected conflict situation, other fields are set by default and can be adjusted if desired.

- **From Collision:** This parameter is set to `True` by default. The simulation will be generated from the road end if the switch is set to `False`. Otherwise, it will be generated from the collision point.
- **From Weibull Distribution:** This parameter is set to `True` by default. If set to `False`, VUT/VRU speed values are entered as speed in km/h. Otherwise, `Weibull Distribution for VUT/VRU speed` is entered, and as the output of these values via shape and scale parameters, corresponding VUT and VRU speeds are obtained.

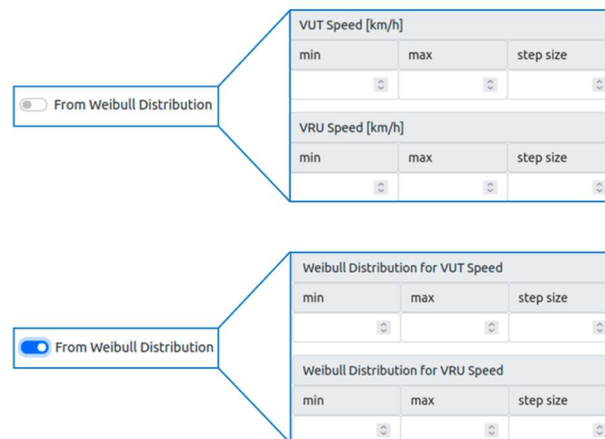


Figure 9-5: If `From Weibull Distribution` switch is `False`, the user is offered to choose `VUT/VRU Speed [km/h]` parameters. Otherwise, to the user may select `Weibull Distribution for VUT Speed` parameters.

- **Conflict Type:** In this dropdown menu, one of the three offered conflict type options can be chosen: `car_ped` (to simulate conflict situation with car and pedestrian), `car_cyc` (to simulate conflict situation with car and cyclist) and `tram_ped` (to simulate conflict situation with tram and pedestrian).
- **Conflict Situation:** It is possible to choose one, more or all stored conflict situations stored in the dropdown menu. Since it is impossible to display all selected conflict situations in the GUI, the graphical display of conflict situations is only displayed if one conflict situation is selected, as shown in Figure 9-6.

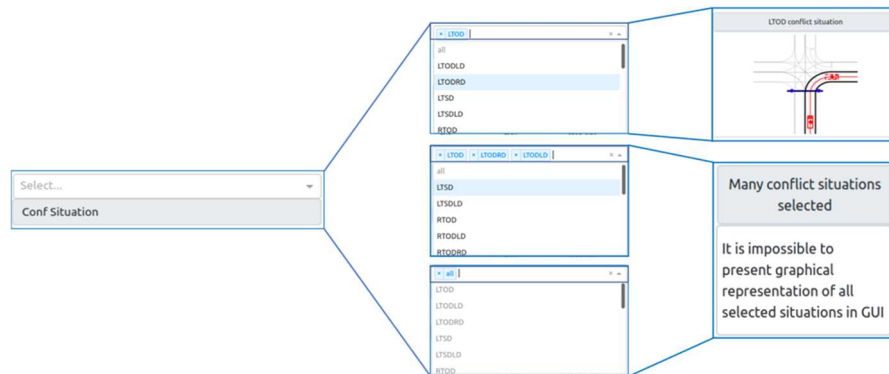


Figure 9-6: User interface to select one or multiple conflict situations

- Severity:** In this dropdown menu, several options can be selected. It is possible to choose one, more or all offered severity levels. The VUT and VRU speed default values are automatically set when the Weibull switch is set to False and the severity option is selected. If the Weibull distribution switch is True then the Weibull Distribution for VUT and VRU values are set. The cumulative distribution functions (CDFs) of the set Weibull distributions are visualised in the GUI as presented in Figure 9-7.

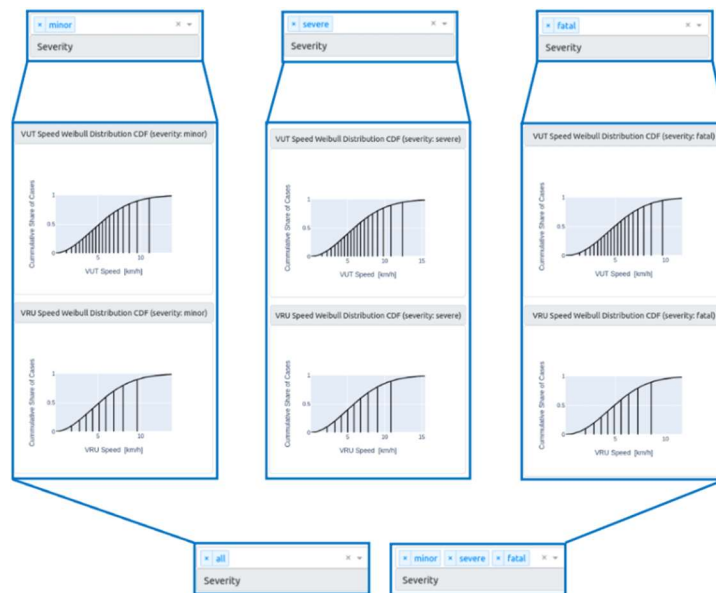


Figure 9-7: Visualisation of Weibull distributions. If From Weibull Distribution switch is True, and values for VUT Weibull Distribution for VUT/VRU Speed are set, Weibull Distribution CDF plots are shown in GUI for the respective severity.

When a conflict directory is generated, it contains various .html files. Therefore, VUT and VRU speed, impact location and friction coefficient parameters are arrays.

- Since each .html file represents one combination of VUT and VRU speed, impact location, and friction coefficient values, the total number of scenarios generated is given by the product of the lengths of these arrays.

- **VUT speed [km/h] or Weibull Distribution for VUT Speed:**
If `From Weibull Distribution` switch is `False`, the user is offered to choose `VUT Speed [km/h]` parameters. Otherwise, it is provided to select `Weibull Distribution` for `VUT Speed` parameters.
- **VUT speed [km/h]:** The most straightforward way for the user to configure the VUT speed array is to select the desired values for the following parameters:
 - **Min:** This parameter represents the first value in the initial VUT speeds array.
 - **Max:** This parameter represents the end of the initial VUT speeds array and is not included in the array.
 - **Step size:** This parameter represents the spacing (difference) between each two consecutive VUT speed values in the array.

If one conflict situation is selected, the default values for `min`, `max` and `step size` are set, but it is possible to manually change these values. If more conflict situations are selected, changing these options is disabled.

Weibull Distribution for VUT Speed: Same as for `VUT Speed` case here also the user defines the array with the following parameters:

- **Min:** This parameter represents the first probability value in the initial Weibull Distribution probability array.
- **Max:** This parameter represents the end probability in the initial Weibull Distribution probability array, and this probability is not included in the array.
- **Step size:** This parameter represents the spacing (difference) between each two consecutive probabilities in the array.

The array created by entering these fields represents the Weibull distribution's input values. In addition, shape and scale values, which are explained in more detail in Simulation matrix for pre-crash simulations (Section 9.5.1.1), are passed as input values for the Weibull distribution. As output, the Weibull function then returns an array of the initial VUT speeds.

- **VRU speed [km/h] or Weibull Distribution for VRU speed:**
if `From Weibull Distribution` switch is `False`, the user is offered to choose `VRU Speed [km/h]` parameters. Otherwise, it is provided to select `Weibull Distribution` for `VRU Speed` parameters.
- **VRU speed [km/h]:** The most straightforward way for the user to configure the VRU speed array is to select the desired values for the following parameters:
 - **Min:** This parameter represents the first value in the initial VRU speeds array.
 - **Max:** This parameter represents the end of the initial VRU speeds array and is not included in the array.
 - **Step size:** This parameter represents the interval between each two consecutive VRU speed values in the array.

If one conflict situation is selected, the default values for `min`, `max` and `step size` are set, but it is possible to change these values. If more conflict situations are selected, changing these options is disabled.

Weibull Distribution for VRU Speed: Same as for `VRU Speed` case here also the user defines the array with the following parameters:

- **Min:** This parameter represents the first probability value in the initial Weibull Distribution probability array.
- **Max:** This parameter represents the end probability in the initial Weibull Distribution probability array; this probability is not included in the array.
- **Step size:** This parameter represents the interval between every two consecutive probabilities in the array.

The array created by entering these fields represents the Weibull distribution's input values. In addition, shape and scale values, which are explained in more detail in "Simulation matrix for pre-crash simulations" (Section 9.5.1.1), are passed as input values for the Weibull distribution. As output, the Weibull function then returns an array of the initial VRU speeds.

- **Impact Location (IL) [%]:** This field is displayed only when `From Collision` switch is set to `True`. It is possible to select more options in this dropdown menu. This parameter represents the impact locations between VRU and VUT, which are defined concerning the centre of the corresponding contour edge.
 - **Add new IL value [%]:** If the user wants to add a value not offered in the `Impact Location` dropdown options, they can enter that value in the range [-50, 50] in the input field and add it by clicking the `Add new IL value [%]` button.

If one conflict situation is selected, the default impact locations are set, but it is possible to change these values. If more conflict situations are selected, changing these values is disabled.

- **Friction Coefficient μ :** This field is displayed only when `From Collision` switch is set to `True`. It is possible to select more options in this dropdown menu, with values between 0.5 and 1.
 - **Add new μ value:** If the user wants to add a value not offered in the `Friction Coefficient` dropdown options, he/she can enter that value in the range [0.5, 1] in the input field and add it by clicking the `Add new μ value` button.

If one conflict situation is selected, the default friction coefficients are set, but it is possible to change these values. If more conflict situations are selected, changing these values is disabled.

- **Number of generated scenarios:** This parameter represents the number of scenarios generated if the `Simulate` button is pressed concerning the previously selected parameters.

Car Configuration

A detailed description of the configuration parameters of the car can be found in Vehicle parameters and setup (Section 9.2.1.1).

AEB Configuration

A detailed description of the AEB parameters can be found in Active Safety System Parameters and Setup (Section 9.2.1.1).

Scenario generation process

The process of generating a scenario proceeds stepwise: iterating through all combinations of given parameters (VRU and VUT speeds, impact locations and mu values) and creating different variations of a given conflict situation, adding each to the dictionary, and finally, saving that dictionary as a PKL file.

The agent dictionary is a nested dictionary. The keys of that dictionary are the names of HTML files or the appropriate combination of VRU and VUT speeds, impact locations and mu value.

Scenario Evaluation

For the scenario evaluation, it is necessary to select available options in the dropdown menus as shown in Figure 9-8. In the first dropdown one can select a pre-simulated scenario catalogue, which is stored in a subfolder with a respective name. With the second dropdown menu a specific AEB configuration can be selected from a list.

Further explanations of the output simulation folder structure can be found in Outputs from pre-crash simulation (9.4.2.1).

When the user selects the values in the dropdown menus, a table is displayed below the dropdown (see Figure 9-8). All generated .html files from the selected folder are listed in this table. The "view sim" hyperlink in the AEB column links to the HTML file selected AEB folder. The hyperlinks in the Baseline column link to a .html file from the related baseline folder. According to the hyperlink colour, we know if a collision happened between the vehicle and the road user. In this way, we can see in which situations there was a conflict in the baseline scenario (red hyperlink) and whether the AEB influenced the collision (if the hyperlink is green).

Since the hyperlink links to a .html file, we can easily find the desired combination of parameters in the table and thus open the AEB and baseline variants of the specific scenario via the hyperlink and compare them.

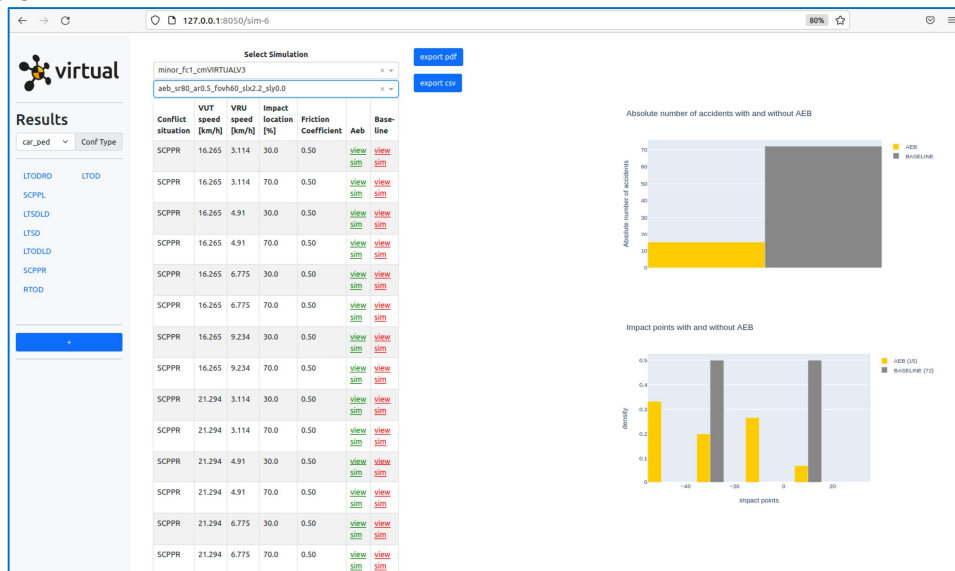


Figure 9-8: Example of output and interface when the user selects the values in dropdown menus. Buttons for exporting .pdf and .csv files and plots are displayed in GUI.

In addition to the table, there are buttons for exporting .pdf and .csv files and plots on which certain information for the scenario being evaluated are visualised.

Further explanations for this can be found in Documentation of Validation of Car Model for Pre-crash Simulation (9.2.3.1) and Postprocessing definitions for pre-crash simulation (9.6.1.1)

9.1.6 User interfaces for in-crash simulation

The following Jupyter notebooks can be used for selecting the in-crash simulations and can be found on the OpenVT platform⁹. As these notebooks are under constant further development please follow the instructions and README given in the VIRTUAL Integrated Safety Assessment Framework VISAFE-VRU repository.

Currently the following Jupyter notebooks and auxiliaries are available:

- **pre_crash_simulation_analysis.ipynb**: This notebook is used to analyse the pre-crash simulation results and creates csv. files with the clustered non-avoided collision scenarios and the related occurrence probability.
- **DoE.R**: This R script can be used to conduct the Design of Experiment with the help of the maximum projection (MaxPro) criterion (Joseph et al., 2020). Input for the DoE are the csv. files created by the
- **pre_crash_simulation_analysis Jupyter notebook**. The result of this script is a csv-file giving the scenarios which should be considered for in-crash simulation.
- **create_folder_structure.ipynb**: This Jupyter notebook can be used to automatically create the simulation input for each collision scenario of the csv. file created with the DoE. Output of this notebook is a folder for each in-crash simulation which includes all necessary LS-Dyna input decks. The parameters are automatically adjusted and an information file is created.
- **post_processing.ipynb**: This Jupyter notebook can be used to automatically assess your simulation results using Dynasaur (Klug et al., 2018; Schachner et al., 2018). For more information on Dynasaur, please visit <https://gitlab.com/VSI-TUGraz/Dynasaur>.
- **post_processing_single.ipynb**: This Jupyter notebook can be used to analyse the results created with Dynasaur for a specific in-crash simulation collision scenario. Output is a pdf-report which includes all the necessary information, such as injury criteria of different body regions and energies.
- **virtual_metamodel.py**: This python script can be used to predict the injury risk for collision scenarios not included in the in-crash simulation based on the results of the in-crash simulations. Output of this python script is a csv. file with predicted injury risks for different body regions and all non-avoided scenarios of the pre-crash simulation.
- **overall_injury_probability.ipynb**: starting from the csv file created by the metamodel, this Jupyter notebook is used to calculate the overall injury probability for specific body regions based on the occurrence probability for each collision scenario. The output of this notebook is a csv file which can be used for the cost benefit analysis.

9.2 JupyterVirtual Models to be tested

9.2.1 Calibration of the vehicle under test

9.2.1.1 Calibration of the vehicle under test for Pre-crash Simulation

The basic car model consists of two components. On the one hand the dynamics, which are implemented as a two-track model, and on the other, a PID controller, which calculates the control signals, gas, brake, and steering angle, based on the difference between a targeted and the actually driven trajectory in the simulation. A detailed description of the basic vehicle model can be found in (Schachner et al., 2020). The vehicle model has a large number of input parameters, related to the PID controllers (i.e. weighting factors), as well as the vehicle dynamics (i.e. max slip). Most of them, effecting the driven trajectory only at high lateral accelerations and can be neglected.

⁹ <https://openvt.eu/wp-4/VISAFE-VRU>

The user can configure geometrical properties, like weight, length, width, wheelbase, centre of gravity or the track width. Further properties, which can be configured by the user, are brake delay and brake gradient.

In order to derive future impact configurations, the vehicle model has been extended with a generic active safety system (Autonomous Emergency Braking), as described in (Barrow et al., 2018; TRL et al., 2018; Gruber et al., 2019; Schachner et al., 2020). The main component is an idealistic sensor model, which spans a segment of a circle and determines intersections to other agents, using a ray-tracing algorithm. The sensor model can be parametrized, sensor location in the car coordinate system, field of view (sensor angle), maximum range, azimuthal resolution. The sensor is able to permanently calculate the time to collision (TTC) by extrapolating the current course of an obstacle. The TTC is further passed to the controller, which triggers an emergency brake if a given threshold is reached.

In the following, a detailed description of the configurable vehicle parameters is given as well as a description of the active safety system.

Vehicle parameters and setup

Vehicle parameters are categorized into brake properties and geometry and mass.

Brake properties

- **Brake Delay [s]:** This parameter represents the reaction time of the brake system.
- **Brake Gradient [m/s³]:** This parameter represents the gradient of the build-up time, which is a limiting factor for reaching a full deceleration.

Geometry and mass

- **Width [m]:** This parameter configures the width of the car.
- **Length [m]:** This parameter represents the length of the car.
- **Distance COG to Front Axle [m]:** Distance of the centre of gravity to the front axle.
- **Weight[m]:** This parameter configures the car's mass.
- **Wheelbase [m]:** Defines the distance between the front and the rear axle.
- **Track Width [m]:** This parameter represents the distance between the centres of the left and right wheel for each axle.

Selectable car models

In order to configure the vehicle parameters, the user can either insert them into the graphical user interface manually, or select one of the existing models, shown in the dropdown. In order to add a vehicle to the list, the `vehicle_catalog.json` can be extended by the user.

```
{
  "VIRTUAL V3": {
    "brake_delay": 0.2,
    "brake_gradient": 35,
```

```

        "width": 2.008,
        "length": 4.953,
        "distance_cog_to_front_axle": 2.45,
        "weight": 2078,
        "wheelbase": 2.984,
        "track_width": 1.63
    },
    ...
}

```

Car geometry and mass

If a certain vehicle model is selected, the predefined values are automatically set in the GUI fields as shown in Figure 9-9. If those default values are altered, they can be stored in the program, which creates a new entry in the JSON file.



Figure 9-9: GUI for the car configuration with visualisation of configurable parameters (right) and interactive fields in which these parameters can be altered (left)

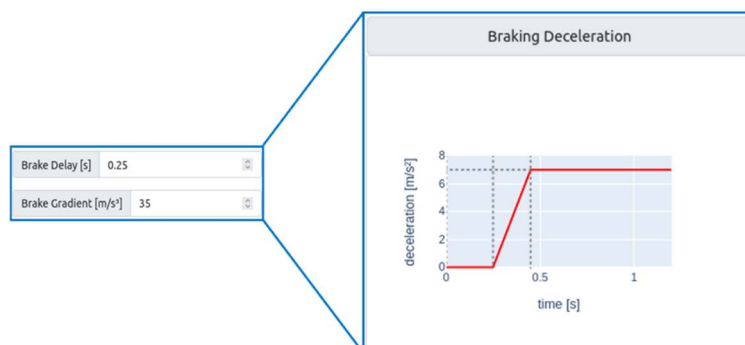


Figure 9-10: Braking deceleration plot for given brake delay and brake gradient parameters set in the GUI

After the user sets the car configuration parameters and generates the desired simulation, the values are saved as `runConfiguration.xml` file in the resulting simulation folder.

```
<Agent id="0">
  <AgentTypeRef>0</AgentTypeRef>
  <Type>Car</Type>
  <Width>2.008</Width>
  <Length>4.953</Length>
  <DistanceCOGtoFrontAxle>1.42</DistanceCOGtoFrontAxle>
  <Weight>2078</Weight>
  <HeightCOG>0.78</HeightCOG>
  <Wheelbase>2.984</Wheelbase>
  <MomentInertiaRoll>1190</MomentInertiaRoll>
  <MomentInertiaPitch>3967</MomentInertiaPitch>
  <MomentInertiaYaw>3967</MomentInertiaYaw>
  <FrictionCoeff>0.8</FrictionCoeff>
  <TrackWidth>1.63</TrackWidth>
  <DistanceCOGtoLeadingEdge>2.45</DistanceCOGtoLeadingEdge>
  <Color>red</Color>
</Agent>
```

Active Safety System Parameters and Setup

Within the AEB configuration, the user can set the desired value for the parameters below. The default values are set. However, if the user wants to generate a conflict scenario with a different AEB configuration, he/she can change the individual parameters.

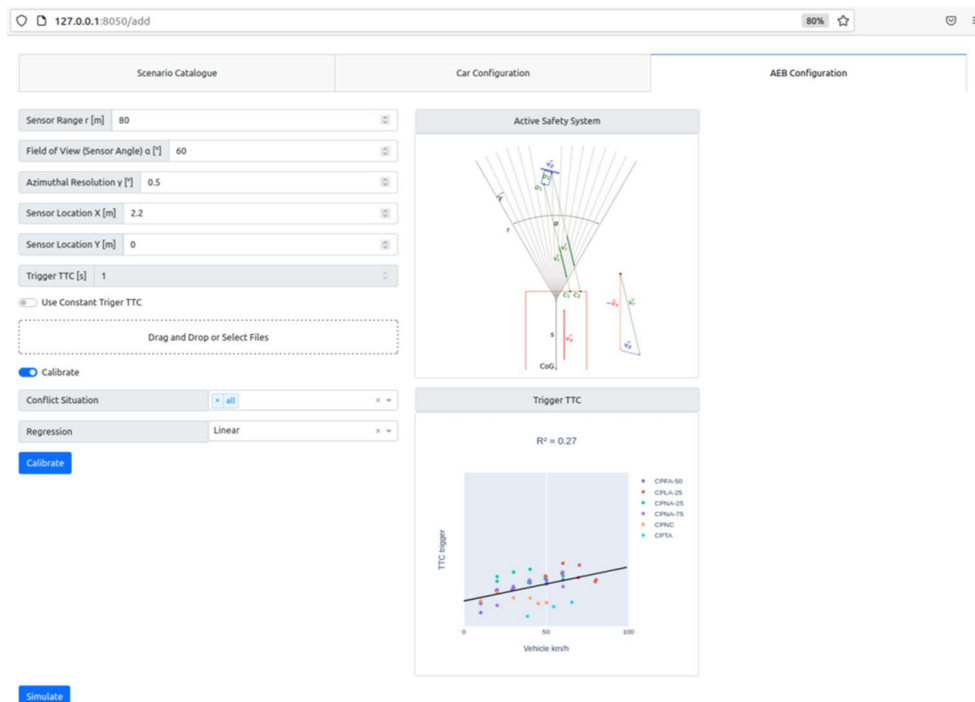


Figure 9-11: GUI for the generic configuration with visualisation of configurable parameters (right) and interactive fields in which these values can be altered (left)

AEB Configuration Parameters:

- **Sensor Range [m]:** This parameter represents the displacement between the sensing radius of the VUT sensor and the VRU that triggers the signal change in the circle segment.
- **Field of View (Sensor Angle) [°]:** This parameter represents the maximum area that a sensor can image.
- **Azimuthal Resolution [°]:** The angle or distance by which two VRUs at the same range must be separated in azimuth to be distinguished by a VUT sensor.
- **Sensor Location X [m]:** This parameter represents the distance of the sensor ahead of the vehicle COG (in driving direction).
- **Sensor Location Y [m]:** This parameter represents the lateral distance of the sensor relative to the vehicle centreline.
- **Sensor Location Y [m]:** This parameter represents the lateral distance of the sensor relative to the vehicle centreline.

- **Trigger TTC [s]:** Trigger TTC configures the threshold for triggering the emergency brake. The parameter can either be selected constant, but also calibrated based on real-world measurements.

By default, the sensor range is 80 m with a field of view of 60°, an azimuthal resolution of 0.5°, positioned 2.2 m ahead of the vehicle CoG. Braking is induced when TTC is less than 1s. Parameters have to be modified to represent the system built into the vehicle under test.

9.2.1.2 Calibration of Car Model for In-crash Simulation

The car models used for in-crash simulations have to reflect the real car in terms of geometry and stiffness. The structural behaviour should be based on component tests and has to be well documented. Strain-rate dependency and the deformation behaviour in the range of deformations for VRU impacts has to be considered.

The vehicle height / spring deflection should be aligned to the "Normal Ride Attitude" as defined in the Euro NCAP pedestrian testing protocol (EuroNCAP, 2019b), reflecting that the vehicle is loaded with the 'unladen kerb weight' and a driver with 75 kg.

9.2.2 Validation

9.2.2.1 Car Model Validation for Pre-crash Simulation

In order to validate the pre-crash simulation, real world tests performed on a test track are compared with simulated results of the developed vru-precrash tool. The scenarios from EuroNCAP (2019a) are well suited and can be re-simulated easily, with a calibrated vehicle model, equipped with a generic AEB system as outlined in chapter 9.2.1.

Simulation of Validation Use Cases

The scenarios of the technical (Euro NCAP, 2019a) can currently be created and simulated through a python script:

```
python generate_and_simulate_euro_ncap.py --destination_dir
    </path/to/storage> --scenario_catalog <path/to/pkl_file>
```

Scenario_catalog: Path to a vru-precrash catalog (.pkl file as described in " **Catlog.pkl** " in Section 9.4.2.1). The catalog contains driving dynamics of real-world tests. Based on the scenario ID, which consists of the scenario_type, vehicle speed and the impact location a corresponding scenario is created and simulated with the calibrated VUT.

Destination_dir: Simulated scenarios are stored in the `dest` directory as .pkl file (vru-precrash catalog format) and can further be used for analysis.

In order to compare simulation and real-world test data, each scenario is aligned through the AEB trigger time. The aligned data is stored in the **destination_dir**, which is used for validation and reporting as shown in Section "Outputs from pre-crash simulation" **Error! Reference source not found.**)

Quality criteria

The generic active safety system is simplified; hence, differences between simulation and real-world test are acceptable. In order to validate the performance of the simulation, with respect to the real-world test, different levels of granularity can be considered.

On the highest level, the scenario outcome can be compared by means of collision occurrence. Four different cases might be observed, as outline in Figure 9-12.

| | | Test | |
|------------|---------------|-----------|---------------|
| | | collision | non collision |
| Simulation | collision | A | B |
| | non collision | C | D |

Figure 9-12: Classification for the comparison between real-world test and simulation with respect to collision occurrence

From the observed results sensitivity (True Positive Rate) and specificity (True Positive Rate) can be calculated.

$$Sensitivity = \frac{A}{A + C}$$

$$Specificity = \frac{D}{D + B}$$

The trigger TTC should be selected such that the sensitivity lies above 50% (True Positive Rate), meaning that the model does not overestimate the performance of the active safety system and is capable to predict most of the collisions.

If no collisions are observed in the physical tests, the lateral distance at the time of complete halt of the car to the VRU should be compared and documented. Deviation of the distance measured in the simulations compared to the tests should be smaller than 20% of the measured value. Thresholds need to be re-evaluated when more data is available.

9.2.2.2 Validation of Vehicle Model for In-crash Simulation

The geometry of the car should be validated by measuring the following values on at least three locations along the vehicle width according to the Euro NCAP pedestrian testing protocol, once in the simulation model and once in the real car

- Bonnet leading edge (BLE) height on the bonnet leading reference line

- Wrap around distance (WAD) of the bonnet rear reference line should be evaluated at 3 locations
- Height of upper bumper reference line
- Height of lower bumper reference line

Furthermore, the lateral distance from one corner reference point and one bumper corner to the vehicle centreline has to be compared.

Deviations have to be smaller than 10% of the measured value between the real and the virtual vehicle model.

The vehicle stiffness has to be validated by comparing the response of impactors in physical tests with signals obtained from the same simulated impacts. Impactors should be thereby as simple as possible. It is recommended to remove the foam layer from the legform impactors and the skin of the headform impactors. Validation reports of the impactors itself must also be provided. Test and simulation response have to be compared for at least three impacts per impact area, covering impacts on the bumper, BLE, bonnet and windshield.

ISO scores of the acceleration of force/moment vs. time signals should be calculated using the method described in ISO/TS 18571:2022. ISO scores must be higher than 0.58¹⁰ to fulfil the validation. Signals should be cut before so that only the relevant area is analysed (no free flight phase). Tests used for validation must not be used for the calibration of the car models. On request of the test institution, tests at other locations might be performed where the car manufacturer would have to predict the responses beforehand.

9.2.3 Documentation of Validation

9.2.3.1 Documentation of Validation of Car Model for Pre-crash Simulation

In order to validate the car model in the pre-crash tool, its performance is assessed with respect to the scenario outcome, meaning a collision or avoided case. If there is a deviation between the simulation and the real-world scenario, the scenario is counted as fail for the validation.

In order to visualize the validation process, a GUI, as shown in Figure 9-13, has been implemented. The GUI takes the aligned data, as generated by the `generate_and_simulate_euro_ncap.py` script and outputs an overview of the validation. In the left sidebar, a list of the validation scenarios is shown. They are coloured either green or red, depending on the correct prediction of the simulation.

¹⁰ Further studies needed to confirm that this is feasible or if higher thresholds are applicable for some signals.

| scenario_id | sim | test |
|--------------------|-----|------|
| CPFA-50-10-day | 0 | 0 |
| CPFA-50-20-day | 0 | 0 |
| CPFA-50-30-day | 0 | 0 |
| CPFA-50-40-day | 0 | 0 |
| CPFA-50-45-day | 0 | 0 |
| CPFA-50-50-day | 0 | 1 |
| CPFA-50-55-day | 0 | 1 |
| CPFA-50-60-day | 0 | 1 |
| CPNA-25-10-day | 0 | 0 |
| CPNA-25-10-night | 0 | 0 |
| CPNA-25-20-day | 0 | 0 |
| CPNA-25-20-night | 0 | 0 |
| CPNA-25-30-day | 0 | 0 |
| CPNA-25-30-night | 0 | 0 |
| CPNA-25-40-day | 0 | 0 |
| CPNA-25-40-night | 0 | 0 |
| CPNA-25-45-night | 0 | 0 |
| CPNA-25-50-day | 0 | 0 |
| CPNA-25-50-night | 0 | 1 |
| CPNA-25-55-day | 1 | 1 |
| CPNA-25-55-night | 1 | 1 |
| CPNA-25-60-day | 1 | 1 |
| CPNA-25-60-night | 1 | 1 |
| CPNA-75-10-day | 0 | 0 |
| CPNA-75-10-night | 0 | 0 |
| CPNA-75-20-day-1 | 0 | 0 |
| CPNA-75-20-day-2 | 0 | 0 |
| CPNA-75-20-night-1 | 0 | 0 |
| CPNA-75-20-night-2 | 0 | 0 |
| CPNA-75-30-day | 0 | 0 |
| CPNA-75-30-night | 0 | 0 |
| CPNA-75-40-day | 0 | 1 |
| CPNA-75-40-night | 0 | 0 |
| CPNA-75-45-day | 0 | 0 |
| CPNA-75-50-day | 0 | 1 |
| CPNA-75-50-night | 0 | 1 |
| CPNA-75-55-day | 0 | 1 |
| CPNA-75-55-night | 0 | 1 |
| CPNA-75-60-day | 0 | 1 |
| CPNA-75-60-night | 0 | 1 |

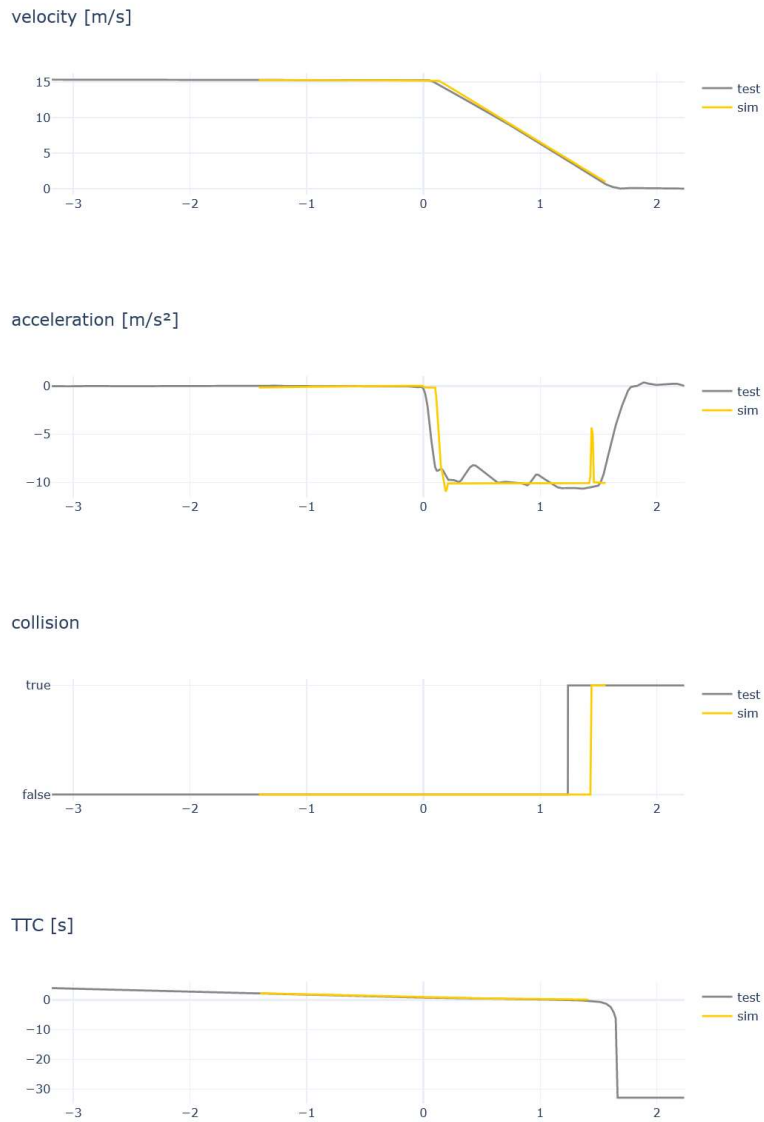


Figure 9-13: GUI to show the validation results. In the left sidebar an overview of the simulated and tested results are shown by the scenario id. In green are the simulations that led to the same output as the real world test. By selecting one of the scenarios, velocity, acceleration collision, and time to collision are shown (right).

9.2.3.2 Documentation of Validation of Car Model for In-crash Simulation

All validation steps need to be properly documented. Templates described in IMVITER deliverables can be used as reference.

To ensure that the vehicle model remains consistent, it is recommended to apply a procedure to ensure consistency of the files, where checksums are calculated of all included files. This checksum

should be included also in the result files to be able to link output files clearly to the simulation input files.

Test data used for validations have to be stored according to ISO-TS 13499. The corresponding simulation outputs have to be available in the same format. The calculated IS-Scores related to the files have to be available in table format for all calculated channels.

9.3 Virtual VRU Models (Measurement Device)

9.3.1 Prerequisites

9.3.1.1 FE Bicycle Models for in-crash simulation

Bicycle Geometry (50F, 50M)

For Simulations with the VIVA+ 50F a bicycle with trapeze frame should be used (Figure 9-15). For Simulations with the VIVA+ 50M a bicycle with diamond frame should be used (Figure 9-16). An overlay of both bicycle models can be seen in Figure 9-14. You can use the bicycle models provided on the OpenVT platform¹¹. If you are using your own bicycle model, make sure to meet the target geometry given in Table 9-1 and Table 9-2. All measurements should be within a $\pm 5\%$ tolerance range.

Both models are provided in rigid and deformable frame configurations. For use in different cases, the bicycle models are also provided in four different pedal positions: left or right foot down (vertical position) and left or right foot in front (horizontal position). The pedal positions can be adjusted to the end user needs by rotating the crank and pedals around the (0,0,0) coordinate.

The end user has a possibility to change the material of the bicycle frame. Originally both models use EN 25CrMo4 steel for the frame, forks and handlebar. This material can be changed to EN AW 7020 AlZn4.5Mg1 aluminium alloy using the included predefined material model.

The provided bicycle models are based on the previous bicycle geometry from TU Graz (Hainisch, 2015). The initial geometry was modified to correspond to the reference values based on the literature review in internal report (WP4-16.9.2021 - Bicycle Type, Sizes and Posture for VIVA+ 50F) and to allow proper positioning of the VIVA+ 50F and VIVA+ 50M models.



Figure 9-14 Overlay of bicycle for VIVA+ 50F (trapeze frame; red) and VIVA+ 50M (diamond frame; blue)

¹¹ <https://openvt.eu/fem/bicycle-models>

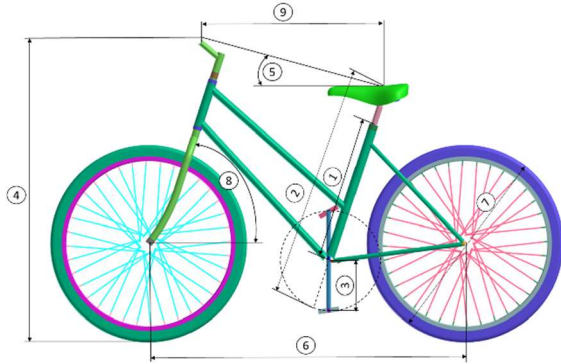


Figure 9-15 Trapeze Frame Bicycle for VIVA+ 50F simulations

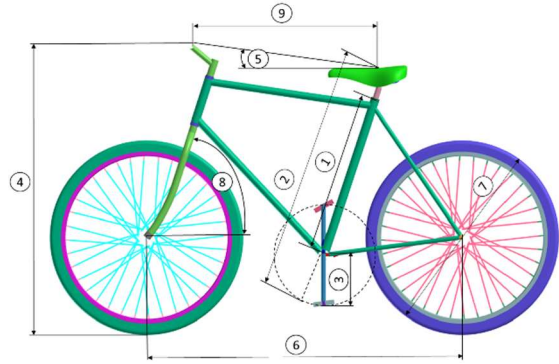


Figure 9-16 Diamond Frame Bicycle for VIVA+ 50M simulations

Table 9-1 Target geometry for trapeze frame VIVA+ 50F

| # | Measurement | Goal |
|----|------------------------------|---------|
| 1 | Frame Size | 480 mm |
| 2 | Saddle Height | 790 mm |
| 3 | Crank Length | 165 mm |
| 4 | Handlebar Height | 1018 mm |
| 5 | Handlebar to Saddle Angle | 14° |
| 6 | Wheelbase | 1062 mm |
| 7 | Wheel Diameter | 660 mm |
| 8 | Head Tube Angle | 66.8° |
| 9 | Handlebar to Saddle Distance | 650 mm |
| 10 | Weight | 11.7 kg |
| 11 | Sitting decline | 68.0° |

Table 9-2 Target geometry for diamond frame VIVA+ 50M

| # | Measurement | Goal |
|----|------------------------------|---------|
| 1 | Frame Size | 550 mm |
| 2 | Saddle Height | 840 mm |
| 3 | Crank Length | 165 mm |
| 4 | Handlebar Height | 992 mm |
| 5 | Handlebar to Saddle Angle | 7° |
| 6 | Wheelbase | 1077 mm |
| 7 | Wheel Diameter | 660 mm |
| 8 | Head Tube Angle | 66.7° |
| 9 | Handlebar to Saddle Distance | 658 mm |
| 10 | Weight | 11.3 kg |
| 11 | Sitting decline | 70.0° |

Bicycle Structure

The bicycle frame, handlebar, forks and crank are modelled as shells to provide more realistic contact response between VIVA+ models and bicycle (Table 9-3). The contacts between bicycle parts are modelled using surface-to-surface and nodes-to-surface contact definitions. To simulate a realistic

contact response between HBM and the bicycle model, the surface-to-surface contact must be defined between them.

Table 9-3 Bicycle parts properties

| Bicycle part | Element type (section) | LS-Dyna material model |
|---------------------|------------------------|---------------------------------|
| Frame | Shell – 2 mm | MAT_PIECEWISE_LINEAR_PLASTICITY |
| Handlebar and forks | Shell – 2 mm | MAT_PIECEWISE_LINEAR_PLASTICITY |
| Crank | Shell – 3 mm | MAT_PIECEWISE_LINEAR_PLASTICITY |
| Pedals | Solid | MAT_PIECEWISE_LINEAR_PLASTICITY |
| Seat post | Shell – 2 mm | MAT_PIECEWISE_LINEAR_PLASTICITY |
| Seat | Shell – 5 mm | MAT_ELASTIC |
| Seat railing | Beam | MAT_PIECEWISE_LINEAR_PLASTICITY |
| Spokes | Beam | MAT_PIECEWISE_LINEAR_PLASTICITY |
| Rims | Shell – 1.5 mm | MAT_PIECEWISE_LINEAR_PLASTICITY |
| Tyres | Shell – 3 mm | MAT_FABRIC |

Due to very scarce data for model validation, the bicycle models were validated only using rigid wall rear impact experimental data (McLundie, 2007) (Figure 9-25). If the bicycle model is intended to be used in another FE-solver, this simulations should be repeated and compared to the LS-Dyna outputs.

9.3.1.2 Shoes

For HBM VRU simulations, shoes should be used that are in accordance with the specifications given in Euro NCAP Technical Bulletin TB024 (Euro NCAP, 2019b). Shoes meeting these specifications are provided for the VIVA+ model on the OpenVT platform¹². The material properties of the VIVA+ shoes are based on Cho et al, 2009). The baseline shoe geometry is based on freely available geometry data¹³. Each shoe consists of the following parts: Fabric outer, Fabric inner, Sole inner, Sole mid and Sole outer. This can also be seen in Figure 9-19 and Figure 9-18.

To fit the shoe on the VIVA+ model, the geometry of the VIVA+ foot (50F and 50M) was used to generate the inner fabric. All other parts are then adjusted on this geometry. The specifications for the 50M and 50F shoes are given in Table 9-4.

¹² <https://OpenVT.eu/fem/shoes>

¹³ <https://free3d.com>

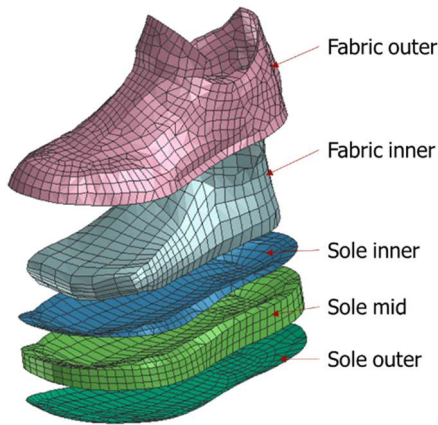


Figure 9-17 Structure of the VIVA+ shoe model

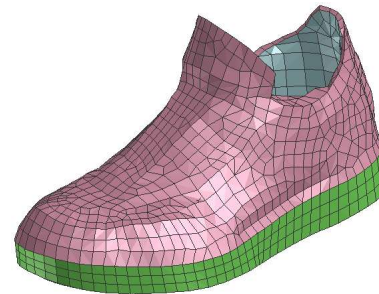


Figure 9-18 VIVA+ Shoe Model

Table 9-4 Specification of VIVA+ shoes example shown for LS-Dyna

| | 50M | 50F |
|--------------------------------------|--|------------|
| Sole thickness (at the heels) | 26.5 mm | 26.5 mm |
| Weight of one shoe | 694 g | 532 g |
| Fabric outer | Section: Shell 1mm; Material: *MAT_ELASTIC (LS-Dyna) | |
| Fabric inner | Section: Shell 1mm; Material: *MAT_ELASTIC (LS-Dyna) | |
| Sole inner | Section: Shell 1mm; Material: *MAT_ELASTIC (LS-Dyna) | |
| Sole mid | Section: Solid; Material: *MAT_ELASTIC (LS-Dyna) | |
| Sole outer | Section: Shell 1mm; Material: *MAT_ELASTIC (LS-Dyna) | |
| Contact Fabric outer to Fabric inner | *CONTACT_AUTOMATIC_SINGLE_SURFACE (LS-Dyna) | |
| Contact right shoe to left shoe | *CONTACT_AUTOMATIC_SINGLE_SURFACE (LS-Dyna) | |
| Contact Foot to Shoe | *CONTACT_AUTOMATIC_SURFACE_TO_SURFACE (LS-Dyna) | |

9.3.2 Model preparation

9.3.2.1 Posture & Geometry

Pedestrian for pre-crash simulation

The pedestrian model is rather simple: It follows a defined trajectory without a dynamic control component. The layout of the model-based design can be obtained from (Schachner et al., 2020). Its dimension follow the pedestrian dummy in the Euro NCAP test protocol (Euro NCAP, 2019a) and has a width of 0.54 m and a length of 0.28 m, the CoG is in the geometric centre of the rectangle. Pedestrian postures are neglected in the pre-crash simulation.

Pedestrian Model for in-crash simulation

For in-Crash simulations the pedestrian model should be positioned according to Euro NCAP Technical Bulletin TB024 (Euro NCAP, 2019b). If you are using the VIVA+ model you can use the prepositioned

pedestrian models provided on the OpenVT platform¹⁴. These models are already positioned according to the Euro NCAP Technical Bulletin TB024 (Euro NCAP, 2019b).

Bicyclist Model for pre-crash simulation

The bicyclist model of the pre-crash simulation follows the same design principles as the pedestrian model and consists of a trajectory following algorithm. Its dimension follow the bicyclist dummy in the Euro NCAP test protocol (Euro NCAP, 2019a) and has a width of 0.67 m and a length of 1.89 m, the CoG is in the geometric centre of the contour rectangle.

Bicyclist Model for in-crash simulation

The cyclist should be positioned according to the values given in Table 9-6 for the 50th percentile female and Table 9-7 for the 50th percentile male. A Stickman where all the values are displayed is given in Table 9-5. To achieve the sitting decline given in Table 9-1 and Table 9-2 the 50th percentile female should be rotated 22° forward around the y-axis and the 50th percentile male should be rotated 20° forward around the y-axis. The positioned VIVA+ 50 F model can be seen in Table 9-8 and the positioned VIVA+ 50M in Table 9-9. These positioned models can be found on the OpenVT platform¹⁵ and can be used for the in-crash simulations. If another HBM for in-crash simulation is used, the reference values given in Table 9-6 and Table 9-7 must be used during the positioning.

¹⁴ https://openvt.eu/fem/viva/vivaplus/-/tree/main/model/positioned_models/

¹⁵ https://openvt.eu/fem/viva/vivaplus/-/tree/main/model/positioned_models

Table 9-5 Reference Posture of Cyclist

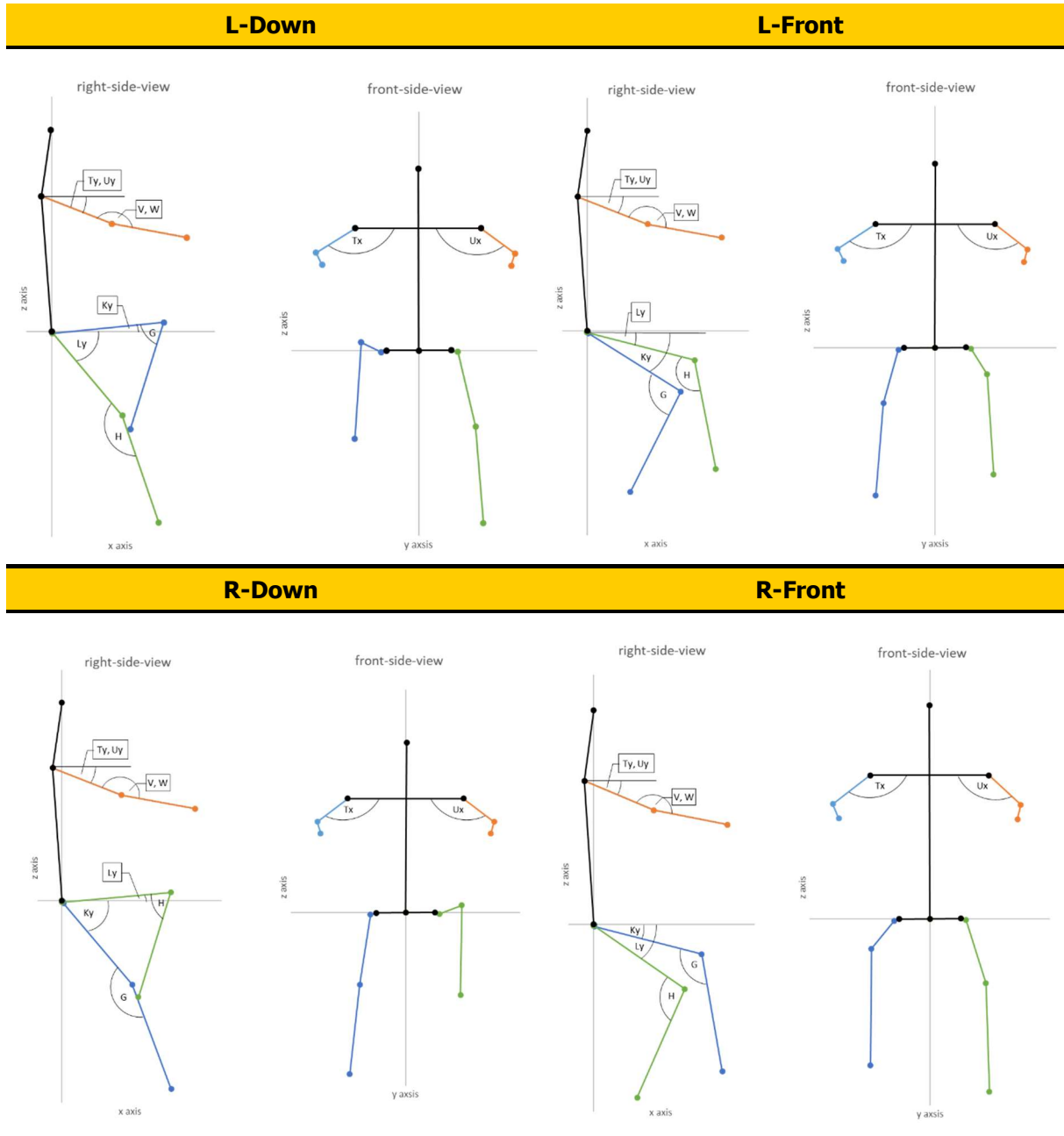


Table 9-6 Reference Posture of 50F Cyclist

| Abbrev. | Measure | L-Down | L-Front | R-Down | R-Front |
|----------------|---|---------------|----------------|---------------|----------------|
| Px | Heel to heel distance longitudinal | 99.627 mm | 289.87 mm | 116.741 mm | 289.28 mm |
| Py | Heel to heel distance lateral | 301.737 mm | 298.85 mm | 285.915 mm | 301.87 mm |
| Pz | Heel to heel distance vertical | 319.531 mm | 79.567 mm | 319.285 mm | 85.482 mm |
| ACz | Height of AC relative to ground level | -- | -- | -- | -- |
| Ky | Right Upper Leg Angle (around Y w.r.t. horizontal) | 4.93° | 34.61° | 52.09° | 15.31° |
| Ly | Left Upper Leg Angle (around Y w.r.t. the horizontal) | 52.03° | 16.23° | 4.59° | 35.28° |
| G | Right Knee flexion Angle (Y) | 68.77° | 99.39° | 161.40° | 115.39° |
| H | Left Knee flexion Angle (Y) | 145.52° | 116.47° | 69.33° | 101.44° |
| Ty | Right Upper Arm Angle (Y w.r.t. horizontal) | 22.67° | 22.69° | 22.727° | 22.66° |
| Uy | Left Upper Arm Angle (Y w.r.t. horizontal) | 22.80° | 22.76° | 22.761° | 22.78° |
| Tx | Right Upper Arm Angle (X w.r.t. horizontal) | 135.27° | 135.29° | 135.27° | 135.30° |
| Ux | Left Upper Arm Angle (X w.r.t. horizontal) | 130.25° | 130.29° | 130.25° | 130.28° |
| V | Right Elbow flexion Angle | 168.29° | 168.29° | 168.26° | 168.31° |
| W | Left Elbow flexion Angle | 168.29° | 168.31° | 168.31° | 168.29° |
| HCx | x-Position of HC relative to AC | -2.411 mm | 0.073 mm | 0.203 mm | -0.235 mm |
| HCz | Height of HC relative to the ground level | -- | -- | -- | -- |

Table 9-7 Reference Posture of 50M Cyclist

| Abbrev. | Measure | L-Down | L-Front | R-Down | R-Front |
|---------|---|-----------|-----------|-----------|-----------|
| Px | Heel to heel distance longitudinal | 120.20 mm | 289.00 mm | 118.30 mm | 276.50 mm |
| Py | Heel to heel distance lateral | 299.60 mm | 292.10 mm | 299.59 mm | 302.40 mm |
| Pz | Heel to heel distance vertical | 321.5 mm | 97.9 mm | 320.6 mm | 98.6 mm |
| ACz | Height of AC relative to ground level | -- | -- | -- | -- |
| Ky | Right Upper Leg Angle (around Y w.r.t. horizontal) | 6.03° | 29.10° | 48.08° | 12.67° |
| Ly | Left Upper Leg Angle (around Y w.r.t. the horizontal) | 46.78° | 13.07° | 6.07° | 28.54° |
| G | Right Knee flexion Angle (Y) | 75.15° | 100.74° | 157.22° | 117.59° |
| H | Left Knee flexion Angle (Y) | 155.23° | 117.42° | 75.32° | 102.38° |
| Ty | Right Upper Arm Angle (Y w.r.t. horizontal) | 24.90° | 24.91° | 24.93° | 24.91° |
| Uy | Left Upper Arm Angle (Y w.r.t. horizontal) | 24.51° | 24.38° | 24.47° | 24.41° |
| Tx | Right Upper Arm Angle (X w.r.t. horizontal) | 114.47° | 115.82° | 116.77° | 116.79° |
| Ux | Left Upper Arm Angle (X w.r.t. horizontal) | 116.50° | 115.89° | 115.77° | 115.91° |
| V | Right Elbow flexion Angle | 169.77° | 169.95° | 169.97° | 170.04° |
| W | Left Elbow flexion Angle | 169.61° | 169.95° | 169.62° | 169.61° |
| HCx | x-Position of HC relative to AC | 9.80 mm | 10.90 mm | 8.50 mm | 12.10 mm |
| HCz | Height of HC relative to the ground level | -- | -- | -- | -- |

Table 9-8 VIVA+ 50F positioned on the trapeze frame

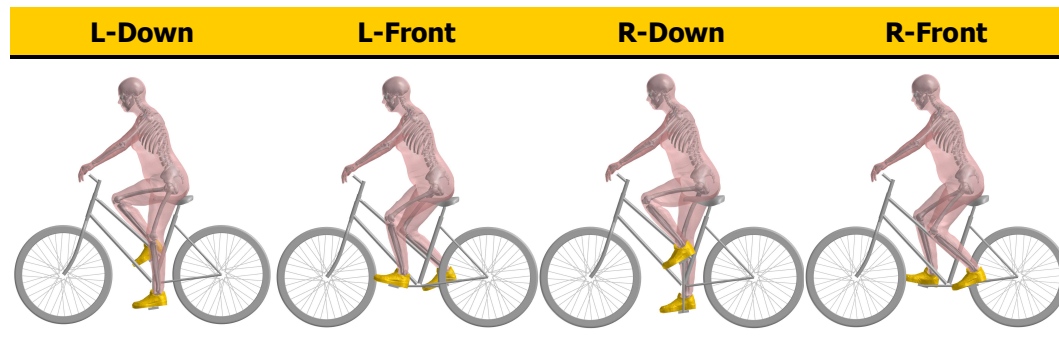
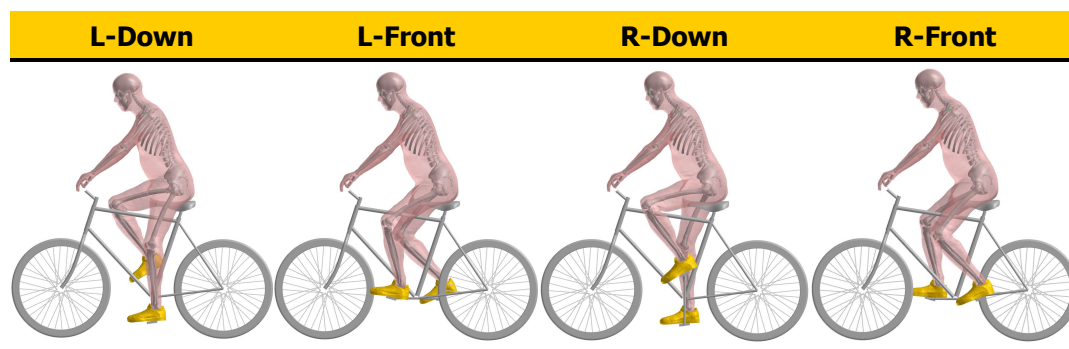


Table 9-9 VIVA+ 50M positioned on the diamond frame



9.3.2.2 Output definitions

VRU-specific outputs in pre-crash simulation

The outputs of the pre-crash simulation are mainly determined by the simulated trajectories, for both the VUT and the VRU. An example of a stored trajectory is shown in Table 9-10.

Table 9-10: Stored trajectory information for the simulated agent (VUT/VRU) in an output frequency of 10ms.

| <i>Time</i> | <i>x</i> | <i>y</i> | <i>h</i> | <i>velocity</i> | <i>closestX</i> | <i>closestY</i> | <i>Collision</i> | <i>TTC</i> |
|-------------|----------|----------|-----------|-----------------|-----------------|-----------------|------------------|------------|
| 0.00 | 2.135515 | 1.424149 | -2.418976 | 2.777778 | inf | inf | <i>False</i> | <i>inf</i> |
| 0.01 | | | | | | | | |

The entire record of all simulated trajectories for each scenario and agent are stored in a .pkl file.

VRU-specific outputs in in-crash simulation

For kinematic assessment of the HBM in-crash simulations, different landmarks should be used. A list of all Landmarks can be found in Table 6-1. The Landmarks are defined according to the ISB

recommendations (Wu and Cavanagh, 1995; Wu et al., 2002; Wu et al., 2005). As output frequency for node histories 0.1ms should be used. In the head centre of gravity, a seatbelt-accelerometer (LS-Dyna) should be used providing local outputs with the xy plane parallel to the Frankfort plane. Please see ANNEX B: HUMAN BODY MODEL OUTPUT of the Euro NCAP Technical Bulletin TB024 (Euro NCAP, 2019b) for more information of how the landmarks should be connected to the HBM. All required landmarks are included in the VIVA+ models by default.

Tissue-based assessment in in-crash simulation

For strain based tissue assessment, specific cortical bones and the knee ligaments should be analysed. A list of cortical bones and ligaments that should be analysed are given in Table 6-2. For these body parts, injury risk curves are available for the strain based assessment. The output frequency for strain values should be 1.0 ms. For LS-Dyna the strain flag (STRFLG) in *DATABASE_EXTENT_BINARY has to be set to 1 to have the strain output also for shell elements in the binary files.

9.3.3 Qualification procedure

9.3.3.1 Anthropometry Requirements

Human Body Models have to be used in two different anthropometries. One should reflect the average female (50F) and the other one the average male (50M) anthropometry. The dimensions should be based on the statistical models available on humanshape.org for the following settings described in Table 9-11. All landmarks should be met with a tolerance of 10 mm.

Table 9-11: Target anthropometries for 50F and 50M models

| | 50F | 50M |
|------------------------|---------|---------|
| Population | US | US |
| Gender | female | Male |
| stature | 1620 cm | 1750 cm |
| BMI | 24 | 25 |
| Sitting height/stature | 0.52 | 0.52 |
| age | 50yrs | 50yrs |

9.3.3.2 Validation of the VRU in-crash Models

The VRU models used for the assessment have to be validated according to the state of the art. Validation setups shared for the VIVA+ models should be used as reference. The overall stiffness should be evaluated with hub impacts (Viano et al., 1989). The full body kinematics should be evaluated using PMHS tests where vehicle models to perform the validations are openly available. For the femur, tibia, pelvis and ribs the stiffness of the isolated bones has to be evaluated as well as strains to be used for tissue-based assessment. The knee ligament elongation has to be validated based on a 4-point bending tests. (Bose et al. 2008). Detailed descriptions of the validation procedures and all related models are available within the VIVA+ validation catalogue on <https://vivaplus.readthedocs.io>.

9.3.3.3 Certification load cases

The pedestrian models have to fulfil the Euro NCAP TB024 to make sure that the overall kinematics are comparable to other models and that the model behaves as it should in the environment used.

9.4 Test setups

9.4.1 Test environment

The test environment should not be changed between the virtual tests and the before described validation and qualification steps. The same models, control setting and solver has to be used for the virtual tests described as for the validation & qualification procedures described before.

Recommended control cards for the VIVA+ models are shared together with the model. If different control settings are needed of the in-crash vehicle model, the validations and certification of the VRU model need to be double-checked.

9.4.1.1 Model preparations (merge model of device with Human Model)

Positioning for pre-crash simulations

The VIRTUAL scenario catalogues are generated in the "from collision" mode, which guarantees an impact for all baseline cases. The initial position of the VRU depends mainly on the conflict situation and the VUT/VRU speeds used for the generation of a particular scenario.

Positioning for in-crash simulation

The HBM should be positioned in front of the car front. It has to be checked that no initial penetrations occur at the beginning of the simulation. The global coordinate system of the HBM should be in the centre of the right and left acetabulum centres AC. For definition of AC please see ANNEX B: HUMAN BODY MODEL OUTPUT of the Euro NCAP Technical Bulletin TB024 (Euro NCAP, 2019b). The coordinate system should be defined that the z-axis is facing upwards and the x-axis is facing forwards. This is exemplarily shown on the VIVA+ 50F pedestrian model where the z-axis is displayed in blue and the x-axis is displayed in red (Figure 9-19).

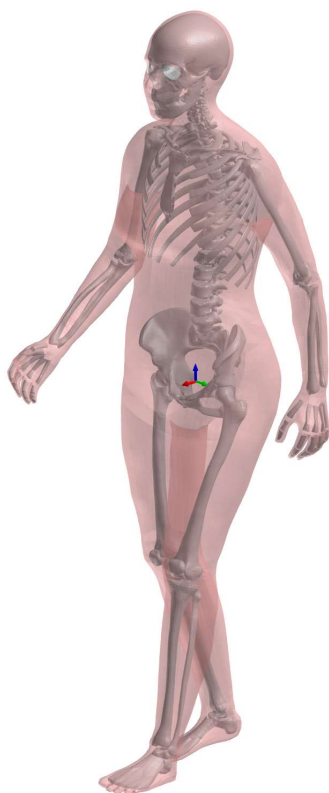


Figure 9-19 Exemplarily coordinate system of the HBM shown on the VIVA+ 50F pedestrian model with z-axis facing upwards (blue) and x-axis facing forwards (red)

The global coordinate system of the car should be in the centre of gravity with the z-axis facing upwards and the x-axis facing forwards (driving direction). This is exemplarily shown for the generic vehicle in Figure 9-20. Here the coordinate system is not in the centre of gravity but as described in ANNEX A: REFERENCE SYSTEMS of the Euro NCAP Technical Bulletin TB024 (Euro NCAP, 2019b) for the generic vehicle. This does not affect the orientation of the coordinate system.

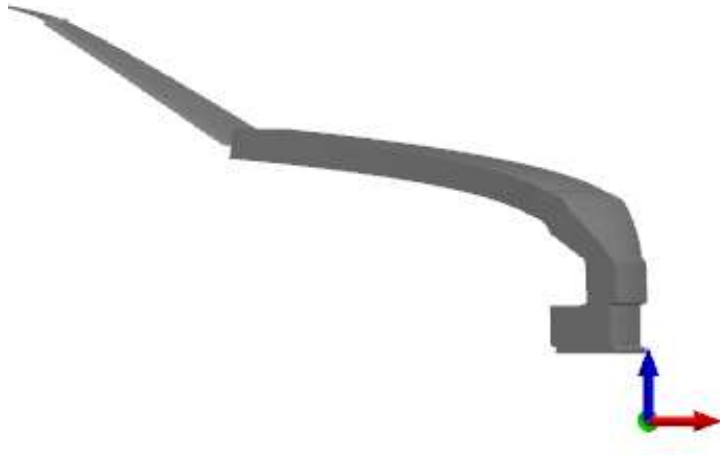


Figure 9-20 Exemplarily coordinate system for car with z-axis facing upwards (blue) and x-axis facing forwards (red)

The global coordinate system of the bicycle should be defined in the bottom bracket with the z-axis facing upwards and the x-axis facing backwards. This is exemplarily shown for the trapeze frame bicycle in Figure 9-21.

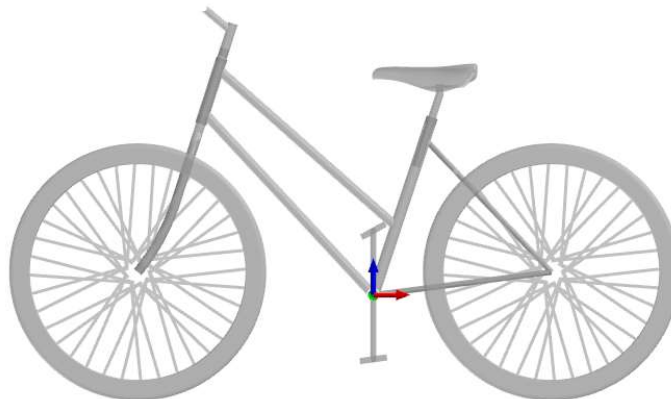


Figure 9-21 Exemplarily coordinate system for the bicycle model with z-axis facing upwards (blue) and x-axis facing backwards (red)

The impact point between HBM and car is defined as shown in Figure 9-22. This means that for an impact point of 0% the origin of the global HBM coordinate system is in line with the center of the car front. -50% means that the origin of the global HBM coordinate system is at the most outer left of the car front and +50% means that the origin of the global HBM coordinate system is at the most outer left of the car front. The car front width is thereby defined as the distance of the exterior points of the bonnet leading edge.

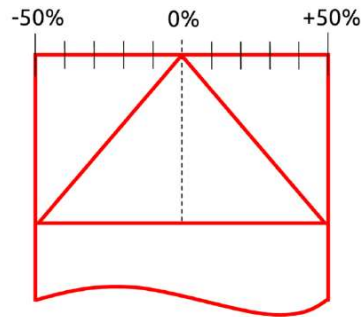


Figure 9-22 Impact Point

The impact angle between HBM and car is defined as shown in Table 9-12. This means that for the 0° position, the axes of the HBM coordinate system and the vehicle system are all pointing in the same direction. For the 90° position, the x-axis of the HBM coordinate system is pointing in positive y-axis direction of the vehicle coordinate system. For the 180° position the x-axis of the HBM is pointing in negative x direction of the vehicle coordinate system and for the 270° position the x-axis of the HBM is pointing in negative y-axis direction of the vehicle coordinate system.

Table 9-12 Impact Angle

| 0° impact angle and 0% impact point | 90° impact angle and 0% impact point | 180° impact angle and 0% impact point | 270° impact angle and 0% impact point |
|-------------------------------------|--------------------------------------|---------------------------------------|---------------------------------------|
| | | | |

The HBMs should be positioned 1mm above the ground so that either the shoes of the pedestrian or the wheels of the bicycle are not impacting the rigid wall which represents the street. Gravity should be used for all simulations.

Posture adjustment

The models should be used in the original posture described in 9.3.2. No further modifications or pre-simulations are needed.

Pre-simulation

No pre-simulation is needed for the VRU assessment. Pre-strains are included in the knee ligaments by default. No effect of initial gravitational loading was observed for the overall kinematics.

Contact Definitions

The contact in the pre-crash simulation is defined by the geometrical overlap of the VUT contour and the VRU. This intrusion is evaluated at each timestep.

For the contact between HBM and vehicle in the in-crash simulations, the sets shown in Table 9-13 and Table 9-14 should be created. With this sets the following contacts should be implemented:

- **Skin Head to whole Vehicle**
- **Skin Torso incl. Hip and Neck to whole Vehicle**
- **Skin left Arm to whole Vehicle**
- **Skin right Arm to whole Vehicle**
- **Skin left Leg to whole Vehicle**

- **Skin right Leg to whole Vehicle**
- **Shoe to whole Vehicle**
- Skin Torso incl. Hip and Neck to Bumper
- Skin left Arm to Bumper
- Skin right Arm Bumper
- Skin left Leg to Bumper
- Skin right Leg to Bumper
- Skin Head to Bonnet
- Skin Torso incl. Hip and Neck to Bonnet
- Skin left Arm to Bonnet
- Skin right Arm to Bonnet
- Skin left Leg to Bonnet
- Skin right Leg to Bonnet

The contacts indicated in bold above should be modelled in LS-Dyna as *CONTACT_AUTOMATIC_SURFACE_TO_SURFACE the other contacts as *CONTACT_FORCE_TRANSDUCER_PENALTY. Similar contacts can be used, if all quality criteria are fulfilled. As explained in the Euro NCAP Technical Bulletin TB024 (Euro NCAP, 2019b) the static and dynamic coefficient of friction between the car and the HBM8 should be set to 0.3 (FS and FD in LS-Dyna). VDC should be set to 20, SOFT=2, SBOPT=3 and DEPTH=5.

Table 9-13 Contact Sets for HBM

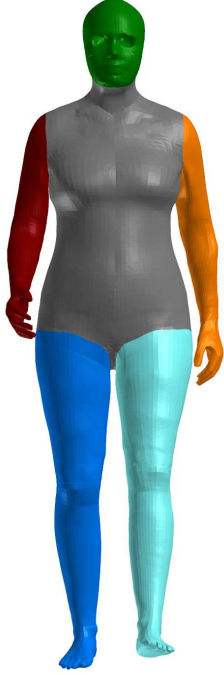
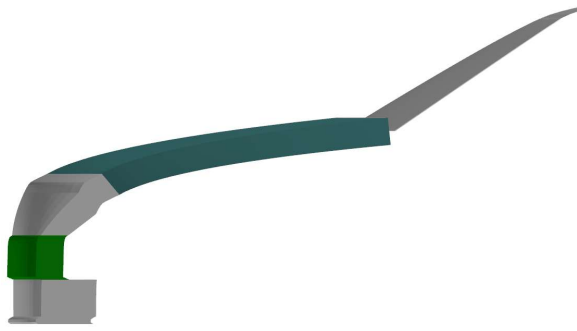
|  | Contact Set |
|--|-------------------------------|
| | Skin Head |
| | Skin Torso incl. Hip and Neck |
| | Skin left Arm |
| | Skin right Arm |
| | Skin left Leg |
| Skin right Leg | |

Table 9-14 Contact Sets for vehicle

|  | Contact Set |
|---|---------------------------------------|
| | Whole Vehicle incl. Bumper and Bonnet |
| | Bumper |
| Bonnet | |

9.4.2 Outputs definitions of test setups

9.4.2.1 Outputs from pre-crash simulation

Depending on the configured scenario catalogue, a corresponding directory is created in the <dest_dir> (passed to the web application on start-up). The hierarchical structure is defined by conflict type, conflict situation, severity, the scenario set up (from road end / from collision) and the chosen car model:

<dest_dir>/<conflict_type>/<conflict_situation>/<severity>_fc<0/1>_cm<>_<car_model>

Scenario Catalogue

From Collision

car_ped Conf Type

x LTOD Conf Situation

x minor Severity

The user's outlined selection would create the following directory: `generated_scenario/car_ped/LTOD/minor_fc1_VirtualV3`. This directory will further contain a `baseline` directory, in which the simulations *without* an active safety system (AEB) of the defined scenario catalogue are stored. For different AEB configurations, a respective directory will be created with a certain identifier, containing information on the system setup consisting of the sensor range, field of view, azimuthal resolution, sensor location, and trigger_ttc.

AEB Configuration

Sensor Range [m] 60

Field of View (Sensor Angle) [°] 60

Azimuthal Resolution [°] 0.5

Sensor Location X [m] 2.2

Sensor Location Y [m] 0.0

The outlined selection would lead to a directory of the following structure.
`aeb_sr60_ar0.5_fovh60_slx2.2_sly0.0_tttc1.0`

When the user generates/runs a particular scenario catalogue, the directory is used to store temporary input and output files for the simulation platform openPASS (`systemConfiguration.xml`, `sceneryConfiguration.xml`, `runConfiguration.xml`, `dataLog.xosc`, `dataLog_0.csv` and `dataLog_1.csv`). Further, `.html` files are created to visualise the scenarios as well as `.pkl` files, containing major quantities of the simulated catalogue to fully reconstruct, evaluate, and visualise the simulated scenarios. In this way, large python objects are stored as binary files.

Table 9-15

| Output file name | Content | Needed for next steps? |
|----------------------------|--|-------------------------|
| Scenario HTML files | Visualisation of scenario | For scenario evaluation |
| Evaluation_data.pkl | Summarised key results – Distribution of collision points, collision velocities, collision angles | For scenario evaluation |

| Catalogue.pk1 | Documents settings for each simulated scenario. | For documentation |
|--------------------------|--|-------------------|
| systemConfigurtion.xml | temporary information for the simulation platform openPASS | No |
| sceneryConfiguration.xml | temporary information for the simulation platform openPASS | No |
| runConfiguration.xml | temporary information for the simulation platform openPASS | No |
| dataLog.xosc | temporary information for the simulation platform openPASS | No |
| dataLog_0.csv | temporary information for the simulation platform openPASS | No |

systemConfiguration.xml, sceneryConfiguration.xml, runConfiguration.xml, dataLog.xosc, dataLog_0.csv and dataLog_1.csv files are generated each time a new .html file is created in the simulation output folder. So for each unique combination of parameters: conflict situation, the initial vehicle speed, impact location, and the friction coefficient mu, these files are updated with information for that scenario. After generating the scenario catalogue, these files contain data only for the last generated scenario, i.e. the scenario defined by the parameters in the name of the previously generated .html file.

Scenario HTML file

.html files are always generated in the resulting simulation directory, with a unique identifier, indicating particular properties and parameters of the scenario (i.e. initial VUT speed). Figure 9-23 shows the rendered content in a web browser. When the user opens the .html file, he/she can see the map of the road showing the model of the car and the model of the virtual road user.

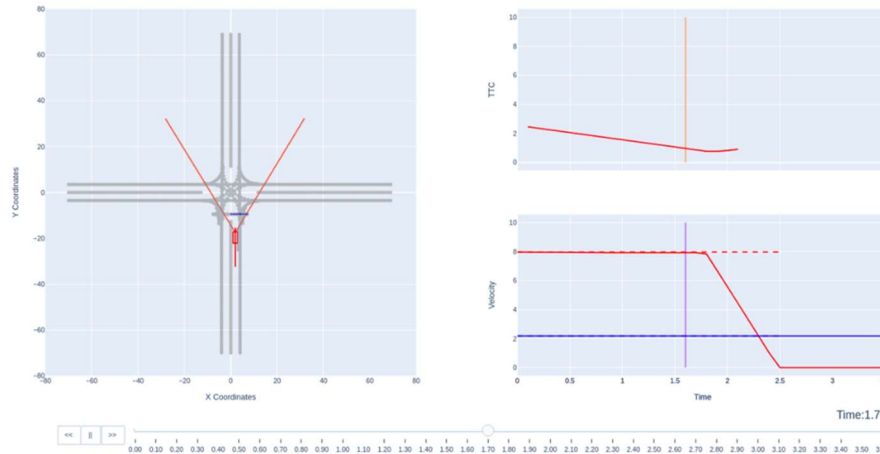


Figure 9-23: Scenario visualisation as plot .html file. The scenario representation consists of the road map, and the temporal evolution of the VUT and the VRU, moving along their simulated trajectories. Next to the road map the TTC over time as well as the velocity over time are shown. A slider represents the simulation time, and can further be used to step to a particular frame.

Catlog.pkl

The top level of the `catalog.pkl` file consists of an entry for each scenario, which is uniquely defined by the conflict situation, the initial VUT and VRU speed, the desired impact location and the friction coefficient μ , i.e. `LTOD_veh5.271_vru0.532_ps0.00_mu0.80`. Every scenario entry consists of two agent entries, `VUT` and `VRU`. Each of them has four further entries called `original`, `observation`, `system` and `agent_config`.

original and observation:

`original` and `observation` tables, contain information on the trajectories of VUT and VRU. This information is presented through positions, velocities and turning angles. The first column in the table represents the time. The `original` table contains the target trajectories, which are passed to the simulation platform, while then observed data from the simulation is added to the `observation` table. Compared to the `original` table, the `observation` table has additional `closestX`, `closestY`, `collision` and `TTC` columns, which are later used in generating the `evaluation_data.pkl` file for the scenario evaluation.

system

`VRU` agent entry has only a saved system file element with a path to the `.xml` system file. However, in the `VUT` agent entry, in addition to the system file, there are two more entries:

`IdealObjectDetector` and `Dynamics_TwoTrack`.

`IdealObjectDetector` contains `AzimuthalResolution`, `FieldofViewHorizontal`, `SensorLocationX`, `SensorLocationY` and `MaxRange` parameters representing the AEB configuration. It is possible to configure it within the GUI according to what kind of scenario we want to generate.

The setting of these parameters in the GUI is described in detail in Active Safety System Parameters and Setup (Section 9.2.2.1).

Dynamics_TwoTrack contains BrakeGradient and BrakeDelay parameters representing the Car configuration. Within the GUI, these parameters are configured according to which car model is selected.

Selecting an existing or defining a new car model is described in more detail in Vehicle parameters and setup (Section 9.2.2.1).

agent_config

Parameters for VUT and VRU geometry and mass are saved in the agent config. Type represents the type of agent and can be a Car, Pedestrian, Tram or Cyclist. For car agent type, Width, Length, DistanceCOGtoFrontAxle, Weight, Wheelbase, and TrackWidth parameters can be set in the GUI. The default values are taken if these parameters are not set in the GUI. Default values for all agent types are defined in the

`<path/to/repository>/<src>/<simlib>/<constants.py>` file.

Evaluation_data.pkl

In the evaluation_data.pkl file, the conflict data is saved in condensed form and used as input for the GUI. Amongst others, it contains information on the collision point, angle and speed between VUT and VRU, as well as the minimal TTC.

9.4.3 Simulation Time

9.4.3.1 Simulation Time for pre-crash simulation

The outcome of the pre-crash simulation is either a collision without intervention, with intervention and reduced collision velocity or an avoidance. For the first case, the simulation prior to the collision should be at least as long as the defined trigger time of the AEB system. For the second and third case, the time prior to the intervention should be as long as the trigger time.

9.4.3.2 Simulation Time for in-crash simulation

The in crash simulations should at least last 100 ms longer than the head impact on the vehicle.

9.5 Virtual test conditions (test runs)

9.5.1 Simulation Matrix

9.5.1.1 Simulation matrix for pre-crash simulations

The VUT settings have to be consistent with the ones used for validation in 9.2.2.1. For all other scenario-specific parameters, the default settings should be used, which lead to the following settings:

- "From Collision" has to be active (as by default) to ensure scenarios are generated with the "From Collision" mode.
- Weibull Distributions have to be used for the definition of the VUT and VRU Parameters ("From Weibull Distribution" is active, as by default).
 - For calculation of initial VUT and VRU speed values shape and scale parameters are used from the .csv files in the `<path/to/repository>/<src>/<coll_statistics_VIRTUAL>` folder. The .csv file has different shape and scale values related to specific conflict situations and severity levels.

- For Weibull distributed VUT speeds, by default 19 probability values are taken, the minimum is set to 0.05, where the maximum is set to 1. The step size is set with 0.05. Using these Weibull distribution parameters, we get 19 initial VUT velocities (5th to the 95th percentile of the initial speeds in 5 percentile steps). For Weibull distributed VRU speeds, by default nine, probability values are taken, the minimum is set to 0.1, max is set to 1 and step size is set to 0.1. The speed values are drawn in the same way as explained above.
- Scenarios are generated with the "From Collision" mode.
 - All conflict situation and severity levels should be selected, the default values for Weibull Distribution parameters are set.
 - New fields are opened in the GUI for entering values for impact location and friction coefficient. Default values for impact location representing the conflict point between the VUT and VRU are -40%, -20%, 0%, 20% and 40%, while the default friction coefficient values representing dry and wet road conditions are 0.5 and 0.8.
 - "All" conflict situations and "all" injury severities should be selected.

9.5.1.2 Simulation matrix for in-crash simulations

The output of the pre-crash simulation is processed via a Jupyter Notebook. This includes converting and rounding the values as well as weighting the simulation results according to their occurrence probability $P(scenario)$. The final step is the normalisation of the occurrence probabilities. In order to reduce the number of data points for further analysis, the simulation results are clustered. As one can see in Table 9-16, the collision angle is clustered in 30° steps. Starting at 0°, the first increment ranges from 345° to 15°, the second one from 15° to 45° and so on. The collision speed of the pedestrian is clustered in 1kph steps for high resolution. For the collision speed of the cyclist and the vehicle, 5kph steps are used due to the bigger range of occurring collision speeds. The collision distance is clustered in bins of 5%, starting at -50% +/-2.5%. The first and the last bin were effectively smaller than the rest of the bins, due to the fact that no accidents occurred below -50% and above 50%.

Table 9-16 List of parameters

| | Pedestrian | | Cyclist | |
|---|------------|---------|-----------|---------|
| | Range | Cluster | Range | Cluster |
| Collision speed vehicle \hat{v}_{veh} [kph] | 0 - 120 | 5 | 0-120 | 5 |
| Collision speed VRU \hat{v}_{VRU} [kph] | 0 - 20 | 1 | 0 - 50 | 5 |
| Collision angle A [°] | 0 - 360 | 30 | 0 - 360 | 30 |
| Collision point CP [%] | -50 - +50 | 5 | -50 - +50 | 5 |

To calculate the occurrence probability of a cluster, the law of total probability, Equation 1, is used.

$$P(B) = \sum_{i=1}^n P(A_i) * P(B|A_i)$$

Equation 1: Total probability (Bartsch and Sachs, 2014)

This leads to the equations for the probability of a certain:

- Collision angle $P(A) = \sum_i P(A|scenario_i) * P(scenario_i)$
- Collision point $P(CP) = \sum_i P(IP|scenario_i) * P(scenario_i)$
- Collision speed of the vehicle $P(\hat{v}_{ve}) = \sum_i P(\hat{v}_{ve} |scenario_i) * P(scenario_i)$
- Collision speed of the VRU $P(\hat{v}_{VRU}) = \sum_i P(\hat{v}_{VRU}|scenario_i) * P(scenario_i)$

$P(scenario_i)$ being the normalised occurrence probability of a certain VIRTUAL testing scenario.

The probabilities for the clustered collision angle, the collision speed of the vehicle/VRU and the collision point were stochastically dependent on each other. Consequently, the law of the total probability in Equation 1 is once again used to calculate the occurrence probability of a clustered collision scenario, which leads to Equation 2:

$$P(A \cap CP \cap \hat{v}_{ve} \cap \hat{v}_{VRU}) = \sum_i P(A \cap CP \cap \hat{v}_{veh} \cap \hat{v}_{VRU}|scenario_i) * P(scenario_i)$$

Equation 2: Occurrence probability of a clustered collision scenario

The occurrence probabilities are ranked in descending order and used as input for the design of experiments (Joseph et al., 2020) in preparation for the in-crash simulation. For further use, the ranked probabilities are saved in a CSV-file with the layout shown in Table 9-17. This step is considered in the pre_crash_simulation_analysis.ipynb¹⁶ notebook.

Table 9-17: Sample probability results table

| | col_angle [°] | col_point [%] | col_speed_veh [kph] | col_speed_vru [kph] | probability |
|-----|---------------|---------------|---------------------|---------------------|-------------|
| 1. | 270 | -40 | 15 | 11 | 0.006149 |
| 2. | 270 | -20 | 10 | 11 | 0.005362 |
| ... | | | | | |

Based on the maximum projection (MaxPro) criterion (Joseph et al., 2020) the cases for the in-crash simulation are selected.

At least 50 cases should be considered for in-crash simulations. The cases should be selected such that 60% of the cases (e.g. 30 cases if you consider 50 in-crash simulations) are selected from the scenarios which represent the upper 50% quantile based on the probability of a clustered collision scenario. The other 40% should then be selected from all scenarios. With the help of the MaxPro criteria a good space filling of the study area can be obtained. This step is implemented in R-Studio¹⁷.

9.5.2 Quality Criteria

9.5.2.1 Pre-crash simulation

If a scenario catalogue is generated “from collision”, each scenario is designed to end in a particular collision point, relative to the centre of the vehicle front, at a particular collision speed. Therefore three different conditions should hold, if a scenario is generated through the standard configurations:

- A collision in the baseline has to occur for each scenario

¹⁶ https://openvt.eu/wp-4/VISAFE-VRU/-/blob/master/pre_crash_simulation_analysis.ipynb

¹⁷ <https://openvt.eu/wp-4/VISAFE-VRU/-/blob/master/DoE.R>

- The default catalogues are designed to have equally distributed collision points. Hence, collision points observed in the baseline simulations have to be as close as possible to the desired ones. A sample result can be seen in Figure 9-24
- The impact speeds in the baseline must not deviate more than 10% from the intended collision velocity

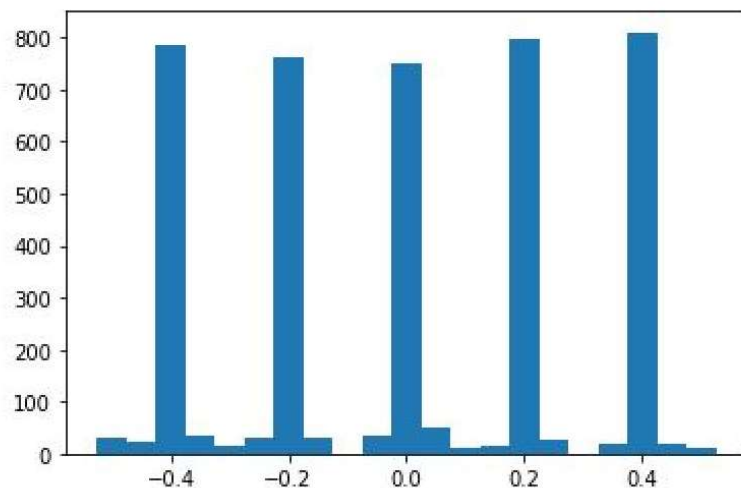


Figure 9-24: Observed collision points in the baseline simulation of a generated scenario catalogue. Peaks can be observed at -40, -20, 0, 20, and 40 percent of the vehicle front.

9.5.2.2 Quality criteria for In-crash simulation

The following quality criteria in line with the Euro NCAP TB024 must be met for all in-crash simulations:

FE surfaces coming in contact do not cross each other.

Surfaces coming in contact do not get trapped in each other (no sticky nodes).

Contact force (between HBM and vehicle) is zero at simulation start.

Total energy remains constant within a 15% tolerance.

Total hourglass energy $\leq 10\%$ of the total energy.

Total contact energy at the simulation start $\leq 1\%$ of the total energy.

Total artificial energy (contact energy and hourglass energy) $\leq 15\%$ of the total energy.

Total artificial mass (from mass-scaling) increase of the overall setup $\leq 3\%$.

Simulations have to run at least until head impact.

Additionally, for the parts where strain-based assessment is performed, the following criteria have to be met:

Hourglass energy of all parts related to the body part where strain-based assessment is performed $<10\%$ of internal energy of these parts.

Added mass of all parts related to the body parts where strain-based assessment is performed $<10\%$ of mass per body part.

9.6 Evaluation of virtual testing results

9.6.1 Postprocessing definitions

9.6.1.1 Postprocessing definitions for pre-crash simulation

The output of each generated scenario catalogue is the `evaluation_data.pkl` file, in which the conflict data is stored. Table 9-18 shows the condensed information, which is used for the evaluation of the scenario catalogue and to derive load cases for the in-crash simulation.

Table 9-18: Outputs of the simulated in-crash catalogue, used to define load cases for the in-crash simulation.

| Scenario ID | min_tccol [s] | vut_vel [m/s] | col_dist [m] | col_angle [%] | col_vru_vel [m/s] |
|------------------------------|------------------|------------------|-----------------|------------------|----------------------|
| SCPPL_veh12_vru2.5_ps0_mu0.5 | 0.2 | 11.9 | 0.3 | -39 | 2.5 |
| SCPPL_veh12_vru2.5_ps0_mu0.8 | 0.3 | 12.1 | 0.35 | -38 | 2.49 |
| ... | | | | | |

9.6.2 Injury Assessments

The following criteria according to the Injury Criteria Manual should be evaluated:

- HIC15
- DAMAGE
- Rib fracture
- Pelvic fracture
- Femur fracture
- Tibia fracture
- Knee injuries

9.6.3 Overall injury assessment

In order to predict the injury probabilities of unavoidable collision scenarios, which are not taken into account by the design of experiments, meta-models are used. The models are based on the python library Scikit-learn (Pedregosa et al., 2011). A Gaussian regression (K. I. Williams, 2006; Duvenaud, 2014) and the results of the 50 in-crash simulations were used within the meta-models to predict the injury criteria of the remaining unavoidable collision scenarios. This step is implemented in the `virtual_metamodel.py`¹⁸ python script for metamodeling and the `overall_injury_probability.ipynb`¹⁹ notebook for the overall injury assessment.

The output must be prepared in a format suitable for the CBA tool for the table "injury probabilities".

9.6.4 Cost-benefit analysis (CBA)

The VIRTUAL cost-benefit calculation tool for vehicle safety systems was developed by Wijnen et al. (2020). The tool converts the reduction of injuries through the safety system into the reduction of

¹⁸ https://openvt.eu/wp-4/VISAFE-VRU/-/blob/master/virtual_metamodel.py

¹⁹ https://openvt.eu/wp-4/VISAFE-VRU/-/blob/master/overall_injury_probability.ipynb

QALYs. The calculated QALYs incorporate disability weights, which account for the severity and the impact on the quality of life of the injury, as well as the duration of quality of life loss. Inserting the injury risks derived in 9.6.3 into the "injury probability" sheet will lead to the calculation of "benefits" in the "CBA" sheet, which can be compared to the costs of introducing a specific safety measure when a baseline is available.

9.6.5 Documentation and Data Specification

The simulation output files (animations and time histories) and tables generated with the Jupyter notebooks must be stored.

The results of the assessment of the in-crash simulations and the cost benefit analysis will be stored as PDF reports. This is currently a work in progress and will be further described in the next version of the protocol.

9.7 References

- Barrow, A., Edwards, A., Smith, L., Khatry, R., Kalaiyaran, A., and Hynd, D. *Effectiveness estimates for proposed amendments to the EU's General and Pedestrian Safety Regulations*. Wokingham, Berkshire, United Kingdom: TRL, 2018.
- Bartsch H.-J., Sachs M. *Taschenbuch mathematischer Formeln für Ingenieure und Naturwissenschaftler*. München: Hanser, 2014.
- Bose, Dipan, Kavi S. Bhalla, Costin D. Untaroiu, B. Johan Ivarsson, Jeff R. Crandall, and Shepard Hurwitz. "Injury tolerance and moment response of the knee joint to combined valgus bending and shear loading." *Journal of biomechanical engineering* (American Society of Mechanical Engineers Digital Collection) 130 (2008).
- Cho, Jin-Rae, Seung-Bum Park, Sung-Hyun Ryu, Sung-Ho Kim, and Shi-Bok Lee. "Landing impact analysis of sports shoes using 3-D coupled foot-shoe finite element model." *Journal of mechanical science and technology* (Springer) 23 (2009): 2583–2591.
- Duvenaud, David. "The Kernel cookbook: Advice on covariance functions." URL <https://www.cs.toronto.edu/~duvenaud/cookbook>, 2014.
- EuroNCAP. "Pedestrian Human Model Certification. TB 024." <https://cdn.euroncap.com/media/56949/tb-024-pedestrian-human-model-certification-v20.pdf>, 2019.
- EuroNCAP "Pedestrian testing protocol." <https://cdn.euroncap.com/media/41769/euro-ncap-pedestrian-testing-protocol-v85.201811091256001913.pdf>, 2019.
- Gruber, Michael, et al. "The effect of P-AEB system parameters on the effectiveness for real world pedestrian accidents." *Proceedings of the 26th ESV Conference Proceedings*. 2019.
- Hainisch, T. *Erstellung von FE Fahrradmodellen zum Abbilden unterschiedlicher Rahmen-Geometrien und -Größen für Crashsimulationen*. Bachelorarbeit, Graz: TU Graz, Institut für Fahrzeugsicherheit., 2015.
- Hertz, Ellen. "A note on the head injury criterion (HIC) as a predictor of the risk of skull fracture." *Proceedings: Association for the Advancement of automotive medicine annual conference*. 1993. 303-312.
- Joseph, V. Roshan, Evren Gul, and Shan Ba. "Designing computer experiments with multiple types of factors: The MaxPro approach." *Journal of Quality Technology* (Taylor & Francis) 52 (2020): 343–354.
- Klug, C., P Luttenberger, M Schachner, J Micorek, R Greimel, and W Sinz. "Postprocessing of Human Body Model Results – Introduction of the Open Source Tool DYNASAUR." *7th International Symposium: Human Modeling and Simulation in Automo*. 2018.
- Larsson, Karl-Johan, Amanda Blennow, Johan Iraeus, Bengt Pipkorn, and Nils Lubbe. "Rib cortical bone fracture risk as a function of age and rib strain: updated injury prediction using finite

- element human body models." *Frontiers in bioengineering and biotechnology* (Frontiers) 9 (2021): 412.
- McLundie, W. M. "Investigation of Two-Wheeled Road Traffic Accidents using Explicit FE Techniques." (Cranfield University) 2007.
- Nusia, Jiota, Jia Cheng Xu, Reimert Sjöblom, Johan Knälmann, Astrid Linder, and Svein Kleiven. "Injury risk functions for the four primary knee ligaments." *Under review (Journal of the Mechanical Behavior of Biomedical Material)*, 2022.
- Pedregosa, Fabian, et al. "Scikit-learn: Machine learning in Python." *the Journal of machine Learning research* (JMLR. org) 12 (2011): 2825–2830.
- Schachner, M, J Micorek, P Luttenberger, and R Greimel. *Dynasaur*. 2018. <https://gitlab.com/VSI-TUGraz/Dynasaur>.
- Schachner, Martin, Wolfgang Sinz, Robert Thomson, and Corina Klug. "Development and evaluation of potential accident scenarios involving pedestrians and AEB-equipped vehicles to demonstrate the efficiency of an enhanced open-source simulation framework." *Accident Analysis & Prevention* (Elsevier) 148 (2020): 105831.
- Schmitt, Kai-Uwe, Peter F. Niederer, Duane S. Cronin, Barclay Morrison III, Markus H. Muser, and Felix Walz. *Trauma biomechanics: an introduction to injury biomechanics*. Springer, 2019.
- Schubert, Alexander, Nico Erlinger, Christoph Leo, Johan Iraeus, Jobin John, and Corina Klug. "Development of a 50th Percentile Female Femur Model." *International Research Council on the Biomechanics of Injury 2021*. 2021. 308–332.
- Snedeker, Jess G., Markus H. Muser, and Felix H. Walz. "Assessment of pelvis and upper leg injury risk in car-pedestrian collisions: comparison of accident statistics, impactor tests and a human body finite element model." Tech. rep., SAE Technical Paper, 2003.
- TRL, CEESAR, ACEA. "General Safety Regulation: accident analysis assesses effectiveness of proposed safety measures." <https://www.acea.auto/publication/general-safety-regulation-accident-analysis-assesses-effectiveness-of-proposed-safety-measures/>, 2018.
- Wijnen, W., Elvik, R., Bützer, D. «Preliminary cost-benefit calculation tool for vehicle safety systems.» *Milestone 6.3 of the H2020 project VIRTUAL*. 2020.
- Williams, Christopher K. I., and Carl Edward Rasmussen. *Gaussian processes for machine learning*. Vol. 2. MIT press Cambridge, MA, 2006.
- Wu, Ge, and Peter R. Cavanagh. "ISB recommendations in the reporting for standardization of kinematic data." *J. Biomech* 28 (1995): 1257–1261.
- Wu, Ge, et al. "ISB recommendation on definitions of joint coordinate system of various joints for the reporting of human joint motion—part I: ankle, hip, and spine." *Journal of biomechanics* (Elsevier) 35 (2002): 543–548.
- Wu, Ge, et al. "ISB recommendation on definitions of joint coordinate systems of various joints for the reporting of human joint motion—Part II: shoulder, elbow, wrist and hand." *Journal of biomechanics* (Elsevier) 38 (2005): 981–992.

9.8 Appendix

9.8.1 Bicycle model validation

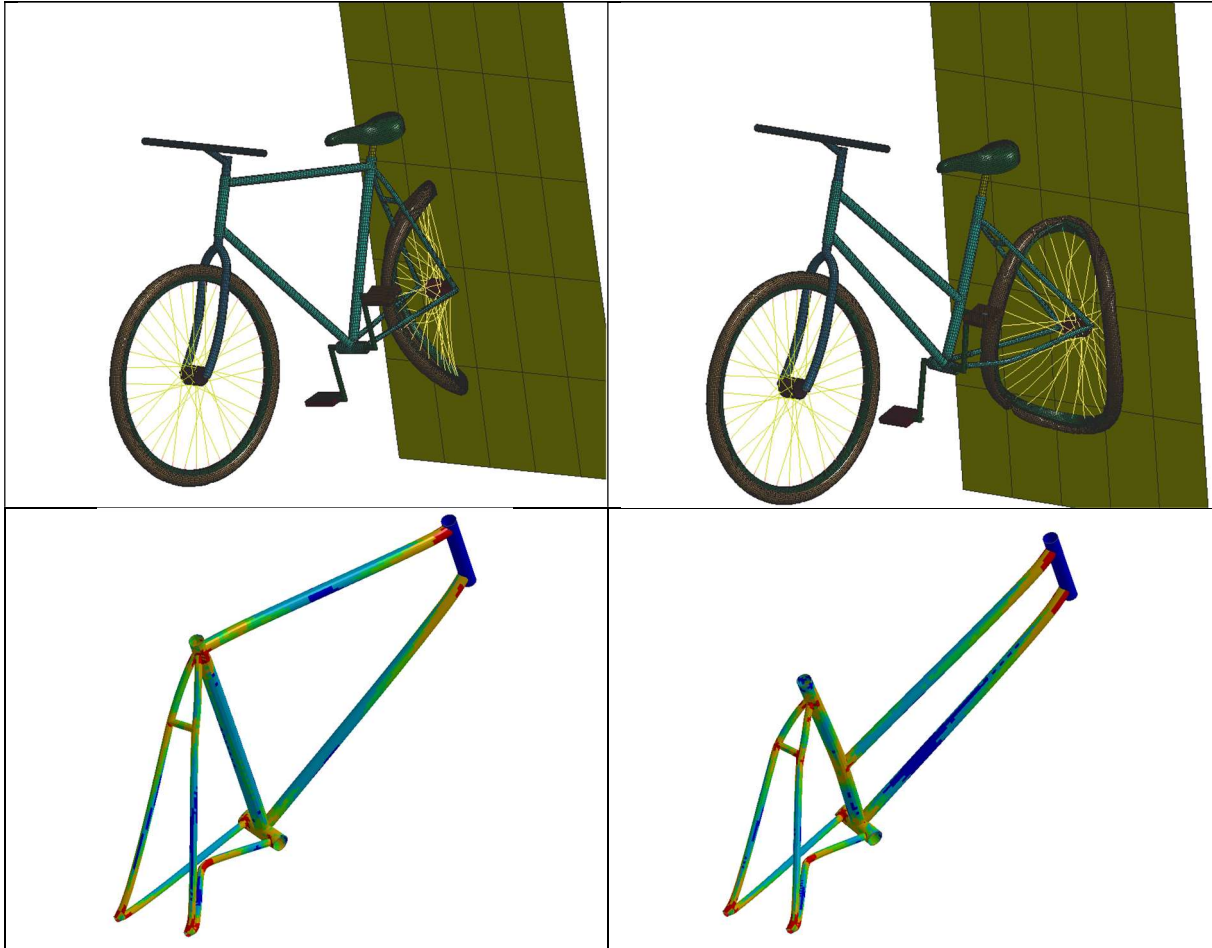


Figure 9-25 Bicycle validation using rigid wall rear impact: diamond model for VIVA+ 50M (left); trapeze model for 50F (right)

10 Appendix E: Articles of the OpenVT Organisation

General regulations

Article 1 – Name and registered headquarters

The association is called *The OpenVT Organisation* and constitutes an association according to Art. 60ff of the Swiss Civil Code.

The OpenVT Organisation is registered at Winkelriedstrasse 27, 8006 Zürich, Switzerland (c/o AGU Zürich).

Article 2 – Neutrality

The OpenVT Organisation is a politically independent and secular association.

Article 3 – Objectives

Objectives of *The OpenVT Organisation* are:

- Run and own The OpenVT platform and the associated domain openvt.eu.
- Provide OpenVT as an open platform for virtual testing (VT) in road safety and injury biomechanics in general.
- Own the copyrights of open source projects related to VT and biomechanics.
- Host open source projects related to VT and biomechanics on The OpenVT platform, maintain them and ensure the sustainable evolution in the future, provide user support.
- Promote and support research related to virtual testing and computer modelling in biomechanics and traffic safety.

Organisation

Article 4 – Authorities

Authorities of *The OpenVT Organisation* are the General Meeting, the Committee and the Auditor.

Article 5 – General Meeting

The General Meeting (GM) convenes at least once per year; this regular assembly is called by the Committee with at least 30 days notice. The call should state the place and time of the GM assembly and the proposed agenda. The GM can convene either in person or remotely. An extraordinary assembly of the GM can be called by the Committee or by a written request of at least one fifth of the members, on 30 days notice.

All members have equal voting rights at the GM. Members not attending the GM assembly may assign their vote to another member. In order for a GM assembly to be valid, at least 40 percent of the members must be present or represented. If the minimum attendance for a valid GM assembly is not met, the Committee immediately calls a new assembly, which takes place at the latest 40 days later and is valid even if the minimal attendance requirement is not fulfilled. Resolutions are passed by a valid GM assembly with the vote of a majority of the members present or represented, by secret ballot if a present member requests so.

The GM elects the members of the Committee and the Auditor by majority vote of the members present or represented, by secret ballot if a present member requests so.

The GM supervises the activities of the Committee and decides on all matters brought to it in a way to follow the objectives of the organisation. The GM accepts or refuses membership applications by resolution.

The GM decides on which Open Source Projects are hosted on The OpenVT platform and supervises their activities.

During the regular assembly, the GM grants discharge, i.e. approves the reports and all actions and decisions of the Committee by resolution. The members of the Committee are excluded from the vote on their own discharge.

The GM may decide to change the articles, except the Objectives (Article 3), by resolution. Requests to change the articles must be announced to all members in writing at least 30 days before the assembly, including the old and new formulation of the articles. The Objectives (Article 3) may be changed in the same way, but require unanimous vote of all members present or represented.

Article 6 – Committee

The Committee consists of a President, a Vice President, a Treasurer and a Secretary. These positions must be held by 4 different persons.

The members of the Committee are elected by the General Meeting from among the full members for a one-year term and can be re-elected.

The Committee is responsible for the day-to-day business of *The OpenVT Organisation*, as well as for preparing and executing the assembly of the General Meeting.

The President is *The OpenVT Organisation's* official representative. The President shall preside at all GM assemblies and, with the concurrence of the GM, shall appoint sub-committees and their chairs as appropriate. The Vice-President shall serve in the President's stead should the President be absent or otherwise unable to serve or act. The Secretary shall record the minutes of all GM assemblies and distribute them to the members for approval during the following meeting. The Treasurer, under the supervision of the GM, shall oversee the receipt of all monies, the deposit thereof into *The OpenVT Organisation* accounts and all payments of *The OpenVT Organisation's* debts and obligations.

Committee members serve unsalaried although they can claim monetary compensation for actual expenses or reimbursement for cash outlay. In certain exceptional situations where a Committee member expends a particularly large amount of time on behalf of the organisation, reasonable compensation may be considered by the GM.

Article 7 Auditor

The Auditor conducts an annual review of the financial administration, cash management and accounting procedures. The Auditor is required to submit a written, signed letter to the GM, verifying whether the financial management of the organisation conforms to acceptable accounting practices. The Auditor may be a member of *The OpenVT Organisation*, a non-member or an independent accountant. The Auditor is elected by the GM for one year and can be re-elected. The Auditor may be dismissed by a majority vote of the GM.

Article 8 – Subcommittees

For each open source project (OSP) hosted on OpenVT, the Committee may decide to form a Subcommittee. The members of the Subcommittees are nominated by the active developers of the corresponding OSP and appointed by the Committee.

The subcommittees shall oversee and govern the development and maintenance of the corresponding OSP. They develop a yearly roadmap and decide on official releases. They can decide to charge an appropriate support fee to cover expenses and hire staff to deal with support requests if needed. The members of the Subcommittees serve unsalaried, with the same exceptions as the Committee members. The Subcommittees report to the General Meeting.

Article 9 – The OpenVT administrators

The OpenVT administrators (OVTA) are appointed by the Committee. The OVTA are responsible for the daily maintenance and administration of The OpenVT platform and server, such as user and content administration. The OVTA serves unsalaried, with the same exceptions as the Committee members.

Membership

Article 10 – Membership

Only natural persons who support the objectives can be members of *The OpenVT Organisation*. The GM defines by resolution a list of additional requirements for new members and a maximum number of members.

Article 11 – Sponsorship

Legal entities as well as natural persons can become sponsors of *The OpenVT Organisation*. Sponsors do not have a vote in the General Meeting. However, they may participate in the assemblies of the General Meeting in a reporting and consultant role. If the sponsor is a legal entity, it may be represented by a person who can but does not have to be member of *The OpenVT Organisation*. If the representative is also member of *The OpenVT Organisation*, his or her right to vote is unaffected by the fact of representing a sponsor.

Article 12 – Nomination

Membership candidates submit a written application to the Committee for approval by the GM, on which the GM decides according to the membership requirements. In order to accept the application, at least two thirds of the members present or represented at the General Meeting assembly have to approve of it. The GM may deny a membership application without specifying the reasons. If the application is accepted, membership takes immediate effect, unless the GM has decided on a non-zero yearly membership fee (in this case, the membership is validated with the payment of the fee). A new member can only be accepted by the GM if including the new member no more than 30% of the members are affiliated with the same organisation or company less than 50% are affiliated with industrial enterprises.

Applications for sponsorship are decided on by the Committee. The sponsorship takes effect as soon as the Committee has accepted the application and at least the minimum sponsoring donation has been paid. The Committee may deny the application without specifying the reasons.

Article 13 – Membership fees

The General Meeting decides on the yearly membership fee and on the minimum yearly amount to be donated by sponsors. While the membership fee can be set to zero, the minimum sponsoring donation must be greater than zero.

Article 14 –Resignation/exclusion

All members and sponsors have the right to resign subject to six months' notice expiring at the end of the calendar year. The Committee may permit a resignation on shorter notice in individual cases. Already paid fees and sponsoring donations cannot be refunded in case of resignation.

Members and sponsors can be excluded by resolution of the GM.

Dissolution

Article 15 – Dissolution

The dissolution of *The OpenVT Organisation* can be pronounced by the General Meeting by unanimous vote of the members. Dissolution requires a vote of at least 75% of the full members. Proxy voting is allowed. The vote on dissolution must be announced by the Committee at least 60 days in advance; a proxy voting form must be provided.

The GM decides by majority vote on the disposition of the assets and properties of *The OpenVT Organisation*. Assets may be given to non-profit organisations based in Europe with similar objectives or to university institutions. Immaterial property may only be given to universities and other public research institutions.

Additional items

Article 16 – Liability

The association limits liability only to the goods of the association according to its property list. Liability of individual members is excluded.

Article 17 – Legal force

These articles were approved by the **General Meeting on October 25, 2021** and came into force immediately.